OCT 15 1991

8/1/91 circulates

NUREG/CR-5743

Approaches to Large Scale Unsaturated Flow in Heterogeneous, Stratified, and Fractured Geologic Media

Technical Compliance Program

Prepared by
R. Ababou

Center for Nuclear Waste Regulatory Analyses
Southwest Research Institute

Prepared for
U.S. Nuclear Regulatory Commission

9551

AVAILABILITY NOTICE

Availability of Reference Materials Cited in NRC Publications

Most documents cited in NRC publications will be available from one of the following sources:

1. The NRC Public Document Room, 2120 L Street, NW., Lower Level, Washington, DC 20555

2. The Superintendent of Documents, U.S. Government Printing Office, P.O. Box 37082, Washington, DC 20013-7082

3. The National Technical Information Service, Springfield, VA 22161

Although the listing that follows represents the majority of documents cited in NRC publications, it is not intended to be exhaustive.

Referenced documents available for inspection and copying for a fee from the NRC Public Document Room include NRC correspondence and internal NRC memoranda; NRC bulletins, circulars, information notices, inspection and investigation notices; licensee event reports; vendor reports and correspondence; Commission papers; and applicant and licensee documents and correspondence.

The following documents in the NUREG series are available for purchase from the GPO Sales Program: formal NRC staff and contractor reports, NRC-sponsored conference proceedings, and NRC booklets and brochures. Also available are regulatory guides, NRC regulations in the *Code of Federal Regulations*, and *Nuclear Regulatory Commission Issuances*.

Documents available from the National Technical Information Service include NUREG-series reports and technical reports prepared by other Federal agencies and reports prepared by the Atomic Energy Commission, forerunner agency to the Nuclear Regulatory Commission.

Documents available from public and special technical libraries include all open literature items, such as books, journal articles, and transactions. *Federal Register* notices, Federal and State legislation, and congressional reports can usually be obtained from these libraries.

Documents such as theses, dissertations, foreign reports and translations, and non-NRC conference proceedings are available for purchase from the organization sponsoring the publication cited.

Single copies of NRC draft reports are available free, to the extent of supply, upon written request to the Office of Administration, Distribution and Mail Services Section, U.S. Nuclear Regulatory Commission, Washington, DC 20555.

Copies of industry codes and standards used in a substantive manner in the NRC regulatory process are maintained at the NRC Library, 7920 Norfolk Avenue, Bethesda, Maryland, for use by the public. Codes and standards are usually copyrighted and may be purchased from the originating organization or, if they are American National Standards, from the American National Standards Institute, 1430 Broadway, New York, NY 10018.

DISCLAIMER NOTICE

This report was prepared as an account of work sponsored by an agency of the United States Government. Neither the United States Government nor any agency thereof, or any of their employees, makes any warranty, expressed or implied, or assumes any legal liability of responsibility for any third party's use, or the results of such use, of any information, apparatus, product or process disclosed in this report, or represents that its use by such third party would not infringe privately owned rights.

NUREG/CR-5743

Approaches to Large Scale Unsaturated Flow in Heterogeneous, Stratified, and Fractured Geologic Media

Manuscript Completed: July 1991
Date Published: August 1991

Prepared by
R. Ababou

T. J. Nicholson, NRC Project Manager

Center for Nuclear Waste Regulatory Analyses
Southwest Research Institute
6220 Culebra Road
San Antonio, TX 78228-0510

Prepared for
Division of Engineering
Office of Nuclear Regulatory Research
U.S. Nuclear Regulatory Commission
Washington, DC 20555
NRC FIN B6664

For sale by the U.S. Government Printing Office
Superintendent of Documents, Mail Stop: SSOP, Washington, DC 20402-9328
ISBN 0-16-035837-X

ABSTRACT

This report develops a broad review and assessment of quantitative modeling approaches and data requirements for large-scale subsurface flow in radioactive waste geologic repository. The data review includes discussions of controlled field experiments, existing contamination sites, and site-specific hydrogeologic conditions at Yucca Mountain. Local-scale constitutive models for the unsaturated hydrodynamic properties of geologic media are analyzed, with particular emphasis on the effect of structural characteristics of the medium. The report further reviews and analyzes large-scale hydrogeologic spatial variability from aquifer data, unsaturated soil data, and fracture network data gathered from the literature. Finally, various modeling strategies toward large-scale flow simulations are assessed, including direct high-resolution simulation, and coarse-scale simulation based on auxiliary hydrodynamic models such as single equivalent continuum and dual-porosity continuum. The roles of anisotropy, fracturing, and broad-band spatial variability are emphasized.

TABLE OF CONTENTS

Page

ABSTRACT iii

LIST OF FIGURES viii

LIST OF TABLES xi

EXECUTIVE SUMMARY xiii

1. INTRODUCTION AND OVERVIEW 1-1

2. SUBSURFACE CONTAMINATION AND HYDROGEOLOGIC SETTING 2-1

   2.1 FIELD OBSERVATIONS AT EXISTING SUBSURFACE CONTAMINATION SITES 2-1
   2.2 HIGH-LEVEL WASTE ISOLATION AND REGULATORY ISSUES 2-3
   2.3 SITE-SPECIFIC HYDROGEOLOGY AND MODELING ISSUES 2-4
   2.4 SUMMARY AND OUTLOOK 2-13

3. FIELD EXPERIMENTS ON FLOW AND TRANSPORT IN HETEROGENEOUS MEDIA 3-1

   3.1 GENERAL CONSIDERATIONS 3-1
   3.2 TRANSPORT EXPERIMENTS IN UNSATURATED SOILS AND UNCONSOLIDATED MEDIA 3-2
   3.3 EXPERIMENTS ON FLOW AND TRANSPORT IN SATURATED FRACTURED ROCKS 3-8
   3.4 OBSERVATIONS OF FLOW AND TRANSPORT IN UNSATURATED FRACTURED ROCKS 3-8

4. LOCAL HYDRODYNAMIC COEFFICIENTS AND CONSTITUTIVE RELATIONS: CONCEPTS, MODELS, AND DATA 4-1

   4.1 HYDRAULIC PROPERTIES OF SATURATED POROUS MEDIA 4-1
   4.2 HYDRAULIC PROPERTIES OF SATURATED FRACTURED MEDIA . . . 4-3

      4.2.1 Approximate Fluid Dynamics of Single Fractures 4-3
      4.2.2 Single Set of Parallel Fractures with Variable Spacing and Apertures 4-6
      4.2.3 Orthogonal Array of Fractures 4-7
      4.2.4 Multiple Sets of Parallel Fractures of Arbitrary Orientations 4-8
      4.2.5 Kozeny-Carman Relation for Fracture Networks 4-14

4.3 HYDRAULIC PROPERTIES OF UNSATURATED POROUS MEDIA . . . 4-15

4.3.1 Equations and Constitutive Relations 4-15
4.3.2 Log-Conductivity Slope and Exponential Conductivity Model 4-17

4.3.2.1 Kirchhoff Transform 4-17
4.3.2.2 Gravity-Driven Advection and Peclet Number 4-18
4.3.2.3 Correlation of Log-Conductivity Slope with Other Parameters 4-19

4.3.3 Functional Conductivity Models of Burdine and Mualem 4-23
4.3.4 Brooks-Corey and Van Genuchten Parametrization of Water Retention Curves 4-24
4.3.5 Combining Brooks-Corey and Van Genuchten Retention Curves with Functional Conductivity Models of Burdine and Mualem 4-24
4.3.6 Scaling Factors in Similar Media Theory 4-28

4.4 UNSATURATED HYDRAULIC PROPERTIES OF FRACTURED POROUS ROCKS 4-30

5. HYDROGEOLOGIC HETEROGENEITY AND SPATIAL STRUCTURE: FIELD DATA AND STOCHASTIC MODELS 5-1

5.1 INTRODUCTION 5-1
5.2 STATISTICAL CONTINUUM HETEROGENEITY OF WATER-BEARING FORMATIONS 5-1
5.3 STATISTICAL CONTINUUM HETEROGENEITY OF UNSATURATED MEDIA 5-9

5.3.1 General Considerations 5-9
5.3.2 Field Data 5-9
5.3.3 Auxiliary Hydrodynamic Models and Cross-Correlations 5-13

5.3.3.1 Conductivity Curve Cross-Correlation 5-14
5.3.3.2 Similar Media Hypothesis 5-14

5.4 FIELD CHARACTERIZATION OF FRACTURED ROCKS AND FRACTURE NETWORKS 5-18

5.4.1 Hydraulic Characterization and Mapping of Fracture Networks 5-18
5.4.2 Hydraulic Characterization of Unsaturated Fractured Rocks 5-22

6. OUTLOOK OF FIELD-SCALE FLOW MODELING FOR HETEROGENEOUS AND FRACTURED UNSATURATED MEDIA 6-1

6.1 GENERAL CONSIDERATIONS 6-1
6.2 CONCEPTUAL APPROACHES TO FIELD-SCALE FLOW MODELING . . 6-2

6.2.1 Direct Simulation Approach 6-2
6.2.2 Indirect Simulation Approach 6-3
6.2.3 Combination of Direct and Indirect Modeling 6-4

6.3 SINGLE EQUIVALENT CONTINUUM MODELS 6-4
6.4 DUAL CONTINUUM MODELS AND FRACTURE/MATRIX FLOW 6-5
6.5 DIRECT MODELING OF PARTIALLY SATURATED FLOW IN FRACTURED ROCK 6-9

6.5.1 Direct Modeling of Flow through Variably Saturated Parallel Plate Fracture Networks 6-9
6.5.2 Direct Modeling of Unsaturated Matrix/Fracture Flow Based on Bulk Unsaturated Fracture Properties 6-11

6.6 HIGH-RESOLUTION MODELING OF UNSATURATED FLOW IN RANDOMLY HETEROGENEOUS AND STRATIFIED CONTINUUM 6.15

6.6.1 Background, Simulation Results, and Analysis 6-15
6.6.2 Computational Aspects of Direct High-Resolution Simulations 6-16

6.6.2.1 Numerical Analysis of Nonlinear Unsaturated Flow 6-16
6.6.2.2 Effects of Heterogeneity on Numerical Accuracy 6-16
6.6.2.3 Algebraic System Solvers 6-19

6.7 OTHER REVIEWS OF MODELING APPROACHES IN THE LITERATURE 6-19

7. SUMMARY AND CONCLUSIONS 7-1

8. REFERENCES 8-1

APPENDIX: ANNOTATED BIBLIOGRAPHY A-1

LIST OF FIGURES

Page

2-1 Idealized Moisture - Flow System Through East-West Section at Yucca Mountain (modified from Montazer and Wilson, 1986, and DOE Site Characterization Plan, 1988). 2-6

2-2 Idealized Moisture - Flow System Through East-West Section at Yucca Mountain (from Peters and Klavetter, 1988) 2-7

2-3 Numerical Grid Used in the Two-Dimensional Flow Simulations (Modified from Rulon et al, 1986). 2-9

3-1 Typical Horizontal and Vertical Movement of Liquids in Hanford Formation Sediments Under Partially Saturated Conditions 3-3

3-2 Progression of Strip-Source Wetting Front up to Day 55 as Observed on the Trench Face, Las Cruces Trench Experiment No. 1 3-5

3-3 Cross-Section Profile of Water Content, from Neutron Probe Readings, During Strip Source Experiment No. 1 at Las Cruces at Jornada Trench Site (Days 10-117). 3-6

3-4 Cross-Section Profile of Water Content, from Neutron Probe Readings, During Strip Source Experiment No. 1 at Las Cruces at Jornada Trench Site (Days 217-737). 3-7

4-1 Parallel Plate Model of Single Fracture (above), and Orthogonal Array of Fractures (below) 4-5

4-2 Two Non-Orthogonal Sets of Parallel Fractures with Variable Apertures and Spacing 4-10

4-3 Relation between Parameter α, Slope of $\ell n K(h)$, and the Fine Particle Fraction of Soils of Table 4-2 4-21

4-4 Water Retention Curve (degree of saturation S) and Relative Conductivity Curve (K_r) versus Dimensionless Suction ($\psi = a\Psi$) According to the van Genuchten-Mualem Model. Parameters from the Las Cruces-Jornada Trench Soil Were used (m = 0.4955). The Solid Circle Indicates the Inflection Point of the Water Retention Curve. 4-26

5-1 Log-Conductivity Records $\ell n K(x)$ in One Spatial Dimension. Top: Mount Simon Borehole Data (from Gelhar, 1976). Bottom: Synthetic Random Function (from Ababou, 1988).. 5-2

5-2 Log-Conductivity Contours in a Vertical Plane. (a) from Sudicky (1986) (Measured at the Borden Tracer Site). (b) by Simulation, Using the Turning Band Method With an Anisotropic Spectrum. 5-5

5-3 One-Dimensional Spectral Density of Measured Log-Conductivity in a Vertical Borehole (black circles) and Fitted Spectral Density Functions. (from Ababou and Gelhar, 1990) 5-7

5-4 Illustration of the Spectral Conditioning Method after Ababou and Gelhar (1990): Log Spectral Density versus Log-Wavenumber (above); Sample Function of Log-Conductivity Process (below) 5-8

5-5 Synthetic Realization of a 1D Gauss-Markov Process with Exponential Covariance Function (log-normal above, Gaussian below) 5-12

5-6 Unsaturated Hydraulic Conductivity versus Capillary Tension Head for the Maddock Sandy Loam 5-15

5-7 Schematic Representation of Suction-Dependent Anisotropy of Conductivity, and Crossing Point of Fracture-Matrix Conductivity Curves 5-16

5-8 Lower Stereonet Projection of Fracture Orientations Observed at Apache Leap Tuff Site, from X-Series Boreholes (Crosses), Y-Series Boreholes (Circles), and Z-Series Boreholes (Squares) [from Yeh et al., 1988] 5-17

5-9 Line Interpretation of Structural Lineaments in the Apache Leap Tuff. Fractures were traced from an aerial photo scaled at 1:14,350. The area bounded by registration marks has been studied in detail (Thornburg, 1990) 5-19

5-10 Line Interpretation of Structural Lineaments in the Apache Leap Tuff. Fractures were traced from an aerial photo scaled at 1:7,180. The University of Arizona field sites are located: [A] Rock knoll heater site, and [B] Inclined boreholes site. The area bounded by registration marks has been studied in detail (Thornburg, 1990). 5-20

5-11 Definition of sets and poles of fractures mapped in the 80m section of the drift wall at the Faney-Augères mine (from Long and Billaux, 1987) 5-21

5-12 Synthetic two-dimensional fracture network in a 100m 100m domain, where each 10m 10m subdomain was generated independently. The total number of fractures is 65,740 (from Long and Billaux, 1987). 5-23

6-1 Conceptual Model of Partially Saturated, Fractured, Porous Medium Showing Schematically the Flow Line Moving Around the Dry Portions of the Fractures 6-10

6-2 Front View of Peeled-Off Three-Dimensional Moisture Plume from Stochastic Flow Simulations 6-11

6-3 Back View of Three-Dimensional Moisture Plume from Stochastic Flow Simulations 6-12

6-4 Conceptual Model of Partially Saturated, From Red, Porous Medium Showing Schematically the Flow Line Moving Around the Dry Portions of the Fractures (Wang and Narasimhan, 1985) 6-14

6-5 Front View of Peeled-Off Three-Dimensional Moisture Plume from Stochastic Flow Simulations 6-16

6-6 Back View of Three-Dimensional Moisture Pattern from Stochastic Flow Simulations; the Cut-Off Moisture Plume Is Visible In Purple and Blue 6-17

LIST OF TABLES

		Page
2-1	Definition of Unsaturated-Zone Hydrogeologic Units and Correlation with Rock Stratigraphic Units	2-5
2-2	Summary of Compilations of Hydrogeologic Properties of Hydrogeologic Units Within the Unsaturated Zone, Yucca Mountain	2-10
2-3	Summary of Hydrologic Characteristics of Major Stratigraphic Units in the Vicinity of Yucca Mountain	2-11
4-1	Comparison of Specific Area of Solids in Vitric and Zeolitized Sub-Units of the Nonwelded Calico Hills Formation; Based on Kozeny-Carman Relation	4-3
4-2	Comparison of Grain Size Distributions and Log-Conductivity Slope for Nine Soils (Modified After Ababou, 1981)	4-20
4-3	Partial List of Single-Point Moments of Hydrodynamic Parameters for the Las Cruces—Jornada Trench Site from 562 Cores	4-28
5-1	Statistical Properties of Measured Three-Dimensional Log-Conductivities (ℓnK) in Saturated Formations, from Hufschmied (1985) and Sudicky (1986)	5-4
5-2	Summary of Statistical Data on the In-Situ Spatial Variability of Unsaturated Soils from the Literature	5-10

EXECUTIVE SUMMARY

A quantitative characterization of large-scale flow and radionuclide transport through the heterogeneous unsaturated fractured rock of Yucca Mountain will be necessary to evaluate compliance with the performance objectives and siting criteria associated with the proposed high-level waste repository (NRC Rule 10 CFR 60.112, 60.113, and 60.122). The pertinent scientific and technical aspects of radionuclide migration at Yucca Mountain will need to be understood so as to demonstrate that the hydrogeologic conditions at the repository site strongly inhibit radionuclide transport to the accessible environment and meet performance criteria. In particular, realistic modeling of the far field heterogeneous flow and radionuclide transport processes at Yucca Mountain requires incorporating the effects of a broad spectrum of anisotropic heterogeneities, from relatively fine scales up to the scales of interest for performance assessment. In the undisturbed geologic setting, examples of geologic features that can have significant overall effect on flow and transport are: persistent narrow discontinuities such as faults and major fractures, inter-unit discontinuities, structural configuration of geologic units, bedding, fine-scale stratification, and variable fracture density, to name a few.

The NRC Research Project on "Stochastic Analysis of Large Scale Flow and Transport in Unsaturated Fractured Rock" was initiated at the Center for Nuclear Waste Regulatory Analyses to investigate the above-mentioned questions of far field modeling (Contract: NRC-02-88-005; starting date: February 2, 1990). The specific objectives of the "Stochastic Project" are as follows:

- To review the literature on field-scale flow-transport in the presence of heterogeneities; to assess available models and data relevant to the subject site; and to select a global modeling approach to large-scale unsaturated flow and transport in heterogeneous, stratified, and fractured rock;

- To develop auxiliary hydrodynamic modeling approaches, numerical algorithms, and probabilistic data processing techniques for incorporation into the global model;

- To implement large-scale simulations for large-scale flow and transport processes in unsaturated, heterogeneous, and fractured rock at the Yucca Mountain repository; to analyze model predictions; and to contribute to model validation activities.

Accordingly, the project was divided in three tasks:

- Task 1 - Review, Analysis, and Initial Development of Modeling Approach;

- Task 2 - Stochastic Submodel Development, Auxiliary Analyses, and Development of Related Numerical Algorithms;

- Task 3 - Large-Scale Flow/Transport Simulation and Input/Output Data Analyses.

The results of literature review, including assessment of field data requirements, and initial stage of model analysis and development, are presented in this Technical Report for Task 1 of the Project. Subsequent reports for Tasks 2 and 3 will be devoted to implementing a suitable modeling strategy for the case of Yucca Mountain, building on the constitutive models reviewed in Chapter 4, and the large-scale modeling approaches reviewed in Chapter 6. The required data for large-scale modeling of flow and tracer transport will be assessed in more detail, building on Chapters 2, 3, and 5.

This report is organized as follows. Chapter 1 introduces the technical and scientific basis of the report. Chapter 2 reviews technical aspects of radioactive and toxic waste contamination, and closes with an analysis of the specific regulatory background and hydrogeologic conditions at the candidate high-level waste repository of Yucca Mountain, Nevada. Chapter 3 examines the effects of heterogeneity on flow and transport based on field observations and experiments. Chapters 4 and 5 define constitutive hydrodynamic models and data requirements for such models. Chapter 4 focuses on the formulation and identification of local parameters for the nonlinear constitutive relations of unsaturated media, while Chapter 5 analyzes large-scale field data in terms of spatial variability and spatial structure. Chapters 2 through 5 include partial reviews of available data, including data directly relevant to the subject site. Chapter 6 is a preliminary review and critical analysis of alternative field-scale flow models in the presence of heterogeneity and fractures. This chapter identifies several areas to be developed for future research. Finally, Chapter 7 recapitulates the main findings and discusses future strategy. An Annotated Bibliography is attached as Appendix. All references quoted in the Appendix as well as in the main text can be found in the overall list of references.

1. INTRODUCTION

This report reviews and develops operational approaches for data analysis and modeling of groundwater flow and radionuclide transport through the deep, partially saturated, inhomogeneous and fractured rock formations of Yucca Mountain, Nevada, the candidate national repository for civilian high-level nuclear waste. Particular attention will be paid to large-scale flow processes in highly heterogeneous, unsaturated or variably saturated, geologic media.

The scientific framework of this particular investigation is subsurface hydrology and porous media hydrodynamics. This field of study is concerned with groundwater flow both below the water table and above the water table, and the transport of contaminants such as radioactive solutes, other toxic solutes, immiscible hydrocarbon liquids, brines, and gases. Subsurface hydrology research has recently become particularly active in the development of generic approaches and experimental designs applicable to the study and modeling of underground toxic waste contamination over large space-time scales. The progress in this area is in response to the increasing public and governmental awareness of environmental pollution problems, either real or potential, due to toxic and radioactive waste disposal sites, particularly in North America, Scandinavia, and parts of Western Europe.

One of the first questions that needs to be addressed in subsurface contamination is the nature of the ambient subsurface flow system. The flow system must be understood in sufficient detail and accuracy in order to obtain reliable simulations and predictions. The next task is then to model the subsurface transport of toxic species within the actual or predicted flow system, based on actual or fictitious release scenarios. The sequence described above assumes the existence of a flow-to-transport hierarchy. This can be justified on physical grounds as follows. It is assumed here as a first approximation that liquid water is the main carrier of toxic species underground, that transport occurs in dissolved form, and that coupling phenomena can be neglected (e.g. groundwater water flow is not affected by variations in concentration or chemical/nuclear reactions of the transported species). Under these assumptions, it becomes clear that the flow system can be studied separately. A study of naturally heterogeneous water flow processes is an essential step towards a better understanding of contaminant transport in complex geologic media. Accordingly, flow processes will be examined here in more comprehensive fashion than mass transport processes. Nonetheless, it should be kept in mind that this report constitutes the first phase of research geared towards modeling large-scale radionuclide transport phenomena.

For purposes of clarity and tractability, the natural complexity of heterogeneous subsurface flow systems can be simplified by separating different types of phenomena. For instance, this report will usually consider separately two distinct types of heterogeneity, the continuous heterogeneity of porous media, and the discontinuous heterogeneity represented by fractures. In addition, two distinct flow regimes will be distinguished, purely saturated flow (in aquifers), and purely unsaturated (in the vadose zone). Nevertheless, this work is concerned with the physics of liquid water flow in the variably saturated regime, which allows for both saturated and unsaturated flow to coexist (e.g. perched water tables).

Purely unsaturated flow processes are, of course, of particular interest in the case of a relatively dry rock repository. Purely saturated flow processes are also worthy of consideration in view of methodological analogies between saturated and unsaturated flow modeling approaches (treatment of heterogeneities and fractures, solution methods, and so on). For these reasons, while this review focuses on the vadose zone, some phenomena and observations pertaining to other types of groundwater systems will also be examined occasionally. Finally, it should be noted that the usual distinction between discontinuous heterogeneity (fracture sets) and continuous heterogeneity (porous medium) can be highly specific and subjective, depending on the particular site, scales of observation, and modeling assumptions. Regardless of the conceptual approach taken, the main goal is to identify and investigate the role of all hydraulically active heterogeneities, and particularly their cumulative effects over large three-dimensional space-time scales.

A screening of the literature indicates that stochastic models may offer the most suitable representation of spatial heterogeneity in natural geologic media. Furthermore, the same stochastic concepts can be used to model the associated flow-transport processes, which are largely inaccessible to observation in their full three-dimensional complexity. Before reviewing field evidence (see for instance Section 2.1 on heterogeneous contaminant migration at actual contamination sites), it will be instructive to give here an overview of recent accomplishments in the mathematical representation and modeling of flow and mass transport phenomena in heterogeneous geologic media.

Stochastic concepts were introduced in the past decade as a means to represent the natural variability of porous formations, such as stratified deposits, fissured soils, and fractured rocks, in a probabilistic framework. In the case of non-fractured media, new statistical formulations of the classical continuum flow and transport equations have been developed and tested. For fractured media, analogous continuum approaches are also being investigated, along with various alternative approaches such as random fracture networks. At the same time, methods of collecting, identifying, and interpreting data also tend to rely more heavily on probabilistic and geostatistical techniques, as can be seen from the increasing literature on this subject (for a recent collection of works on parameter identification in hydrogeology, see Bachu, 1991). In summary, current research in subsurface hydrology is evolving towards increased use of stochastic methods. This follows the earlier evolution of surface hydrology towards stochastic time series analysis (Box and Jenkins, 1976). The stochastic representation of geophysical variability in multidimensional space is comparatively more recent and generalizes some of the techniques previously used for one-dimensional time series. The scientific basis of the stochastic approach to subsurface hydrodynamics and transport is essentially as follows:

(1) Classical quasi-linear equations governing local transport of fluids and species, e.g. Richards equation for unsaturated water flow;

(2) Mathematical theory of random functions of space or random fields, useful in statistical continuum models;

(3) Mathematical theories of geometric probability, e.g. random fracture networks for statistical discontinuum models;

(4) Solution methods for classical and stochastic partial differential equations, e.g. perturbation and probabilistic solution methods;

(5) Homogenization theory and effective transport coefficients for composite and random media, e.g. effective moisture capacity, hydraulic conductivity, and hydrodynamic dispersivity;

(6) Linear estimation and optimization theory, applied to the collection and identification of hydrogeologic data in multidimensional space and time.

In addition, the classical deterministic equations of subsurface hydrodynamics remain at the basis of the stochastic approaches to be considered in this report. In particular, it is assumed throughout that Darcy-type flow equations adequately model flow processes on local scales. Finally, advanced numerical techniques will be required for efficiently solving the flow and transport equations resulting from stochastic approaches (see Chapter 6 for numerical flow simulations). The numerical aspects will be investigated in more detail in subsequent reports.

2. SUBSURFACE CONTAMINATION AND HYDROGEOLOGIC SETTING

2.1 FIELD OBSERVATIONS AT EXISTING SUBSURFACE CONTAMINATION SITES

The current U.S. strategy for future disposal of civilian high-level radioactive waste is burial in relatively dry rock, hundreds of meters below the ground surface and above the water table. At present, to our knowledge, no toxic waste repository of this kind exists on any continent. On the other hand, it has been common practice to dispose of low-level radioactive wastes and other toxic chemicals above the ground or at shallow depths. In addition, liquified toxic wastes and high-level wastes are sometimes stored in tanks on or near the surface. In short, the implication is that the hydrologic flow regime at many existing toxic waste emplacements is predominantly unsaturated or variably saturated. For this reason alone, observations of accidental leakage at toxic and low-level waste sites may be indicative, to a degree, of the possible performance of the unsaturated hydrogeologic barrier envisioned for high-level waste isolation.

Examples of low-level and other hazardous waste sites are landfills, surface impoundments (such as lined evaporation ponds), and uranium mill tailings (buried at shallow depths). Unsaturated zone contamination also occurs in the case of potentially harmful chemicals applied over large surfaces at relatively small concentrations, e.g. in irrigated areas where fertilizers are provided in solution with irrigation waters. Finally, there is evidence of numerous industrial sites where, presumably, leakage of pollutants has taken place and developed primarily in the vadose zone. However, such accidental leakage usually remains undetected until the contaminant reaches a major and extensively monitored groundwater system (observation and pumping wells), and/or until it causes major damages such as diseases and deaths in local communities via contamination of drinking water (e.g. town of Woburn, Massachusetts). In other words, while vadose zone contamination sites are numerous, contaminant migration has rarely been observed in the unsaturated zone per se. Some of the few cases where accidental contamination was actually monitored in the unsaturated zone are discussed below.

In 1973, a major leak of contaminated liquid in unsaturated, stratified glacio-fluvial deposits was detected beneath one of the tanks of the high-level waste liquid storage facility of Hanford, Washington. The total amount that leaked into the vadose zone was estimated at one fifth of the 500,000 gallons (2000 m^3) of high-level radioactive liquid waste initially contained in the tank. The contaminant movement at this site is now being extensively monitored. In 1978, significant radionuclide concentrations were detected as far as 30 meters in depth, and 25 meters laterally from the edge of the tank, (Routson et al., 1979). The vadose zone transport was subsequently simulated numerically by Smoot and Sagar (1990), among others.

Another observation of large-scale vadose zone contamination was reported by Trauntwein et al. (1983) and Kent et al. (1982), in a field study of leakage from a 500 m x 1000 m waste disposal evaporation pond located over a deep, layered clay/sand soil. After twenty years of leakage, water contaminated with organo-metallic compounds reached a depth of 100 meters, and extended laterally over a distance of at least two kilometers in all directions. The surprisingly

large lateral spread could be explained by the presence of horizontal clay lenses, which may have produced perched groundwater zones.

Finally, another study by Purtymum (1973) reported observations of tritium (^3H) contamination near waste storage shafts in dry ashflows of rhyolite tuff. The scale of observation was about 20m vertically and 15m laterally. Soil moisture and tritium data obtained from soil samples indicated lateral movement, especially at the contact between two ashflows.

In addition, a number of large-scale observations of vadose zone transport from controlled experiments and tracer studies are available. These will be discussed later in this report (Chapter 3). Gelhar et al. (1984) reviewed pertinent field observations, including existing contamination sites like the ones discussed above, prior to 1984. However, while the observations reviewed here and in Gelhar et al. (1984) concern the vadose zone, none deals with a contamination site directly analogous, in terms of environment and scales, to the type of repository envisioned for permanent disposal of large quantities of high-level wastes.

According to the concept developed in the U.S., the purpose of a permanent high-level waste geologic repository is to provide a natural and stable barrier to the migration of leaking radionuclides for a time on the order of ten thousand years, i.e. very large by human standards although short in geologic time units. In particular, there must be a proven hydrologic barrier to contaminant migration. A number of options and concepts have been considered for high-level waste disposal in the conterminous United States. One of the initial options which has been studied, then abandoned, is the deep burial of sealed cannisters in saturated formations of very low permeability, such as *unfractured* basalt, tuff, or granite. The option which is now actively studied is the burial of radioactive wastes in very dry unsaturated porous formations located in arid and sparsely populated regions. This option is our main concern here.

Winograd (1981), one of the early proponents of dry or unsaturated geologic repositories, first discussed the possibility of burying high-level wastes at depths of 15 m to 85 m in valley-fill deposits inside the man-made Sedan crater at Yucca Flat, Nevada. In that particular environment, the annual rainfall is only 125 mm/year (5 inches/year) and the water table is about 600 meters deep. The current design investigated by the U.S. Department of Energy (DOE) and the U.S. Nuclear Regulatory Commission (NRC) is the burial of sealed canisters deep inside unsaturated fractured tuffs at Yucca Mountain, Nevada. The climatic conditions and depth to water table at Yucca Mountain are roughly similar to those of the Sedan crater site discussed above.

In his review of the Sedan Crater site, Winograd estimated that the net downward percolation rate (velocity) of water through the unsaturated valley-fill could be on the order of 2 mm/year, i.e., 200 meters per hundred thousand years. Current estimates of net percolation at Yucca Mountain are on the same order (or less). The time unit chosen here is suggestive of the time scale of interest for high-level, slowly decaying radioactive wastes. The implication is that, in order to assess the hydrogeologic performance of the site as a contaminant barrier, the pattern of contaminant migration must be evaluated on space-time scales of hundreds of meters (or kilometers) and millenia (or tens of millenia). Furthermore, this assessment needs to be replicated for several hydroclimatic scenarios. Combining these large-scale requirements with the need to account for spatial heterogeneity and fracturing of Yucca Mountain formations results in challenging problems of data processing and modeling.

The remainder of this report focuses on hydrogeologic observations, experiments, and modeling approaches relevant to the Yucca Mountain site as a potential candidate repository for high-level waste storage. The current regulatory concepts pertaining to hydrogeologic isolation of high-level wastes are analyzed in the next section (Section 2.2). The hydrogeologic characteristics and modeling requirements of the Yucca Mountain site, the main object of this research, will then be discussed in more detail in Section 2.3.

2.2 HIGH-LEVEL WASTE ISOLATION AND REGULATORY ISSUES

The modeling objectives will be better understood through a review of pertinent regulatory issues concerning high-level waste isolation. This section analyses aspects of the current federal regulations pertaining to hydrogeologic isolation of high-level nuclear wastes in permanent geologic repositories, particularly as they relate to *far field* radionuclide transport due to variably saturated liquid water movement in the undisturbed hydrogeologic setting of Yucca Mountain. Non-isothermal processes, liquid/gas phase changes, air movement, complex chemical interactions, and coupled hydro-thermo-mechanical processes will be ignored throughout. On the other hand, large-scale flow and transport processes in the naturally heterogeneous subsurface environment will be emphasized.

The Nuclear Waste Policy Act of 1982 required the NRC to evaluate license application(s) submitted by the DOE to construct and operate a permanent high-level radioactive waste geologic repository. In 1987, the Yucca Mountain site was singled out by Congress, by the Nuclear Waste Policy Amendments Act, as the sole candidate repository for permanent disposal of up to 70,000 tons of high-level nuclear wastes. The waste would be constituted mostly of spent fuel from commercial nuclear power plants. The total quantity of commercial spent fuel anticipated by the year 2020 has been estimated at 100,000 tons (U.S. General Accounting Office, 1988). If licensed, therefore, the candidate repository is destined to store a major fraction of the national stock of commercial high-level wastes.

The regulations issued by the NRC (10 CFR Part 60) and by the U.S. Environmental Protection Agency (EPA Standard 40 CFR Part 191) include criteria to ensure long-term isolation based on a multiple-barrier concept. While the EPA standard relates to overall system performance (see for instance Bonano et al., 1989; and Sagar 1991), the NRC rule contains specific regulations related, in particular, to hydrogeologic isolation.

The NRC regulations in 10 CFR Part 60 require, in particular, that the geologic setting for a high-level waste repository exhibit a combination of conditions that provide reasonable assurance of waste isolation. It must be demonstrated that the hydrogeologic conditions at the repository site strongly inhibit radionuclide transport to the accessible environment. The requirement of reasonable assurance of hydrogeologic waste isolation has been codified by NRC in terms of groundwater travel time (10 CFR 60.113(a)(2)):

> *"The geologic repository shall be located so that pre-waste-emplacement groundwater travel time along the fastest path of likely radionuclide travel from the disturbed zone to the accessible environment shall be at least 1,000 years or such other travel time as may be approved or specified by the Commission."*

Following NRC's definition in 10 CFR Part 60, the term groundwater is understood here to include all water below land surface. The accessible environment includes both the geosphere (atmosphere, land surface, oceans, etc.) and the portion of the lithosphere inside a controlled area. The latter extends laterally at most ten kilometers away from the boundary of the underground facility in all horizontal directions (10 CFR 60.2). But, if radionuclides reach the water table through the unsaturated zone, subsequent transport through the saturated zone may possibly constitute a relatively faster route to the accessible environment. Accordingly, it is implicitly assumed in this report that the water table is equivalent to the accessible environment, an assumption which can be discarded later for purposes of global performance assessment.

Future modification of the 1,000 year rule for travel time was not ruled out by NRC (10 CFR 60.113(b)). The travel time rule quoted above makes implicit use of probabilistic ("likely") terminology. This interpretation of the rule raises a question directly relevant to this project: how "likely" should the fastest path of radionuclide travel time be, for the performance criteria to be met? Another key question concerns the definition and estimation of the fastest radionuclide travel pathway. Compliance with current and/or future environmental standards may possibly require a different formulation of the problem, i.e., characterization of the distribution of travel pathways and of the total mass of radionuclides that will be transported per unit time through each given class or group of pathways. Therefore, in addition to the distribution of travel times, the distribution of radionuclide mass flux densities (mass per unit time crossing a unit area) can possibly be viewed as a meaningful performance criterion. Finally, due to the presence of heterogeneities on many different scales, travel times and other *observables* need to be characterized unambiguously with respect to prescribed scales of averaging in space and time. The latter point, scale dependence, seems essential and has been increasingly addressed in the hydrology literature. The modeling approach to large-scale flow and transport should be selected with the above considerations in mind.

2.3 SITE-SPECIFIC HYDROGEOLOGY AND MODELING ISSUES

In the case of the Yucca Mountain site, the questions raised above are complicated by the highly heterogeneous and nonlinear nature of the subsurface flow processes. It will be useful to summarize here the main aspects of the hydrogeologic conditions prevailing at the site. Yucca Mountain hydrogeologic data will be considered further in subsequent chapters (3, 4, and 5). The annotated bibliography, in the Appendix, discusses a number of publications focused on the specific hydrogeologic properties of the subject site.

The Yucca Mountain site lies within the southern Great Basin, in southeastern Nevada. For a recent collection of works of the geophysical characteristics of the region around the site, see Carr and Yount (1988). The repository zone as envisioned by the DOE would be located deep in unsaturated tuffs of the Topopah Spring unit, about 300 meters below land surface and 250 meters above the water table (see DOE's Site Characterization Plan, 1988: sections 3.9.1, 3.9.2, 3.9.3, and references therein). The hydrogeologic/stratigraphic setting at the repository site is summarized in Table 2-1 from DOE's Site Characterization Plan (Table 3-22, p. 3-139), and is schematically illustrated in Figure 2-1 from the Site Characterization Plan (1988, Figure 3.40) and Figure 2-2, from Peters and Klavetter (1988, Figure 1). The arrows represent hypothetical flow pathways as hypothetical pathways as envisioned by the above-quoted authors. A three-dimensional description of the stratigraphy in the vicinity of the repository, depicted as a series

Table 2-1. Definition of unsaturated zone hydrogeologic units and correlation with rock-stratigraphic units (from DOE Site Characterization Plan, 1988)

Rock-Stratigraphic Unit		Hydrogeologic Unit	Approximate Range of Thickness (m)	Lithology [b]
Alluvium		QAL	0-30	Irregularly distributed surficial deposits of alluvium and colluvium
Paintbrush Tuff	Tiva Canyon Member	TCw	0-150	Moderately to densely welded, devitrified ash-flow tuff
Paintbrush Tuff	Yucca Mountain Member	PTn	20-100	Partially welded to nonwelded, vitric and occasionally divitrified tuffs
Paintbrush Tuff	Pah Canyon Member	PTn	20-100	Partially welded to nonwelded, vitric and occasionally divitrified tuffs
Paintbrush Tuff	Topopah Spring Member	TSw	290-360	Moderately to densely welded, devitrified ash-flow tuffs that are locally lithophysae-rich in the upper part, includes basal vitrophyre
Tuffaceous beds of Calico Hills		CHn: CHnv / CHnz	100-400	Nonwelded to partially welded ash-flow tuffs: Vitric / Zeolitized
Crater Flat Tuff	Prow Pass Member	CHn: CHnv / CHnz	100-400	Nonwelded to partially welded ash-flow tuffs: Vitric / Zeolitized
Crater Flat Tuff	Bullfrog Member	CFu	0-200	Undifferentiated, welded and nonwelded, vitric, devitrified, and zeolitized ash-flow and air-fall tuffs

[a] Sources: Montazer and Wilson (1984) and as noted in footnotes
[b] Lithology summarized from Ortiz et al. (1985).

QAL - Quarternary Alluvium
TCw - Tiva Canyon welded unit
PTn - Paintbrush nonwelded unit
TSw - Topopah Spring welded unit
CHn - Calico Hills nonwelded unit
CHnv - Calico Hills nonwelded vitric unit
CHnz - Calico Hills nonwelded zeolitized unit
CFu - Crater Flat undifferentiated unit

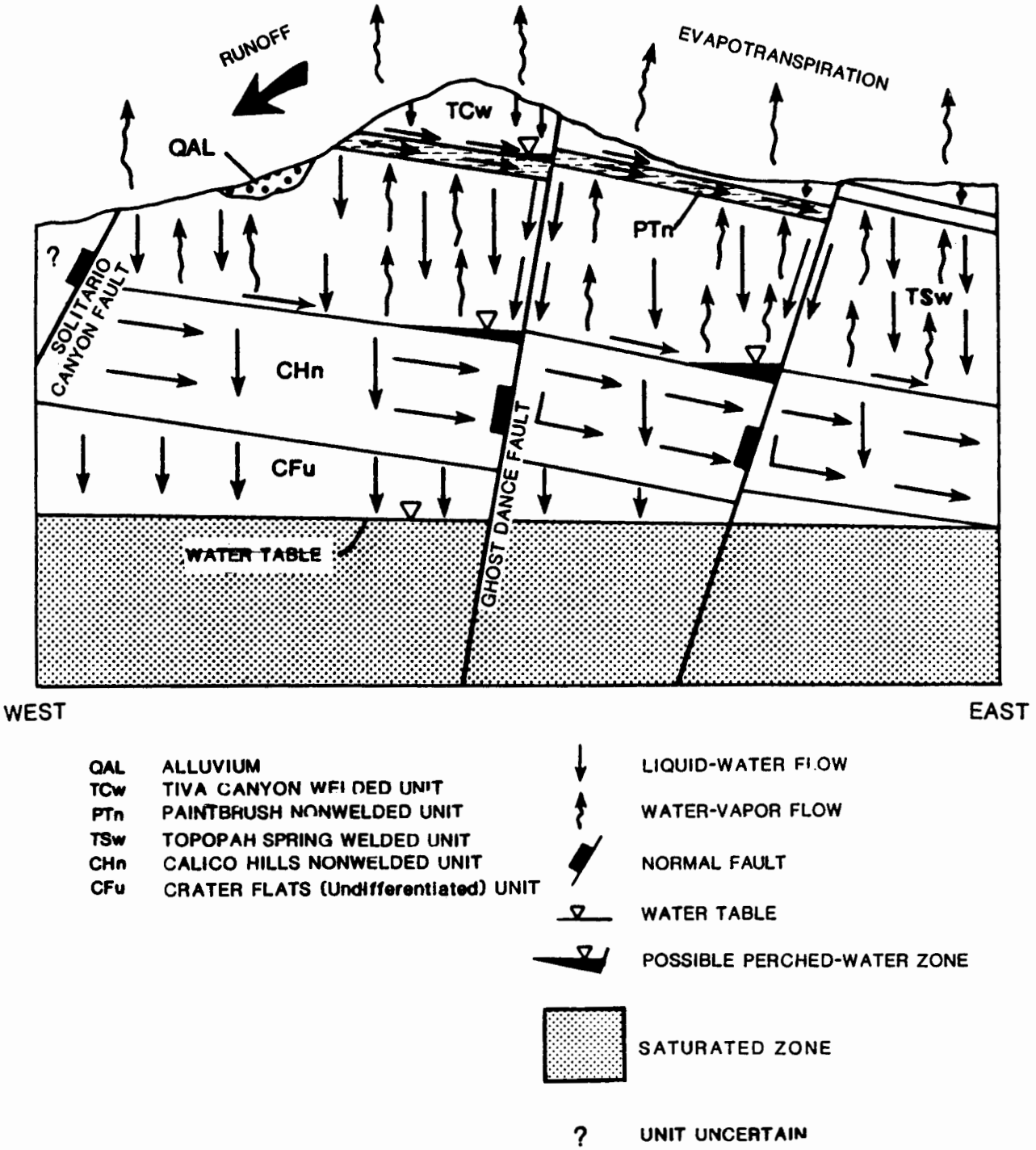

Figure 2-1. Idealized moisture - flow system through East-West section at Yucca Mountain (modified from Montazer and Wilson, 1986, and DOE Site Characterization Plan, 1988)

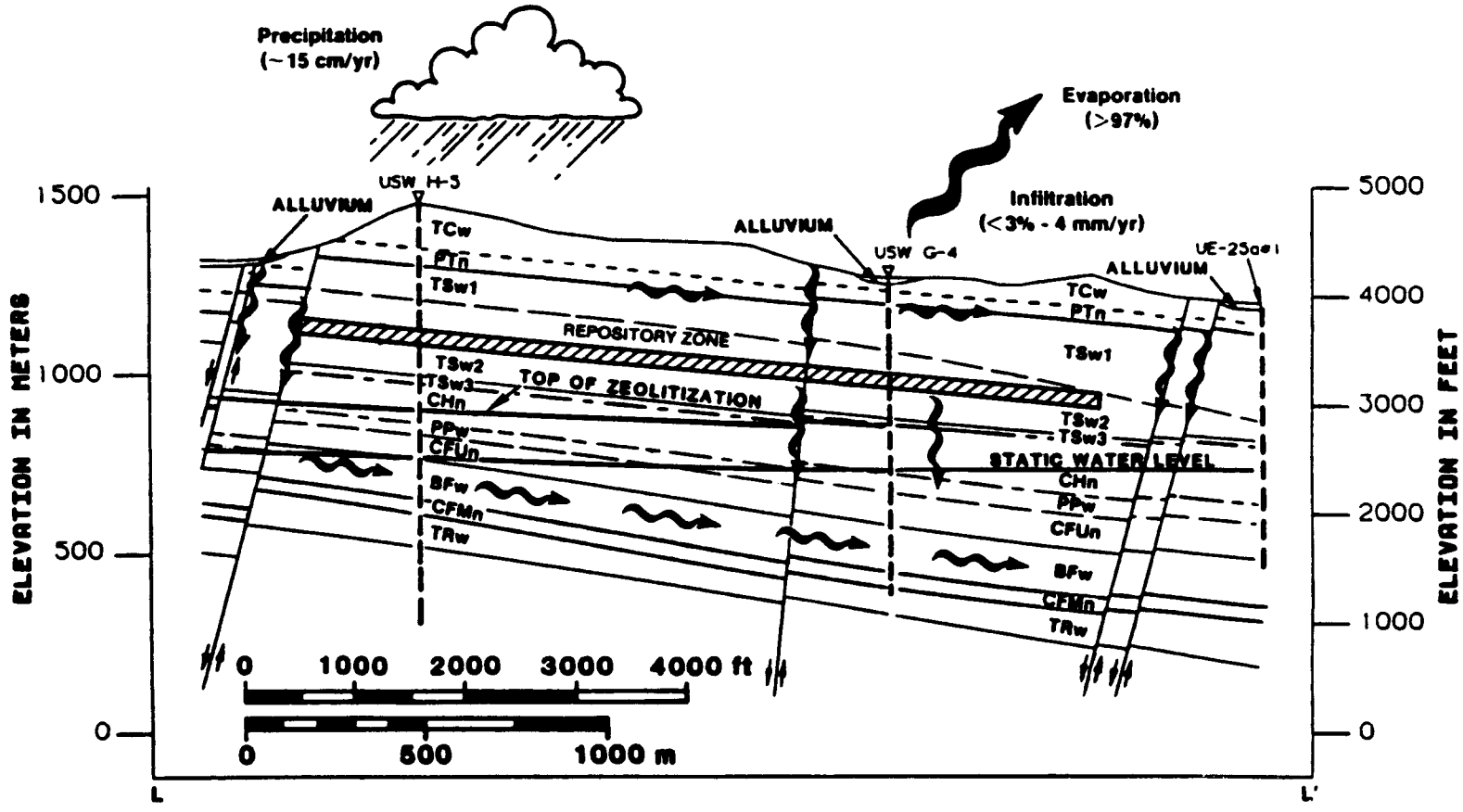

Figure 2-2. Idealized moisture - flow system through East-West Section at Yucca Mountain (from Peters and Klavetter, 1988)

of two-dimensional isopach contours of thickness of geologic units, can be found in the Site Characterization Plan (1988, Figure 3-41, p. 3-198) and in Sinnock et al. (1986).

In addition to the presence of markedly distinct geologic units and tectonic faults, the geologic units are themselves variously fractured. The Topopah Spring unit (TSn) where the repository would be located is a low porosity welded tuff that is believed to be "densely fractured", while the underlying Calico Hills unit (CHn) is a higher porosity nonwelded tuff with seemingly much lower fracture density (Site Characterization Plan, 1988, p.3-144). A variety of quantitative data and qualitative observations on the degree of fracturing and hydraulic conductivity of Yucca Mountain units (both above and below the water table) are available. See the DOE Site Characterization Plan (1988, Section 3.9) and references therein; available hydraulic data are indicated on p. 3-144, pp. 3-181/3-185, pp. 3-197/3-199, pp. 3-203/3-205, and some limited flow simulation results are discussed in pp. 3-209/3-213. Peters et al. (1986b) and Sinnock et al. (1986) implemented one-dimensional models of flow at Yucca Mountain, while Rulon et al. (1986) simulated two-dimensional steady flow based on the vertical cross-sectional grid depicted in Figure 2-3 (from Rulon et al, 1986, and Site Characterization Plan, 1988, Figure 3-45, p. 3-211). In addition, Tables 2-2 and 2-3 from DOE's Site Characterization Plan (1988, Tables 3-26 and 3-27) present a compilation of in-situ and laboratory data on porosity, saturated conductivity, and fracture density within each hydrological unit. Finally other in-situ hydraulic data analogous to Yucca Mountain are available from the G-Tunnel Experiment in partially welded tuff at the Nevada Test Site, Rainier Mesa, Nevada. These data are currently being compiled for the Phase I INTRAVAL report (INTRAVAL*, 1991, Appendix A: G-Tunnel Experiments).

The net annual infiltration from rainfall and surface water over Yucca Mountain is believed to be on the order of 0.1-1.0 mm/year on average, for a mean annual rainfall of about 150 mm/year. Larger values of net infiltration or recharge have also been advanced (4.5 mm/year). About 75 percent of the rain falls over a period of six months, between October and April. For a discussion of available hydroclimatic data, see DOE Site Characterization Plan (1988, pp. 3-203/3-205) and the annotated bibliography (Appendix). It must be emphasized that the mean values given above do not take into account the more extreme rainfall rates that may occur due to interannual fluctuations, interseasonal fluctuations, and individual storms. In addition, they only reflect contemporary rainfall and infiltration conditions. Simplified models of subsurface flow with periodic boundary conditions indicate that fluctuations of infiltration occuring at the surface are damped at depth, and that the damping factor increases with frequency. However, this conclusion is based essentially on a linearized theory, and needs to be confirmed in the case of the nonlinear unsaturated flow equation, particularly in view of the following facts: 1) the ground surface at Yucca Mountain is fractured since the "highly fractured" Tiva Canyon unit crops out throughout most of the repository (Site Characterization Plan, 1988, p. 3-203); 2) rainfall occurs in bursts and the rainfall rate is far from periodic at any time scale accessible to observation; 3) the interactions between rainfall intensity, infiltration, ponding, and runoff are not well understood; and 4) the linear theory of damping applied to the nonlinear unsaturated flow equation may be overly inaccurate under certain conditions such as 1 through 3 above.

---

*INTRAVAL - An International Project to Study Validation of Geosphere Transport Models. Unsaturated Zone Test Cases, in Phase I Final Report. T.J. Nicholson, ed. To be published by Swedish Nuclear Power Inspectorate. Stockholm, Sweden.

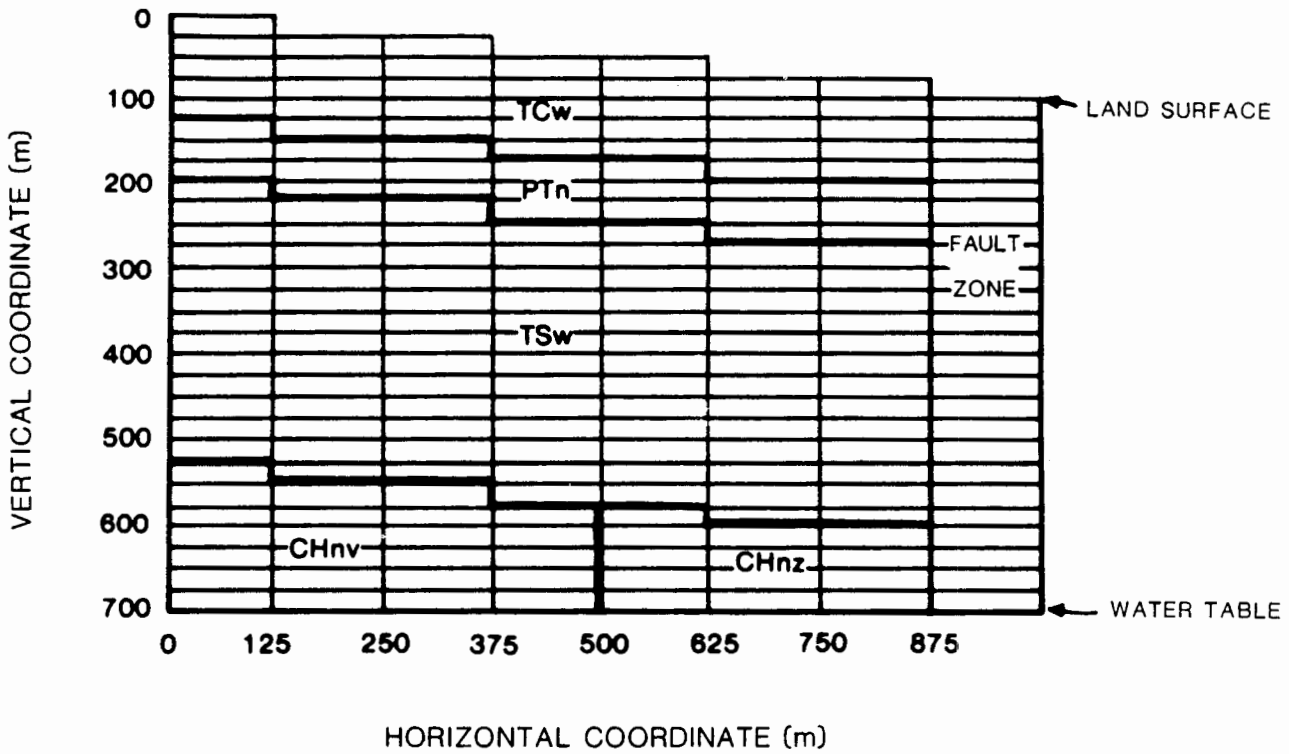

TCw	TIVA CANYON WELDED UNIT
PTn	PAINTBRUSH NONWELDED UNIT
TSw	TOPOPAH SPRING WELDED UNIT
CHnv	CALICO HILLS NONWELDED VITRIC UNIT
CHnz	CALICO HILLS NONWELDED ZEOLITIC UNIT

Figure 2-3. Numerical grid used in the two-dimensional flow simulations (modified from Rulon et al., 1986)

Table 2-2. Summary of compilations of hydrogeologic properties of hydrogeologic units within the unsaturated zone, Yucca Mountain (from DOE Site Characterization Plan, 1988)

Hydro-geologic unit[a]	Source of data	Range of thickness (m)	Grain density (kg/m^3)[b]	Fracture density ($no./m^3$)[c]	Porosity[b]	Saturated matrix hydraulic conductivity (m/s)
TCw	(d)	0-150	ND[f]	10-20	0.12	2×10^{-11}
	(e)	ND	2,490	ND	0.08	9.7×10^{-12}
PTn	(d)	20-100	ND	1	0.46	1×10^{-7}
	(e)	ND	2,350	ND	0.40	3.9×10^{-7}
TSw	(d)	290-360	ND	8-40	0.14	3.5×10^{-11}
	(e)	ND	2,580	ND	0.11	1.9×10^{-11}
CHnv	(d)	100-400	ND	2-3	0.37	5×10^{-8}
	(e)	ND	2,370	ND	0.46	2.7×10^{-7}
CHnz	(d)	100-400	ND	2-3	0.31	9×10^{-11}
	(e)	ND	2,230	ND	0.28	2.0×10^{-11}

[a]Hydrogeologic units are defined on Table 3-22.
[b]See Chapter 2 for more details
[c]Scott et al. (1983).
[d]Montazer and Wilson (1984).
[e]Peters et al. (1984) and Peters et al. (1986b).
[f]ND = no data

Table 2-3. Summary of hydrologic characteristics of major stratigraphic units in the vicinity of Yucca Mountain (from DOE Site Characterization Plan, 1988)

		In situ (field) analyses					Laboratory analyses (cores)					
							Saturated matrix hydraulic conductivity		Matrix porosity[e]			
Stratigraphic unit	Typical character	Saturated thickness (m)	Transmissivity[b] (m^2/d)	Average hydraulic conductivity[c] (m/d)	Well or hole tested	Reference[d]	m/d	No. of samples	%	No. of samples	Well or hole analyzed	Reference[d]
Topopah Spring Member	Moderately to densely welded tuff	167	120	0.7	J-13	7	3×10^{-7} to 2×10^{-4}	5	4 - 33	5	J-13	7
							7×10^{-7} to 5×10^{-4}	18	6 - 30	24	UE-25a#1	1
							8×10^{-7}	1	12	1	UE-25b#1	4
Tuffaceous beds of Calico Hills	Zeolitised, nonwelded tuff, vitric tuff	148	(82)	0.5	UE-25b#1	4	4×10^{-6} to 3×10^{-4}	6	20 - 34	7	UE-25a#1	1
Prow Pass Member of Crater Flat Tuff	Nonwelded to moderately welded tuff	116	167	1.44	USW H-1	2	6×10^{-6} to 1×10^{-4}	3	28 - 29	3	USW H-1	6
		135	150	1.1	USW H-1	6	2×10^{-6} to 1×10^{-3}	8	10 - 25	12	UE-25a#1	1
		174	36 - 142[f]	0.2 - 0.8[f]	USW H-4	9	6×10^{-7} to 1×10^{-3}	5	17 - 30	18	USW G-4	5
		150	(65)	0.4	UE-25b#1	4						
		111	14	0.01	UE-25p#1	3						
Bullfrog Member of Crater Flat Tuff	Nonwelded to densely welded tuff	125	0.8	0.006	USW H-1	6	3×10^{-6} to 1×10^{-3}	10	19 - 34	9	USW H-1	6
		119	70 - 276[f]	0.6 - 2.3[f]	USW H-4	9	2×10^{-4} to 1×10^{-3}	3	17 - 34	3	UE-25a#1	1
		159	(65)	0.4	UE-25b#1	4	2×10^{-4} to 5×10^{-4}	2	24 - 27	6	USW G-4	5
		132	(7)	0.05	UE-25p#1	3						
Tram Member of Crater Flat Tuff	Nonwelded to moderately welded ashflow and bedded tuffs	284	2×10^{-3}	7×10^{-6}	USW H-1	6	4×10^{-6} to 4×10^{-4}	9	18 - 26	9	USW H-1	6
		354	0.7	0.002	USW H-3	8						
		352	70 - 276[f]	0.2 - 0.8[f]	USW H-4	9						
		183	(3.3)	0.02	UE-25p#1	3						
Lithic Ridge Tuff and older tuffs	Partially welded ashfall tuffs	594	0.001	2×10^{-6}	USW H-1	6	6×10^{-5} to 3×10^{-4}	2	9 - 17	2	USW H-1	6
		110	0.1	1×10^{-3}	USW H-3	8						
		371	>10	>0.03	UE-25p#1	3						
Lone Mountain Dolomite and Roberts Mountain Formation	Carbonate rocks Paleosoic age (lower) carbonate aquifer of Winograd and Thordarson, 1975	>561	106	0.2	UE-25p#1	3						

[a]Interpretive analyses from in situ testing at some drillhole not completed yet, including those from drillholes USW G-4, USW H-6, and UE-25c#1, 2, 3.

[b]Determined from pumping tests, borehole-flow surveys, and slug-injection tests; parentheses indicate approximate value because reported values reflect more than one stratigraphic unit. See references cited for details of individual drillholes tested.

[c]Obtained by dividing transmissivity by saturated thickness, which in some cases may not agree with values reported in the cited reference. Productive zones are typically thin, fractured intervals rather than a generally-uniform rock matrix; therefore, the porous-media concept of hydraulic conductivity is not necessarily appropriate.

[d]1. Anderson (1981); 2. Barr (1985); 3. Craig and Robison (1984); 4. Lahoud et al. (1984); 5. Peters et al. (1984); 6. Rush et al. (1984); 7. Thordarson (1983); 8. Thordarson et al. (1984); 9. Whitfield et al. (1985).

[e]DOE's Site Characterization Plan, 1988, Chapter 2: Geoengineering.

[f]Lower value based on straight-line method of pumping-test analysis; higher value based on Theis-recovery method; see Whitfield et al. (1985).

Under the ambient conditions just described, it appears likely that any radionuclides hypothetically released from the repository zone will be transported predominantly in the unsaturated flow regime (stricto sensu). However, locally saturated flow conditions and perched water tables may also occur in the vadose zone, possibly due to short and intense rainfalls, or due to extreme climatic fluctuations on larger time scales. Therefore, in this work, the term "unsaturated" will include partially saturated as well as unsaturated conditions, unless stated otherwise. In addition, this report is concerned with fully three-dimensional groundwater flow systems, characterized by the presence of horizontal as well as vertical flow paths, as both types of pathways may eventually carry radionuclides to the "accessible environment". The possible exit points of transported radionuclides are the lateral compliance boundaries (near horizontal pathways), the regional water table (downward pathways), and the ground surface (upward pathways). Since this investigation is limited to the case of single-phase water flow, upward flow of water vapor and air will not be considered. Upward liquid flow due to surface evaporation can be taken into account within the present framework, but will not be emphasized at this stage. For all practical purposes, the main concerns here will be the horizontal and downward movements of liquid water in variably saturated or unsaturated environments.

Because of the natural heterogeneity, stratification, and fracturing of the porous rock, significant variability of flow and radionuclide pathways and travel times is expected to occur at Yucca Mountain. Formation heterogeneity spans a broad range of scales, from sub-millimeter scales up to dekameter scales. For instance, the effective aperture of hydraulically active fractures is typically on the order of 0.1-1 mm or less. This is obviously much smaller than the meso-scale heterogeneity suggested by the stratigraphic data (thickness of geologic units): the thickness of the fractured and welded Topopah Spring unit (TSw2), where the repository would be located, is over 200 m on average, and the thickness of the non-welded "non-fractured" vitric Calico Hills unit (CHnv), beneath the repository, is about 15 m on average. Furthermore, two major sets of fractures and faults have been identified at Yucca Mountain, the first one striking north-northwest, and the second one striking north-northeast, both steeply dipping to the west (Site Characterization Plan, 1988, pp. 3-184/3-185). The second set is believed to be more open and therefore more conductive (Scott et al., 1983; Erickson and Waddell, 1985), which tends to enhance three-dimensional anisotropy. On the other hand, surface maps of fracture outcrops indicate a positive horizontal trend of fracture density from north to south-southeast, probably owing to the presence of large-displacement faults in the south. Finally, a large-scale negative trend of hydraulic conductivity with depth may occur due to the closing of fractures under increased lithostatic stress. There is at least circumstancial evidence that this may be the case at Yucca Mountain. Rush et al. (1984) confirmed the lithostatic closure of fractures by comparing small core conductivities to pumping test conductivity data at several depths down to 790 m in a deep drill hole.

These diverse scales of anisotropic heterogeneity are to be compared with the global length scales of interest for flow and transport modeling, typically hundreds of meters vertically and on the order of 1-10 kilometers horizontally. The disparity of scales and the inherent three-dimensionality of heterogeneity contribute greatly to the difficulty of modeling such a system. Both large-scale inter-unit heterogeneity and finer sub-unit heterogeneity, including fractures of various orientations, need to be considered for realistic three-dimensional simulations. Indeed, experimental research conducted in the last decade has shown that formation heterogeneity

enhances the large-scale, three-dimensional dispersion of tracer particles transported by water (Gelhar et al. 1984). These observations have been confirmed by theoretical means in idealized cases (Gelhar and Axness 1983, Dagan 1987, Newman 1990, Newman et al. 1990, Ababou and Gelhar 1990). The presence of near horizontal strata or fractures can also increase the horizontal/longitudinal spreading of radionuclides, relative to isotropic porous media. On the other hand, the presence of vertical fractures may lead to contrary effects, depending on ambient moisture and on the interplay between porous rock and fracture hydraulic properties. These are some of the key questions that should be addressed by detailed simulations.

Finally, the occurrence of erratic high-intensity rainfall events can drastically perturb the subsurface flow regime compared to a simple average steady flow model. One possible way to approach the problem is to assume that the shortest significant time scale of climatic inputs to the system is storm duration, typically on the order of hours or less. The storm time scale is significantly smaller than the time scale of the solar cycle (one year), and indeed much smaller than the global time scale of interest for contaminant migration, (10^3-10^4 years or more). A direct numerical approach to hydroclimatic variations at the storm scale would require slicing time very finely and may be overly prohibitive in three spatial dimensions. Yet, the possible effects of intense but short storm events, as opposed to steady inputs, cannot be discounted. It is not known in advance what form of time-averaging can best represent the mean climatic conditions and net infiltration for Yucca Mountain. These simple considerations suggest that short transient effects may have to be addressed separately via simplified modeling (see for instance Wang and Narasimhan, 1985).

2.4 SUMMARY AND OUTLOOK

In summary, realistic modeling of heterogeneous flow and transport processes at Yucca Mountain will require incorporating effects of relatively small scale variability over large scales of simulation. For this reason, particular emphasis will be placed on the use of stochastic models to account for spatial variability in large scale unsaturated flow and radionuclide transport under the hydrogeologic conditions just described. As will be seen, applying a stochastic approach to the Yucca Mountain site requires auxiliary models to represent unknown data, sub-scale phenomena, and separate processes. Efficient numerical implementation is also an essential requirement and an integral part of model development. Indeed, the computational feasibility of the whole approach conditions in part the degree of success that can be achieved by way of stochastic modeling. Last, but not least, the availability of required data also conditions the choice of the detailed modeling approach to a great extent. The reason for using stochastic modeling is precisely to reduce the data requirements while still integrating spatial variability into the picture. Chapters 4 and 5 will specifically analyze hydrodynamic data required for fractured, unsaturated formations, and will suggest methods to define, identify, and process suitable input data for simulation models of the kind envisioned here. The next chapter analyzes currently available observations of groundwater flow and transport processes in the field.

3. FIELD EXPERIMENTS ON FLOW AND TRANSPORT IN HETEROGENEOUS MEDIA

3.1 GENERAL CONSIDERATIONS

As mentioned earlier in Section 2.1, accidental leaks from waste dumps, industrial plants, and other near-surface sources of pollution, contaminate the vadose zone before reaching the water table of local or regional groundwater flow systems. Residence times in the vadose zone can be very large in dry climate, but are usually relatively short, say on the order of years to tens of years, for shallow aquifers and non-arid hydroclimatic environments. Direct quantitative observations of vadose zone contamination sites are relatively sparse; some were described earlier in Section 2.1. On the other hand, a large volume of information is available from extensive monitoring of saturated contaminant transport in a number of groundwater systems worldwide (e.g. Long Island aquifer in New York state, to give one example). Similarly, there is a well established tradition in the area of field-scale modeling of contamination plumes in saturated flow systems.

Although the hydrodynamics of saturated flow systems are qualitatively different from vadose zone processes, it may be instructive to briefly consider the methodological issues that have arisen in that area. The main fact to be recognized is that groundwater velocities are not directly measured in actual engineering practice, even in the case of shallow unconsolidated aquifers. Thus, to *predict* the fate of contaminants in groundwater flow systems requires a reliable simulation of groundwater velocities based on other type of information more readily accessible to measurement. The current engineering practice is a subtle and complex mixture of numerical simulation and model calibration. Most often, the numerical model is based on a coarse-mesh and a two-dimensional, vertically averaged approximation of the governing flow-transport equation. Calibration is typically based on in-situ measurements of past and present hydraulic heads and solute concentrations, in combination with initial estimates of transmissivity from pumping tests, conductivity and dispersivity data from small cores. Qualitative geologic information is also used to various degrees, particularly for zoning the parameters of the coarse-mesh simulation model.

However, this empirical approach has had very limited success in extrapolating (predicting) the fate of contaminants into the future. The review report by Gelhar et al. (1984) contains a comprehensive assessment and interpretation of available field observations of saturated flow transport up to 1983. A major conclusion from their review is that models based on a simple extrapolation of small-scale data, e.g. using "representative" constant values of conductivity and dispersivity from laboratory-scale measurements, often fail to predict phenomena occurring over large space-time scales, particularly concerning the magnitude and degree of anisotropy of contaminant dispersion. In actual practice, contaminant dispersion is found to be scale-dependent, increasing roughly linearly with scale of contamination due to aquifer heterogeneity. This is confirmed by new experimental research on aquifer contamination, which is now oriented increasingly towards large-scale controlled experiments involving detailed three-dimensional measurements of both aquifer properties and contaminant plumes. See for example the natural gradient tracer tests at the Borden aquifer (Sudicky, 1986) and the Twin Lakes aquifer (Moltyaner, 1990).

3.2 TRANSPORT EXPERIMENTS IN UNSATURATED SOILS AND UNCONSOLIDATED MEDIA

Observations in the field (rather than in the laboratory) reveal the complexity of unsaturated flow processes in heterogeneous media. Figure 3-1 shows the spatial structure and evolution of the wetted zone during an infiltration experiment in the Hanford sediments (Routson et al., 1979, Figure 2.5). The wetted zone in this case is remarkably asymmetric and has pronounced lateral spreading. To explain these features statistically requires a model of three-dimensional variability that includes the effects of stratification, e.g., statistical anisotropy.

A number of field plot experiments have been conducted for characterizing the unsaturated hydraulic properties of agricultural soils and the infiltration properties of small watershed. Until recently, however, these experiments were mostly confined to surficial soils, i.e. no more than two meters in depth. Controlled experiments of unsaturated contaminant migration on large three-dimensional domains are limited by serious technical difficulties in measuring water movement and solute concentration in unsaturated media. Gelhar et al. (1984) gives a review of controlled experiments, as well as natural tracer studies and actual contamination site studies, up to the year 1983. (Some of the most interesting observations of real contamination sites were discussed earlier in Section 2.1 and will not be repeated here.) Among the three-dimensional controlled experiments reviewed by Gelhar et al. (1984), only five had scales of observations significantly greater than two meters in depth (6-10 m vertically, and 3-20 m horizontally). One experiment was conducted in a caisson backfilled with excavated sandy material (DePoorter et al., 1982a,b), while the others were conducted by irrigating field plots (Johnston et al., 1983; Mann, 1977; and Supkow, 1974) and groundwater recharge ponds (Prill 1977).

Prill (1977) analyzed moisture contents in layered alluvial deposits, down to 10 meters beneath and 10 meters or more around recharge ponds (15 m in diameter). The initial moisture was low and the application rate was high. Lateral movement was found to be insignificant, while water was detected as far as 10 m beneath the pond. Incidentally, this is to be contrasted with the evaporation pond contamination site discussed earlier (Section 2.1), where vertical movement down to 100 m in depth was accompanied by horizontal movement as far as to 2000 m laterally (Kent et al. 1982; Trauntwein et al., 1983). On the other hand, Johnston et al. (1983) reported considerable differences in vertical flow movement between different parts of a 4.4 m x 2.3 m plot, corresponding in depth to different weathering profiles and to the presence or absence of deep root channels descending from the surface. Where such root channels were absent, no water was conducted beneath the sand and gravel topsoil in spite of the presence of large continuous voids in the underlying weathered profile. Overall, these observations strongly suggest that unsaturated flow and transport processes may be highly sensitive to the interplay between material properties (structure) and hydrologic conditions (moisture contents and flow rates).

New field-scale experiments are now being conducted or initiated for observing three-dimensional unsaturated flow and transport processes in naturally heterogeneous media. The set of three-dimensional strip-source experiments being conducted at the Jornada trench site near Las Cruces, New Mexico, is documented in Wierenga et al. (1986a), Wierenga et al. (1986b), Wierenga

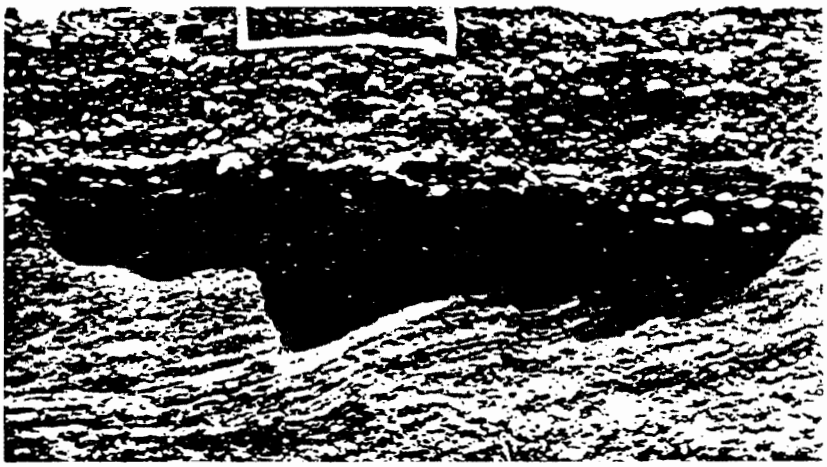

(a) After 6 hours

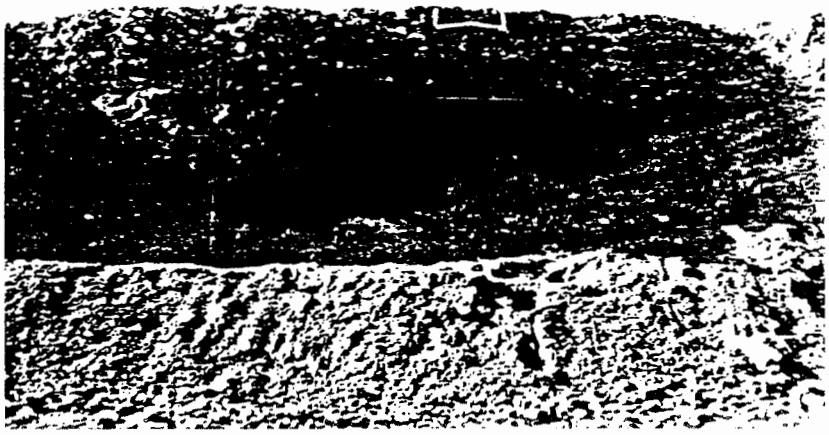

(b) After 24 hours

Figure 3-1. Typical horizontal and vertical movement of liquids in Hanford formation sediments under partially saturated conditions. Taped area outlines position of water addition (Routson et al., 1979).

(1988), Wierenga et al. (1989), and in INTRAVAL* (1991, Appendix C: Las Cruces Trench Experiments). An observation trench 26.5 m long, 4.8 m wide and 6.0 m deep was constructed. In the first strip-source experiment ("Plot 1"), a 9 m long by 4 m wide strip was selected for controlled application of water and tritium tracer through a drip irrigation system. Irrigation was started on May 27, 1987, and ended on June 6, 1987 after eighty-six days of infiltration at a mean daily rate of 17.9 mm/day on the 9 m x 4 m strip. Actually, water was applied four times a day for seventeen minutes per application; the dripper spacings were 15 cm x 15 cm. Direct surface evaporation was prevented by a pond liner cover, although the trench face itself was probably subject to evaporation. Tritium was added to irrigation water from time $t = 0$ (May 27, 1987) and was stopped on June 6, 1987, after ten days of injection. The total millicuries at $t =$ 10 days amounted to 72 mCi for 7200 liters of water, or 0.36 mCi/mm (millicuries per millimeter of applied water); note however that 7200 liters/36 m^2/10 days = 20 mm/day, which differs from the announced mean rate of 17.9 mm/day.

Moisture movement was monitored by visual inspection at the trench face, with an array of tensiometers placed on a 0.5 m x 0.5 m grid on a vertical cross-section located 0.5 m away from the trench wall, and with an array of neutron probes (transverse spacing: 1-2 m; maximum depth: 1.5-6.0 m). The soil was initially dry; the initial moisture content measured by neutron probes was heterogeneous and ranged between five percent and ten percent. At time $t = 86$ days, the moisture plume reached a depth of approximately six meters and extended laterally one meter away from each side of the irrigation strip. The wetting front appeared to be very steep, and there was no sign of preferential flow: see Figure 3-2 from Wierenga (1988, Figure 2). Observations on the advance of the tritium front can be found in Elabd et al. (1988). The natural drainage of the moisture plume was subsequently monitored with the neutron probes (until to date). At time $t = 330$ days, the lateral spread was about 3 m away from each side of the strip, and the moisture plume appeared more heterogeneous (layered) than at earlier times. Figure 3-3 and Figure 3-4 depict contour plots of moisture content up to time $t = 737$ days. Infiltration was stopped at time $t = 86$ days. Moisture migrates under natural gravity drainage conditions from time $t = 86$ days to time $t = 737$ days. A second strip-source experiment with narrower strip-source and more comprehensive tracer studies is under way as part of INTRAVAL Phase II validation studies [see INTRAVAL, 1991, Appendix C (to be published)]. However, the ongoing drainage at the first experimental plot described above is of interest because of the relatively large space-time scales of wetting and draining (roughly 10 m x 10 m x 10 m x 4 years to date).

The ambient moisture at the Jornada site is quite low. Climatic conditions are qualitatively similar to Yucca Mountain (annual rainfall at the Jornada site is 230 mm/year, compared to 150 mm/year at Yucca Mountain). The geologic setting, however is drastically different. The Jornada soil is layered but not distinctly fissured, and does not seem to produce preferential vertical flow, at least for the particular flow rate of the infiltration experiment.

The Jornada strip-source experiment No. 1 has been simulated by a number of methods [INTRAVAL, 1991 (to be published)], including stochastic simulations by Ababou (1988), and

---

*INTRAVAL - An International Project to Study Validation of Geosphere Transport Models. Unsaturated Zone Test Cases, in Phase I Final Report. T.J. Nicholson. Ed. To be published by Swedish Nuclear Power Inspectorate. Stockholm, Sweden.

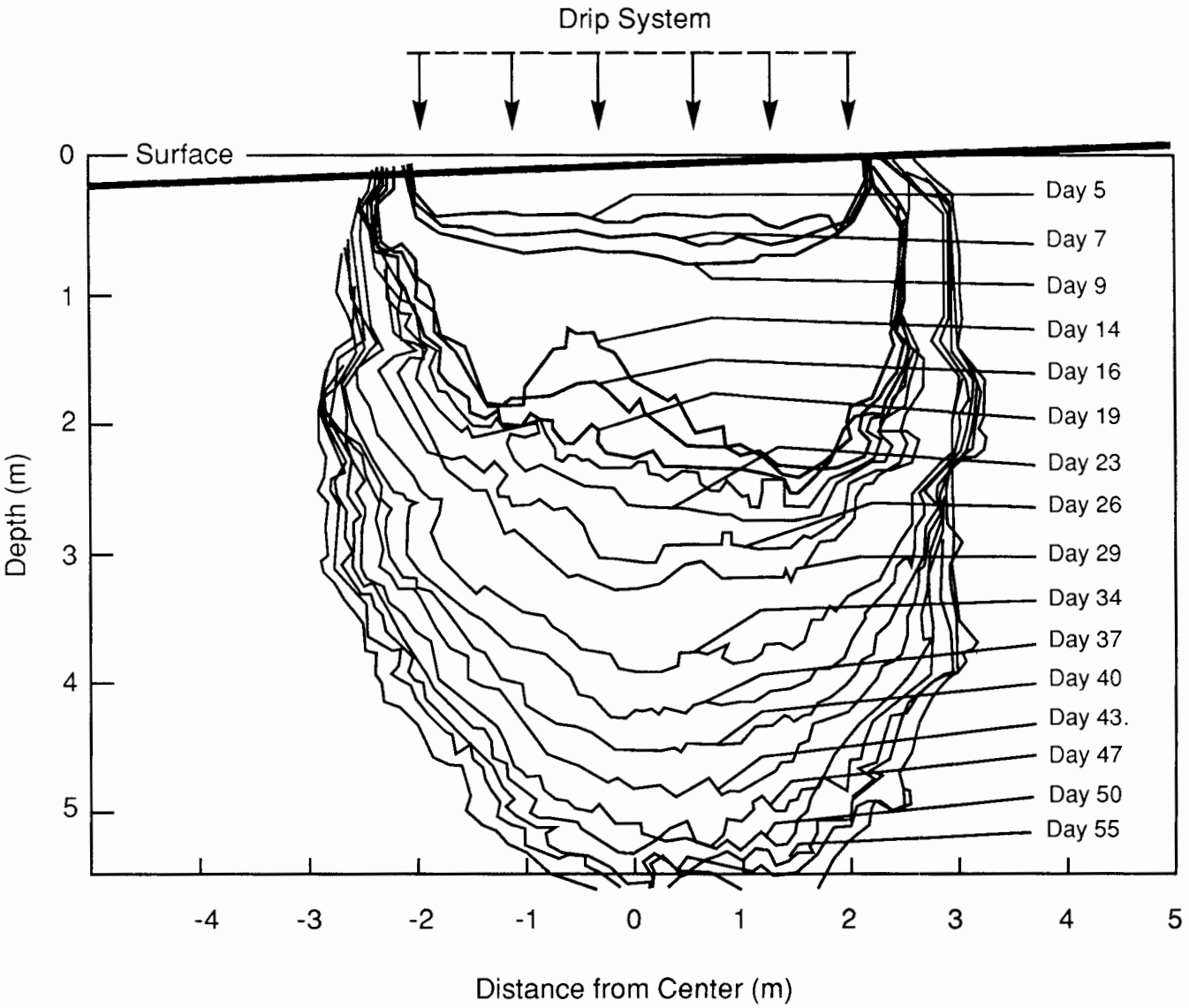

Figure 3-2. Progression of strip-source wetting front up to day 55 as observed on the trench face, Las Cruces Trench Experiment No. 1 (from Wierenga, 1988)

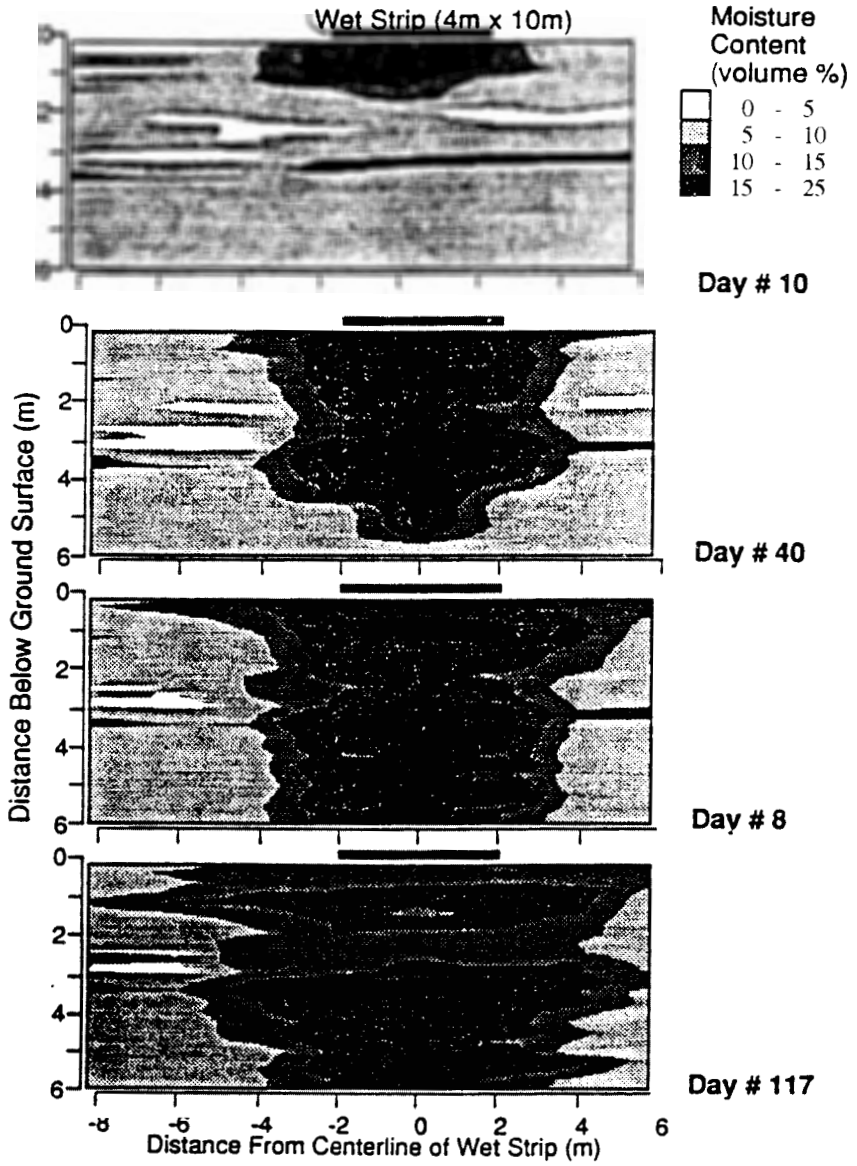

Figure 3-3. **Cross-section profile of water content, from neutron probe readings, during strip-source experiment no. 1 at Las Cruces at Jornada Trench Site (Days 10-117)**

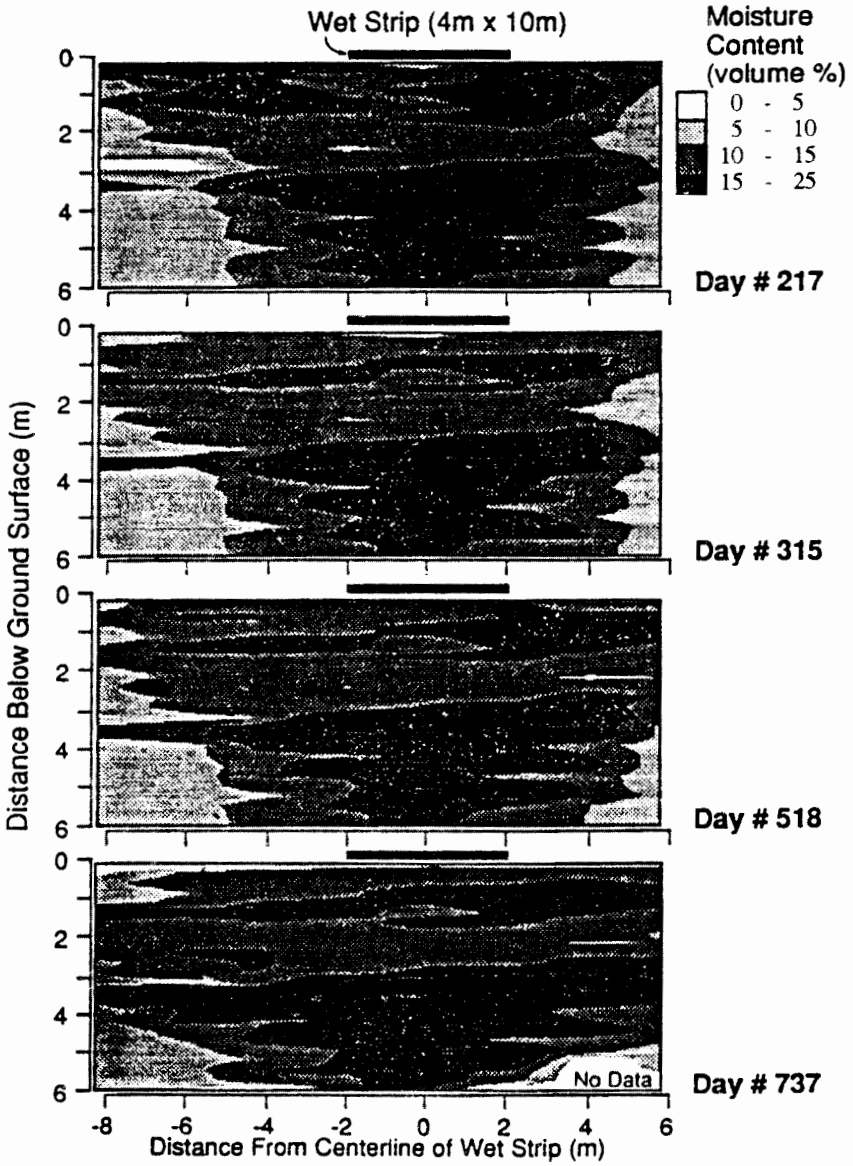

Figure 3-4. **Cross-section profile of water content, from neutron probe readings, during Strip-Source Experiment No. 1 at Las Cruses Jornada Trench Site (Days 217-735)**

Polmann et al. (1988). The latter authors simulated the two-dimensional mean pressure field based on theoretical effective coefficients (Mantoglou and Gelhar, 1987a,b,c), while the former authors used a direct single-realization approach based on three-dimensional random field representation of soil properties. A strip-source moisture plume analogous to the first Jornada trench experiment was simulated and analyzed by inspection of transects and cross-sections of pressure fields (Ababou, 1988). In addition, fully three-dimensional graphic visualizations of moisture plume are presented and discussed by this author in INTRAVAL [1991, Appendix C (to be published)]. To date, it appears that the single-realization unsaturated flow simulation by Ababou (1988) is the only one to represent the effects of three-dimensional soil variability and stratification in detail.

The results of several other three-dimensional unsaturated flow and tracer transport experiments in soils have been reported in the literature, including:

- McCord et al. (1988, 1991) and McCord and Stephens (1989);
- McIntosh (1990);
- Roth et al. (1988), Roth (1989a) and Roth (1989b);
- Stephens et al. (1988) and Bowman et al. (1990).

Some notable features of these experimental investigations are as follows. McCord et al. observed anisotropic behavior of unsaturated flow on a shallow hill-slope sand. McIntosh studied the migration of a tracer plume through a 40 meter thick alluvial deposits and reported several non-classical effects (plume bimodality and variable dispersivity). Roth et al. reported the existence of fast flow paths through a small fraction of soil macropores, as indicated by relatively dense sampling of tracer concentrations from a trench wall. Finally, Stephens et al. reported significant lateral movement after 80 days of a drip irrigation experiment which wetted the soil down to 7 meters vertically and 2-3 meters laterally. These studies are described and discussed in more detail in the Annotated Bibliography (Appendix).

3.3 EXPERIMENTS ON FLOW AND TRANSPORT IN SATURATED FRACTURED ROCKS

In the case of distinctly fractured rock formations, results from a few large-scale experiments on saturated flow and tracer transport are available, particularly from drift experiments in crystalline formations: STRIPA drift experiments in Sweden (Neretnieks et al. 1989), Grimsel drift experiments in Switzerland (see NAGRA Bulletin, 1988), and Faney-Augères drift experiment in a uranium mine in France (see BRGM, 1987, Cacas et al., 1990a&b, Long and Billaux, 1987, and references therein). Since these large experiments concern the saturated flow regime, they will not be discussed in any more detail here. See, however, section 5.4 for comprehensive fracture network data collected at some of these sites, e.g. at the Faney-Augères mine drift.

3.4 OBSERVATIONS OF FLOW AND TRANSPORT IN UNSATURATED FRACTURED ROCKS

A number of uncontrolled experiments have been conducted for observing large-scale flow and migration of environmental tracers in unsaturated fractured formations, including experiments conducted in the vicinity of Yucca Mountain and at the nearby Nevada Test Site. A general source of information concerning field observations in the vicinity of Yucca Mountain is the DOE Site Characterization Plan (1988) and references therein. Two different types of field-scale experiments are analyzed below, one conducted from a tunnel in fractured tuffs at the Nevada Test Site (Russell et al., 1987), and the other conducted at the ground surface on a coastal plain sandstone (Gvirtzman et al., 1988).

In their study of the Rainier Mesa flow system, Russell et al. (1987) monitored flow rates and tracer concentrations in a tunnel located about 500 m above the water table and 400 m below the top of the mesa, which has an altitude of 2200 m on average. This experiment was motivated by the fact that continuous discharge was known to occur at tunnel seeps. Isotopic composition of tunnel discharge was similar to that of present day precipitation, indicating that tunnel discharge water is from recent precipitations. Qualitative correlation between discharge rate fluctuations and precipitation record, based on visual inspection, seemed to indicate a hydraulic response lag time of four months. However, statistical cross-correlation techniques applied to discharge and precipitation records did not show any statistically significant correlation. Alternative methods based on tracers encountered some difficulties as well. Dye tracers applied to the topographic low (Aqueduct Canyon on the mesa) remained undetected at the tunnel seeps for (at least) two years and a quarter. This may be due to the lack of significant winter recharge events during these two years, or simply to the fact that the fractures at the selected site (Aqueduct Canyon) were not connected to the fracture system intercepted by the tunnel. Finally, statistical cross-correlations between stable isotope contents of tunnel water and rainwater did not show correlation at any time lag: tunnel water isotopic composition was in fact quasi-constant in time, perhaps due to mixing, in spite of the observed fluctuations of rainwater composition. This study illustrates some of the difficulties in obtaining quantitative information on variably saturated flow through fractured rocks in-situ. It should be noted that the stratigraphy of the Rainier Mesa is analogous to that of Yucca Mountain. However, recharge is thought to be significantly greater at Rainier Mesa (possibly 15 mm/yr) than at Yucca Mountain (possibly 0.1-1 mm/year).

The uncontrolled natural tracer experiment by Gvirtzman et al. (1988) provides indirect information on the relative role of porous matrix and fissure network in a dry calcareous sandstone under semi-arid conditions (Southern Coastal Plain of Israel). These authors evaluated the annual percolation rates through porous matrix and fissures by comparing 40 meter deep vertical profiles of contemporary tritium and moisture concentrations, with thirty-five year records of rainfall and rainwater tritium content. Bomb tritium can be identified using the known date of atmospheric thermonuclear tests (in the mid-fifties) as a point of reference. Comparison of moisture profile and rainfall record indicated, overall, that evapotranspiration losses reduced the mean annual input to 55 mm/yr, from a mean annual rainfall of 510 mm/yr. The record of net recharge was not known directly. A high anomaly of tritium content was observed at depths of 30-40 meters, just above the water table. This was interpreted as the result of fast flow through eucalyptus root channels in the near surface, and through stratigraphic inhomogeneities in depth.

Based on tritium mass balance on the 30-40 m horizon, Gvirtzman et al. (1988) conclude that about 40 mm/yr of water percolated through the matrix pores at a velocity of 1.1 m/yr, while an additional amount of more than 20 mm/yr percolated faster via root channels and fissure network (with this interpretation, the total amount of net recharge is higher than the 55 mm/yr estimated by moisture content balance down to 40 meters depth). The flow rate and velocity of "pore water" at this site appear to be relatively high compared to the mean annual flow regime at Yucca Mountain.

4. LOCAL HYDRODYNAMIC COEFFICIENTS AND CONSTITUTIVE RELATIONS: CONCEPTS, MODELS, AND DATA

4.1 HYDRAULIC PROPERTIES OF SATURATED POROUS MEDIA

The hydraulic properties of saturated porous media are the saturated hydraulic conductivity K_s (m/s), or the intrinsic permeability k (m^2), and the saturated volumetric water content θ_s (dimensionless). The saturated conductivity is related to permeability by:

$$K_s = \frac{\rho g}{\mu} k = \frac{g}{\nu} k \tag{4.1}$$

where g is the acceleration of gravity, ρ the fluid density, μ its dynamic viscosity, and $\nu = \mu/\rho$ its kinematic viscosity. While K_s is fluid dependent, k is not (permeability k is intrinsic to the porous medium). The saturated water content θ_s is closely related to the porosity, or at least to the accessible porosity p. It will be assumed for all practical purposes that the two concepts are equivalent ($\theta_s \approx p$). Other properties, such as specific storativity are related to the mechanical properties (compressibility) of the fluid and porous medium. These mechanical properties will not be discussed, as they are largely irrelevant for unconfined flow processes occurring in the vadose zone.

The concepts of saturated hydraulic conductivity (or permeability) and saturated water content (or porosity) can be extended to the case of fractured media and fractured/porous media. In general, for fractured/porous media, the hydraulic conductivity is orientation-dependent, e.g., it is a second-rank symmetric tensor, rather than a scalar (more on this below). Assuming for the time being that the medium is locally isotropic, the scalar saturated hydraulic conductivity is identifiable via Darcy's equation (Darcy, 1856):

$$\vec{q} = -K_s \vec{\nabla} H \tag{4.2}$$

where $\vec{q}$ is the specific discharge rate, or flux density per unit area of the porous medium (m/s), and H is the total hydraulic potential or hydraulic head, sum of a pressure potential and gravitational potential, expressed as the equivalent height of a column of water (m). That is:

$$H = \frac{P + \rho g z}{\rho g} \tag{4.3}$$

Finally, an equivalent fluid velocity (by no means equal to the actual pore velocity) is defined by dividing flux by saturated water content:

$$\vec{v} = \vec{q}/\theta_s$$

The "velocity" thus defined characterizes the motion of conservative tracers transported as solutes through the saturated medium. Note that this tracer velocity may be different from, the celerity of a wetting front during downward infiltration. The latter corresponds to the celerity of a

moisture disturbance through the unsaturated medium, while the former corresponds to the (average) velocity of a fluid packet.

In view of the data compiled in the Site Characterization Plan (1988), and by various authors, e.g., Wang and Narasimhan (1988, Table 2), representative values of saturated conductivity in the different stratigraphic units of Yucca Mountain are in the range 1-1000 mm/year, and the porosities are in the range 0.1-0.5. The largest conductivity, as well as porosity, occur in the Paintbrush nonwelded tuff (PTn). Some of the smallest conductivities, as well as porosities occur in the Topopah Spring welded units (TSW1 and 2), and in the Tiva Canyon welded unit (TCw) which crops out at the surface. The Calico Hills nonwelded zeolitic unit (CHnz) underlying the repository has the smallest conductivity (0.5 mm/yr), but a relatively large porosity (0.30). These numbers presumably reflect small core measurements and are considered to represent "matrix properties."

There is, however, great variation within units. For instance, in the welded tuff of the Topopah Spring unit which contains and overlies the repository, there is a range of three orders of magnitude for K_s among eighteen cores collected at Well UE-25a#1 (Site Characterization Plan, 1988, Table 3-27, pp. 3-182). At the same well, measured values of "matrix" porosity ranged between 0.06 and 0.30 among 24 core samples. The K_s values within the nonwelded Calico Hills unit are no less heterogeneous: the range spans two orders of magnitudes among six core samples. Wang and Narasimhan (1988) indicate that, according to geologic logs, the non-welded units are in general more heterogeneous than the welded units. These data are however insufficient to characterize the three-dimensional structure of these heterogeneous hydraulic properties.

Attempts at correlating permeability to porosity have often been unsuccessful, except for synthetic porous media such as glass bead filters, etc. The most widely known formula is the Kozeny-Carman relation, which is based on a semi-empirical model of Poiseuille flow through pore conduits. Expressing the hydraulic diameter of pores in terms of porosity, p, and specific surface area of the solid per unit volume of solid, s_o, leads to the Kozeny-Carman relation (Dullien, 1979):

$$k = \frac{p^3}{5s_o^2(1 - p)^2} \tag{4.4}$$

The Kozeny-Carman formula, being scalar rather than tensorial (i.e. isotropic rather than orientation-dependent) is clearly inapplicable to anisotropic and/or fractured materials. In spite of the recognized failure of Eqn. (4.4) to accurately predict permeability from porosity in natural geologic media, it is suggestive of the general type of relation one should expect: permeability increases with porosity and decreases with specific surface area. Media with high total porosity made of very fine pores can be less conductive than media with smaller total porosity, but coarser pores.

For example, comparing average "matrix properties" of the vitric and zeolitized nonwelded Calico Hill units (CHnv and CHnz) as given by Wang and Narasimhan (1988, Table 2), indicates that the zeolitized unit has approximately the same porosity as the vitric unit but is much less conductive, which suggests a larger specific area of the solid structure. Using Eqns. (4.1) and

(4.4) leads to estimates of s_o, the specific area of solids per unit volumes of solid, and of $\sigma_o = s_o (1 - p)$, the specific area of solids per unit volume of the porous medium. The results, reported in Table 4-1, were obtained by converting all variables to S.I. units (International System units) and inserting the standard values of water viscosity and density at 20 °C. Thus, $K = 10^{-8}$ m/s corresponds to $k = 1.021739 \times 10^{-15}$ m^2, i.e. $k/K = 1.021739 \times 10^{-7}$ K in S.I. units. While the estimates in Table 4-1 are probably very crude, they suggest that the specific area of the zeolitized matrix is one order of magnitude larger than that of the vitric matrix (say 1-10 km^2 per m^3 for the vitric sub-unit, and 10-100 km^2 per m^3 for the zeolitized sub-units). It will be seen in the next section that a tensorial analog to the Kozeny-Carman relation can be obtained for simple fracture systems in tight, impermeable rock matrix.

Table 4-1. Comparison of specific area of solids in vitric and zeolitized sub-units of the nonwelded Calico Hills formation, based on Kozeny-Carman relation

	K mm/yr (m/s)	p	s_o (m^2/m^3)	σ_o (m^2/m^3)
CHnv (vitric)	107.2 ($3.4\ 10^{-9}$)	0.3541	$7.83\ 10^6$	$5.06\ 10^6$
CHnz (zeolitized)	0.535 ($1.7\ 10^{-11}$)	0.3064	$8.30\ 10^7$	$5.76\ 10^7$

4.2 HYDRAULIC PROPERTIES OF SATURATED FRACTURED MEDIA

This section analyzes the effective anisotropic conductivity and porosity in the case of multiple oriented sets of parallel fractures embedded in an impervious rock matrix. Although only steady saturated flow is examined here, a similar approach can also be applied to unsaturated flow under certain conditions (see for instance Section 4.3.2.3). The approach to saturated fracture flow presented below can be generalized, and will be useful in the future to analyze unsaturated matrix fracture flow, although significant modifications of the method will certainly be required.

4.2.1 Approximate Fluid Dynamics of Single Fractures

We discuss here the flow of a liquid through an infinite planar fracture. Consider a single fracture lying in the horizontal plane (x,y). The equations of motion, conservation of mass and momentum, are expressed by the Navier-Stokes equation for a viscous incompressible liquid with constant viscosity:

$$\frac{1}{g}\frac{D\vec{V}}{Dt} = -\frac{1}{\rho g}\vec{\nabla}(p + \rho g z) + \frac{\nu}{g}\vec{\nabla}^2 \cdot \vec{V} = \vec{J} + \frac{\nu}{g}\vec{\nabla}^2 \cdot \vec{V} \tag{4.5}$$

where $\rho g z$ is the potential of external forces (gravity), $\vec{J}$ is the total hydraulic potential gradient with a minus sign (called hydraulic gradient for short), $\vec{\nabla}^2\vec{V}$ is the vector-Laplacian ($\nabla^2 V_x$, $\nabla^2 V_y$, $\nabla^2 V_z$), and $D\vec{V}/Dt$ is defined, for each component, by $DV_x/Dt = \partial V_x/\partial t + \vec{\nabla} \cdot (V_x \vec{V})$, etc. For an incompressible fluid, mass conservation requires $\vec{\nabla} \cdot \vec{V} = 0$, and $D\vec{V}/Dt$ reduces to the material derivative:

$$\frac{D\vec{V}}{Dt} = \frac{\partial \vec{V}}{\partial t} + (\vec{V} \cdot \vec{\nabla})\vec{V} \tag{4.6}$$

The Navier-Stokes equation can be simplified based on the following, clearly stated assumptions:

- The flow is locally quasi-steady, slow and non-turbulent; neglecting both inertial terms and transient effects leads to $D\vec{V}/Dt \approx 0$.
- The partial derivatives of velocity in the (x,y) directions (fracture plane) are negligible with respect to derivatives in the z direction (normal to the fracture plane); in other words spatial velocity fluctuations are slower and smoother along the fracture plane.
- The flow is approximately parallel to the fracture plane: $V_z = 0$.
- The flow is viscous, and satisfies a no-slip boundary condition at the fracture walls: $V_x = V_y = 0$ at $z = \pm (b/2)$, where b represents fracture aperture.

With these simplifications, the resulting equation is easily solved by direct integration along the z-axis. This yields:

$$\vec{V} = \frac{g}{2\nu}\left(\frac{b^2}{4} - z^2\right)\vec{J} \tag{4.7}$$

Since we assumed $V_z = 0$, both the velocity and hydraulic gradient vectors have zero components perpendicular to the fracture. Integrating again along the z-axis yields the average velocity $\vec{v}$ for the fracture:

$$\vec{v} = \frac{b^2}{12}\frac{g}{\nu}\vec{J} \tag{4.8}$$

This result can be extended to the case of a plane fracture with arbitrary orientation with respect to the natural coordinate system (x,y,z) (Figure 4-1). Let (x',y') designate the local coordinate system in the plane of the fracture. The arguments previously used in the (x,y) plane are still valid in the (x',y') plane. So we obtain again Eqn. (4.8), together with:

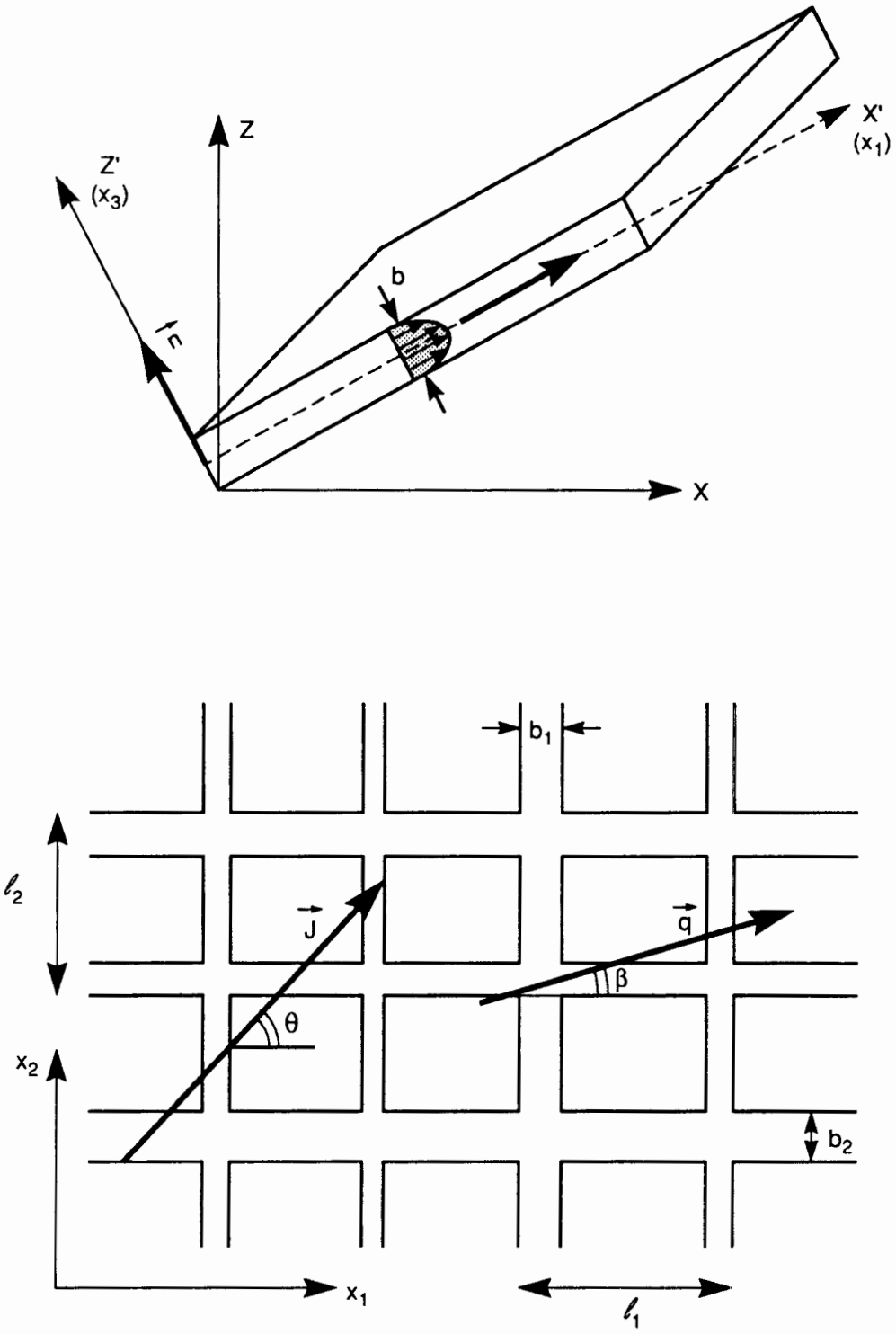

Figure 4-1. **Parallel plate model of single fracture (above) and orthogonal array of fractures (below)**

$$\vec{v} \cdot \vec{n} = \vec{J} \cdot \vec{n} = 0 \tag{4.9}$$

since no flow is allowed perpendicular to the fracture. Here again, $\vec{n}$ is the unit vector normal to the fracture plan. Equations (4.8) and (4.9) correspond to the parallel plate model, which has been widely used in the literature on fracture flow. Note that, since $\vec{v}$ is proportional to b^2, the discharge rate per unit width of fracture is proportional to b^3, whence the name "cubic law" to designate Eqn. (4.8).

4.2.2 Single Set of Parallel Fractures with Variable Spacing and Apertures

The parallel plate model developed above can be applied to a family (set) of parallel fractures embedded in an impervious matrix. The fracture apertures and the spacings between fractures can be variable, e.g. with specified random distributions. However, each individual fracture is assumed, as before, to be a parallel plate of constant aperture. The previous results can be applied to each individual fracture of the parallel set. An average specific discharge for the entire set of parallel fractures is then obtained by simple superposition. This procedure is exact, provided that the rock matrix is impervious, as we assume here.

For a parallel set of N fractures let the total discharge rate per unit fracture width: $\vec{Q} = \Sigma_{k=1}^{N} b_k \vec{v}_k$. Define the average *specific discharge rate* of the fracture set, $\vec{q}$, as follows:

$$\vec{q} = \frac{\vec{Q}}{\Sigma_{k=1}^{N} \ell_k} = \frac{1}{\Sigma \ell_k} \sum b_k \vec{v}_k \tag{4.10a}$$

where ℓ_k represents fracture spacings and b_k fracture apertures ($b_k \ll \ell_k$). Note that the specific discharge rate is an areal flux density per unit area of the fractured medium. Substituting Eqn. (4.8) in (4.10a) gives finally:

$$\vec{q} = \left(\frac{\Sigma b_k^3}{\Sigma \ell_k} \right) \frac{1}{12} \frac{g}{\nu} \vec{J} \tag{4.10b}$$

Furthermore, let us define the mean fracture spacing L and the "cubic-mean" aperture B as follows:

Deterministic Case	Random Case	
$B^3 = \frac{1}{N} \sum_1^N b_k^3$	$B^3 = E(b^3)$	(4.11)
$L = \frac{1}{N} \sum_1^N \ell_k$	$L = E(\ell)$	

This yields the simpler expression:

$$\vec{q} = \frac{B^3}{12L}\frac{g}{\nu}\vec{J} \tag{4.12}$$

In addition, we still require the condition: $\vec{q} \cdot \vec{n} = \vec{J} \cdot \vec{n} = 0$, which expresses that no flow occurs along the direction $\vec{n}$ normal to the fracture set.

4.2.3 Orthogonal Array of Fractures

The previous results are now extended to the case of two parallel fracture sets of infinite lengths intersecting at right angles. It is also assumed that each fracture set is characterized by a whole distribution of apertures and spacings (Figure 4-1). The more general case with non-orthogonal fractures will be treated later in the next section.

Using the previous parallel plate model for calculating the contribution of each set of parallel fractures, and superposing linearly the specific discharges of each set, yields the overall discharge rate for the array of orthogonal fractures. The linear superposition method is an approximation which becomes exact in the special case where the prescribed hydraulic gradient vector is aligned with one of the parallel sets. The (approximate) specific discharge rate for arbitrary orientation of hydraulic gradient is:

$$\begin{aligned} q_1 &= \frac{g}{12\nu}\frac{B_2^3}{L_2}J_1 \\ q_2 &= \frac{g}{12\nu}\frac{B_1^3}{L_1}J_2 \end{aligned} \tag{4.13}$$

where B_i and L_i are the mean fracture aperture and cubic-mean fracture spacing for fracture set No. i (i=1,2), as defined by Eqn. (4.11). Now, let:

$$\vec{q} = \begin{pmatrix} q_1 \\ q_2 \end{pmatrix}; \qquad \vec{J} = \begin{pmatrix} J_1 \\ J_2 \end{pmatrix}; \qquad \frac{q_2}{q_1} = \tan\beta\ ; \qquad \frac{J_2}{J_1} = \tan\theta \tag{4.14}$$

It follows that the direction of flux (β) is related to the direction of hydraulic gradient (θ) by the simple relation:

$$\tan\beta = \left(\frac{B_1}{B_2}\right)^3 \frac{L_2}{L_1}\tan\theta \tag{4.15}$$

Owing to the linear superposition approximation, the discharge rate vector Eqn. (4.13) is related to hydraulic gradient by a linear Darcy-type equation analogous to that of a single fracture. However, the effective Darcy law is now clearly directional (anisotropic). By analogy with the case of anisotropic porous media, the effective permeability tensor $\bar{\bar{k}}$ is such that:

$$\vec{q} = \frac{g}{\nu} \bar{\bar{k}} \cdot \vec{J} \tag{4.16}$$

Moreover, using the coordinate system aligned with fracture sets No. and No. 2, Eqn. (4.13) shows that the effective permeability tensor is given by:

$$\bar{\bar{k}} = \begin{pmatrix} k_{11} & 0 \\ 0 & k_{22} \end{pmatrix} \tag{4.17}$$

with:

$$\begin{aligned} k_{11} &= \frac{1}{12} \frac{B_2^3}{L_2} \\ k_{22} &= \frac{1}{12} \frac{B_1^3}{L_1} \end{aligned} \tag{4.18}$$

The effective anisotropy ratio for this fractured medium is therefore:

$$\frac{k_{11}}{k_{22}} = \left(\frac{B_2}{B_1}\right)^3 \frac{L_1}{L_2} \tag{4.19}$$

It is interesting to note that a 1000-fold increase of permeability can be obtained either by a 1000-fold increase of fracture density or by a 10-fold increase of fracture aperture.

4.2.4 Multiple Sets of Parallel Fractures of Arbitrary Orientations

In this section, the anisotropic effective conductivity is analyzed for a more general fracture network comprising M sets of parallel fractures, each set having a different orientation, aperture distribution, and fracture spacing distribution.

The previous linear superposition method will be used again here. This implies that the driving force acting on liquid movement within each individual fracture is assumed to be constant and equal to the "average" or "far field" hydraulic gradient $\vec{J}$. This approximation tends to neglect interactions between fracture flow geometry and hydraulic head fluctuations. The hydraulic gradient $\vec{J}$ at any point within a given fracture is therefore assumed to be a constant force field with known magnitude and orientation. This approximate method was developed by Snow (1969) to obtain the effective anisotropic conductivity of fracture sets. A similar method was used by Bear and Bachmat (1966, 1967) in their statistical capillary tube model of a porous medium (see Bear, 1972). Shapiro and Bear (1985) later extended Snow's linear superposition method by taking into account the fact that the hydraulic gradient in an individual fracture is generally not the same as the average hydraulic head gradient. Sagar and Runchal (1984) analyzed the case of finite size fractures, which does not lead to a unique and symmetric effective

conductivity tensor. The forthcoming developments follow essentially Snow's approach for infinite fractures.

For a given fracture, the hydraulic gradient $\vec{J}$ is assumed independent of the particular orientation of the individual fracture, and does not necessarily lie in the fracture plane. Therefore, the equation expressing the parallel plate velocity ($\vec{v}$) of an individual fracture must be modified as follows:

$$\vec{v} = \frac{b^2}{12}\frac{g}{\nu}[\vec{J} - (\vec{J}\cdot\vec{n})\vec{n}] = \frac{b^2}{12}\frac{g}{\nu}\vec{J}' \tag{4.20}$$

where $\vec{J}$ denotes that component of the vector $\vec{J}$ that is parallel to the fracture plane. Note that the requirement $\vec{v}\cdot\vec{n} = 0$ is automatically satisfied by Eqn. (4.20) for each individual fracture. This equation can be expressed equivalently as follows using indicial notation:

$$v_i = \frac{b^2}{12}\frac{g}{\nu}[\delta_{ij} - n_i n_j]J_j \tag{4.21}$$

where $\vec{V} = (v_1, v_2, v_3)$ is the average fluid velocity in the individual fracture.

In the case of M intersecting sets of fractures, each set being composed of a series of parallel fractures, the linear superposition approximation leads to:

$$q_i = \frac{1}{12}\frac{g}{\nu}\sum_{m=1}^{M}\frac{B_m^3}{L_m}[\delta_{ij} - n_{i,m}n_{j,m}]J_j = \hat{K}_{ij}J_j \tag{4.22}$$

where q_i is the average discharge rate or areal flux density vector, B_m represents the cubic-mean aperture and L_m is the mean fracture spacing for the mth fracture set, as defined earlier in Eqn. (4.11). In addition, $n_{i,m}$ is the ith component of the unit vector normal to the mth fracture set. The fracture set index, m, runs from 1 through M. Extensions of Eqn. (4.22) to the case of a continuous distribution of fracture orientations is possible; in this case the index m would be replaced by a variable angle between 0 and 2π. In the particular case of rectangular array of cracks with vectors $\vec{J}$, $\vec{q}$ lying in the plane orthogonal to the two sets of cracks, Eqn. (4.22) reduces to the simpler expression given earlier in Eqn. (4.13).

By way of example, we now apply Eqn. (4.22) to the case of two non-orthogonal sets of parallel fractures (M=2). For simplicity, both sets are assumed parallel to the z axis so that the three-dimensional flow problem can be reduced to a planar problem in (x,y). The intersecting fracture sets form an array of parallelogram blocks, as shown in Figure 4-2. The (x,y) axes are chosen such that the fracture sets are inclined at angles $+\alpha$ (set No. 1) and $-\alpha$ (set No. 2) with respect to the x axis. Thus, the normals to these sets are given by the unit vectors:

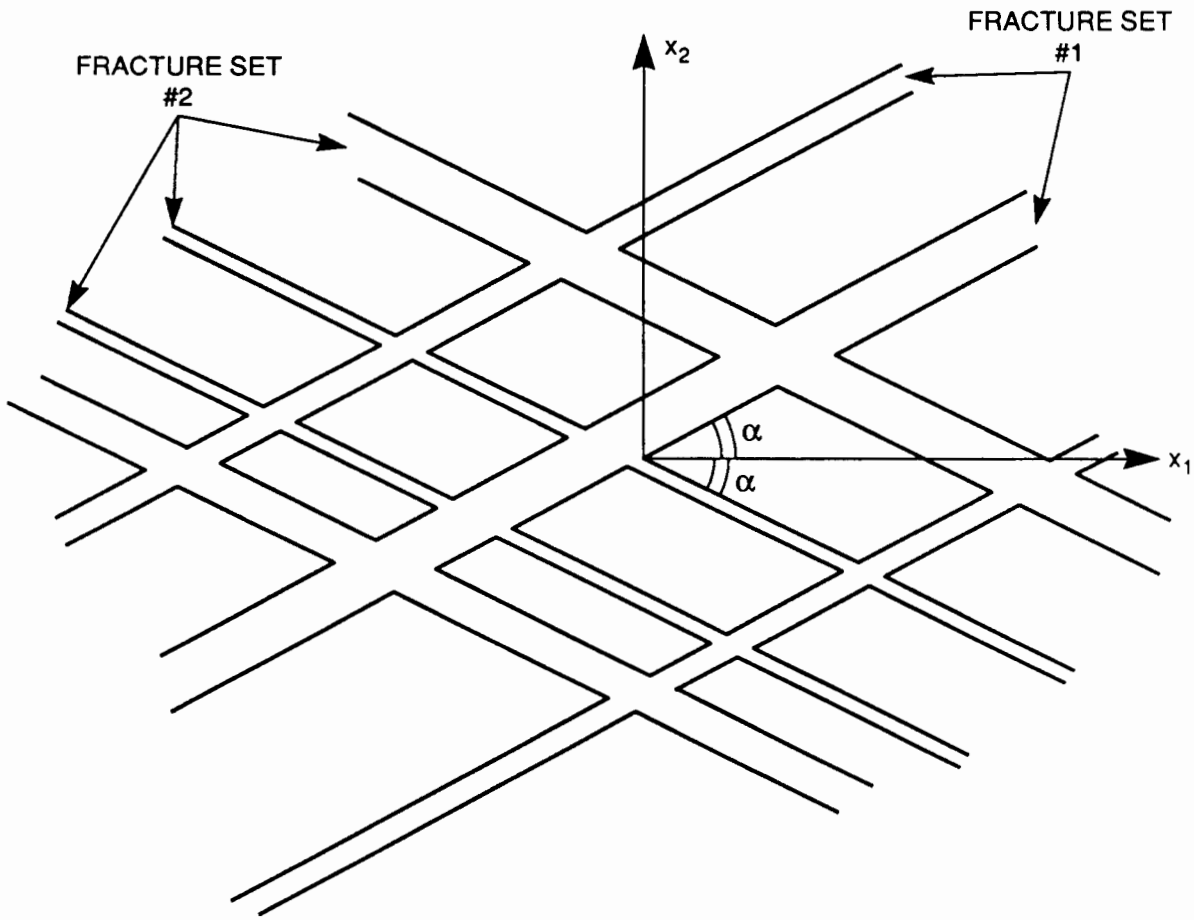

Figure 4-2. Two non-orthogonal sets of parallel fractures with variable apertures and spacings

$$\vec{n}_1 = \begin{pmatrix} -\sin\alpha \\ \cos\alpha \\ 0 \end{pmatrix} ; \qquad \vec{n}_2 = \begin{pmatrix} \sin\alpha \\ \cos\alpha \\ 0 \end{pmatrix} \tag{4.23}$$

From Eqn. (4.22), the general expression of effective conductivity tensor for M fracture sets is:

$$\hat{K}_{ij} = \frac{1}{12} \frac{g}{\nu} \sum_{m=1}^{M} \frac{B_m^3}{L_m} [\delta_{i,j} - n_{i,m} n_{j,m}] \tag{4.24}$$

where the cubic mean aperture for each set (m=1,2) is defined by:

$$B_m^3 = \frac{1}{N_m} \sum_{k=1}^{N_m} b_k^3 \quad \text{or} \quad B_m^3 = E(b_m^3) \tag{4.25a}$$

and the mean fracture spacing for each set (m=1,2) is defined by:

$$L_m = \frac{1}{N_m} \sum_{k=1}^{N_m} \ell_k \quad \text{or} \quad L_m = E(\ell_m) \tag{4.25b}$$

Note that each set is comprised by N_m fractures which can be unequally spaced and can have different apertures. Equation (4.24) clearly shows that the conductivity is a well defined, unique, symmetric, second-rank tensor: this is a result of the analysis, rather than a hypothesis. Here, the fractures were assumed to be of infinite extent. Sagar and Runchal (1984) showed that the conductivity is no longer a unique second rank tensor when finite fracture sizes are considered.

Specializing the previous equations for the problem at hand (Figure 4-2), with i=1 for the x-axis, i=2 for the y-axis, and i=3 for the z-axis, yields the six components of the conductivity tensor as follows:

$$\hat{K}_{11} = \frac{1}{12} \frac{g}{\nu} \left\{ \frac{B_1^3}{L_1} [1 - \sin^2\alpha] + \frac{B_2^3}{L_2} [1 - \sin^2\alpha] \right\} = \frac{1}{12} \frac{g}{\nu} \left\{ \frac{B_1^3}{L_1} + \frac{B_2^3}{L_2} \right\} \cos^2\alpha \tag{4.26a}$$

$$\hat{K}_{22} = \frac{1}{12} \frac{g}{\nu} \left\{ \frac{B_1^3}{L_1} [1 - \cos^2\alpha] + \frac{B_2^3}{L_2} [1 - \cos^2\alpha] \right\} = \frac{1}{12} \frac{g}{\nu} \left\{ \frac{B_1^3}{L_1} + \frac{B_2^3}{L_2} \right\} \sin^2\alpha \tag{4.26b}$$

$$\hat{K}_{33} = \frac{1}{12}\frac{g}{\nu}\left\{\frac{B_1^3}{L_1} + \frac{B_2^3}{L_2}\right\} \tag{4.26c}$$

$$\hat{K}_{13} = \hat{K}_{23} = \hat{K}_{31} = \hat{K}_{32} = 0 \tag{4.26d}$$

$$\hat{K}_{12} = \hat{K}_{21} = \frac{1}{12}\frac{g}{\nu}\frac{1}{2}\left\{\frac{B_1^3}{L_1} - \frac{B_2^3}{L_2}\right\}\sin 2\alpha \tag{4.26e}$$

Alternatively, the permeability tensor $\hat{k}_{ij}$ may be used instead of conductivity. The conductivity tensor is related to the permeability tensor by a relation analogous to Eqn. (4.1), that is:

$$\hat{K}_{ij} = \frac{\rho g}{\mu}\hat{k}_{ij} = \frac{g}{\nu}\hat{k}_{ij} \tag{4.27}$$

According to Eqns. (4.26), the effective permeability tensor is of the form:

$$\hat{k}_{ij} = \begin{bmatrix} \hat{k}_{11} & \hat{k}_{12} & 0 \\ \hat{k}_{21} & \hat{k}_{22} & 0 \\ 0 & 0 & \hat{k}_{33} \end{bmatrix} \tag{4.28}$$

and its non-zero components are given by:

$$\hat{k}_{11} = \frac{1}{12}\left(\frac{B_1^3}{L_1} + \frac{B_2^3}{L_2}\right)\cos^2\alpha \tag{4.29a}$$

$$\hat{k}_{22} = \frac{1}{12}\left(\frac{B_1^3}{L_1} + \frac{B_2^3}{L_2}\right)\sin^2\alpha \tag{4.29b}$$

$$\hat{k}_{12} = \hat{k}_{21} = \frac{1}{24}\left(\frac{B_1^3}{L_1} - \frac{B_2^3}{L_2}\right)\sin 2\alpha \tag{4.29c}$$

$$\hat{k}_{33} = \frac{1}{12}\left(\frac{B_1^3}{L_1} + \frac{B_2^3}{L_2}\right) \tag{4.29d}$$

The form of these equations suggests defining a new quantity k_m, *the effective longitudinal permeability* of fracture set No. m. In view of Eqns. (4.12) and (4.18), we have:

$$k_m = \frac{1}{12}\frac{B_m^3}{L_m} = \frac{1}{12}\frac{E(b_m^3)}{E(\ell_m)} \tag{4.30}$$

Substituting Eqn. (4.39) in Eqn. (4.29) yields a simple expression for the three-dimensional effective permeability tensor:

$$\hat{k}_{ij} = \begin{bmatrix} (k_1 + k_2)\cos^2\alpha & \frac{1}{2}(k_1 - k_2)\sin 2\alpha & 0 \\ \frac{1}{2}(k_1 - k_2)\sin 2\alpha & (k_1 + k_2)\sin^2\alpha & 0 \\ 0 & 0 & (k_1 + k_2) \end{bmatrix} \tag{4.31a}$$

Note that the principal directions of permeability become aligned with (x,y,z) if and only if $k_1 = k_2$. Otherwise, the principal directions must be calculated by rotating (x,y) so as to diagonalize the permeability tensor (axis z is a principal direction and need not be transformed). Let (x_1',x_2',x_3') designate the principal coordinate system where the permeability tensor becomes diagonal. We already know that $x_3' = x_3$. The angle γ between x_1 and x_1', defined as the rotation angle that transforms x_1 into x_1', is given by Bear (1972, Eqn. 5.6.14):

$$\tan 2\gamma = \frac{2k_{12}}{k_{11} - k_{22}} \tag{4.31b}$$

Inserting the tensor components of Eqn. (4.31a) in Eqn. (4.31b) gives, after some manipulations:

$$\tan 2\gamma = \frac{k_1 - k_2}{k_1 + k_2}\tan 2\alpha \tag{4.31c}$$

The principal permeability components, $\hat{k}_{ij}'$, are (Bear 1972, Eqn. 5.6.22):

$$\begin{aligned} k_{11}' &= \frac{k_{11} + k_{22}}{2} + \left[\left(\frac{k_{11} - k_{22}}{2}\right)^2 + k_{12}^2\right]^{1/2} \\ k_{22}' &= \frac{k_{11} + k_{22}}{2} - \left[\left(\frac{k_{11} - k_{22}}{2}\right)^2 + k_{12}^2\right]^{1/2} \end{aligned} \tag{4.31d}$$

Inserting the tensor component $\hat{k}_{ij}$ of Eqn. (4.31a) in Eqn. (4.31d) gives, after a few manipulations:

$$k_{11} = \frac{1}{2}(k_1 + k_2) + \frac{1}{2}[(k_1 + k_2)^2 - 4k_1k_2 \sin^2 2\alpha]^{1/2}$$

$$k_{22} = \frac{1}{2}(k_1 + k_2) - \frac{1}{2}[(k_1 + k_2)^2 - 4k_1k_2 \sin^2 2\alpha]^{1/2} \tag{4.31e}$$

In the special case $k_1 = k_2 = k$, the coordinate system of Figure 4-2 is the principal coordinate system, and we have:

$$\hat{k}_{ij} = \begin{bmatrix} 2k\cos^2\alpha & 0 & 0 \\ 0 & 2k\sin^2\alpha & 0 \\ 0 & 0 & 2k \end{bmatrix} \tag{4.32}$$

Finally, observe that $\alpha = 45°$ corresponds to the special case of an orthogonal array of fractures, which was treated earlier.

4.2.5 Kozeny-Carman Relation for Fracture Networks

Finally, it is now shown that the permeability tensor given by Eqns. (4.31) has the form of a Kozeny-Carman relation generalized to the anisotropic case. For each fracture set #m (m = 1,2), let us define the specific area of voids per volume of medium (σ_m) and the porosity (p_m) due to that fracture set alone:

$$\sigma_m = \frac{2}{L_m}$$

$$p_m = \frac{B_m}{L_m} \tag{4.33}$$

The total specific area and porosity of the fractured medium is then obtained by collecting the contributions of the two fracture sets, as follows:

$$\sigma_o = 2\frac{(1 + 1)}{(L_1 + L_2)} = \frac{4}{L_1 + L_2}$$

$$p = \frac{B_1 + B_2}{L_1 + L_2} \tag{4.34}$$

Comparing Eqns. (4.33) and (4.34) to Eqn. (4.30), the effective longitudinal permeability k_m can be expressed in terms of the partial porosity and specific area of fracture set No. m:

$$k_m = \frac{4p_m^3}{\sigma_m^2} = \frac{4p_m^3}{s_m^2(1 - p_m)^2} \tag{4.35}$$

where s_m is the specific area of fracture set No. m per volume of solid. Note that Eqn. (4.35) is analogous to the Kozeny-Carman relation (4.4). But since the principal components of the permeability tensor depend on both $(k_1 + k_2)$ and $(k_1 - k_2)$, it can be concluded that the permeability tensor of a fractured medium depends on the partial porosities p_m, specific areas σ_m, and orientations of *each set* of parallel fractures, and does not depend directly on the total porosity and total specific area given by Eqn. (4.34). With this provision, Eqns. (4.31) through (4.35) can be considered as a tensorial generalization of Kozeny-Carman for fractured media. Moreover, a similar behavior may be expected for unsaturated flow. In that case, the whole pressure-dependent conductivity curve would be anisotropic, and each conductivity component would be related to the partial porosities and partial specific areas of all fracture sets.

4.3 HYDRAULIC PROPERTIES OF UNSATURATED POROUS MEDIA

4.3.1 Equations and Constitutive Relations

The Darcy equation (Darcy, 1856) was extended by Buckingham (1907) and Richards (1931) to the case of unsaturated flow, assuming that the movement of the air phase has no effect on liquid flow and that air is freely connected to the atmosphere. For isotropic media, the Darcy-Buckingham equation takes the form:

$$\vec{q} = -K(h)\vec{\nabla}(h + z) \tag{4.36}$$

where $h = P/\rho g$ is the water pressure head relative to atmosphere air pressure, $h + z = H$ is hydraulic head, z is vertical upwards, and $K(h)$ is the unsaturated hydraulic conductivity, which can be decomposed as follows:

$$K = K(h) = K_s \cdot K_r(h) \tag{4.37}$$

where $K_r(h)$ denotes the "relative" unsaturated conductivity function. Since $0 \le K \le K_s$, it follows that $0 \le K_r \le 1$.

On the other hand, mass conservation requires that the rate of change of moisture content match the divergence of flux. That is:

$$\frac{\partial\theta}{\partial t} = -\vec{\nabla} \cdot \vec{q} = +\vec{\nabla}(K(h)\vec{\nabla}(h + z)) \tag{4.38}$$

Since there are two unknowns for only one equation, a second constitutive relation is needed for moisture content as a function of pressure head:

$$\theta = \theta(h) = \theta_r + (\theta_s - \theta_r)S(h) \tag{4.39}$$

In this equation, θ represents the volumetric moisture conent (m^3 water per m^3 medium), θ_s is the saturated water content (which was assumed earlier to be equivalent to porosity), θ_r is the residual water content, and S represents the degree of saturation. Since $\theta_r \leq \theta \leq \theta_s$, it follows that $0 \leq S \leq 1$. Note that the concept of "residual water content" is not well defined and can be interpreted in various ways. At infinitely large negative pressure potential ($h \rightarrow -\infty$) it is expected that $\theta \rightarrow 0$, i.e. the residual water content should be zero. However, θ_r is often used as an adjustment parameter for fitting curves of the form (4.39) to experimental data within limited ranges of pressure head.

The specific moisture capacity is defined by:

$$C(h) = \frac{\partial \theta}{\partial h} \tag{4.40}$$

This coefficient appears in the h-based version of the unsaturated flow equation (4.38), or Richards equation:

$$C(h)\frac{\partial h}{\partial t} = \vec{\nabla}(K(h)\vec{\nabla}(h + z)) \tag{4.41}$$

On the other hand, the moisture diffusivity:

$$D(h) = \frac{K(h)}{C(h)} \tag{4.42}$$

appears in the θ-based version of the unsaturated flow equation, that is:

$$\frac{\partial \theta}{\partial t} = \vec{\nabla}(D(\theta)\vec{\nabla}h + K(\theta)\vec{\nabla}z) \tag{4.43}$$

where $D(\theta) = D(h(\theta))$ and $K(\theta) = K(h(\theta))$. It is important to recognize that the latter equation cannot be used to model partially saturated flow with both positive and negative pressures. No such restriction exists for Eqns. (4.38) and (4.41). The mixed-variable equation (4.38) is preferred for numerical models, due to its mass-conservative form (e.g. Ababou, 1988).

Finally, in the case of anisotropic media, the unsaturated conductivity function is expected to be generally direction-dependent. A simple extension of the Darcy-Buckingham equation (4.36) would be to assume that conductivity is a pressure-dependent tensor, that is:

$$\vec{q} = -\,\overline{\overline{K}}(h) \cdot \vec{\nabla}(h + z) \tag{4.44a}$$

or, using indicial notations along with Einstein's rule of implicit summation over repeated indices:

$$q_i = - K_{ij}(h) \cdot \frac{\partial}{\partial x_i} (h + z) \tag{4.44b}$$

However, this may be too restrictive. Other types of orientation-dependent conductivity functions may be more realistic. Consider for instance the case where both K_s and $K_r(h)$ depend, separately, on the orientation of hydraulic gradient. If both K_s and $K_r(h)$ are second-rank tensors, then $K(h) = K_s K_r (h)$ will not necessarily be a second-rank tensor. One possible point of view is that $K(h)$ is approximately a second-rank tensor, as well as $K_s = K(\theta)$. Adopting this point of view precludes the use of a tensor for *relative* conductivity.

Several functional forms of isotropic $K(h)$ and $\theta(h)$ have been proposed in the literature, some based on semi-empirical models of unsaturated flow through idealized porous media. The functional forms to be discussed below include the exponential Gardner model for $K(h)$, the Burdine and Mualem functional models for $K(\theta)$ and $K(h)$, the van Genuchten model for $\theta(h)$, the Brooks-Corey model for $\theta(h)$, and combinations of van Genuchten and Brooks-Corey with the Mualem functional model. In addition, the possibility of extending Kozeny-Carman for unsaturated media will be discussed.

4.3.2 Log-Conductivity Slope and Exponential Conductivity Model

The exponential conductivity model was initially proposed by Gardner and later used extensively by Philip and others to obtain analytical solutions of nonlinear infiltration equations (Philip, 1969; Warrick and Lomen, 1976). Ignoring spatial variability here, the exponential model is:

$$\begin{aligned} K(h) &= K_s \exp\{\alpha(h - h_b)\} && \text{if } h \le h_b \\ K(h) &= K_s && \text{if } h \ge h_b \end{aligned} \tag{4.45}$$

The most interesting property of this model resides in the fact that the slope α of log-conductivity versus pressure has a physical meaning, related to pore size distribution. For pressures less than the air entry pressure (bubbling pressure h_b) the model stipulates that:

$$\frac{\partial \ln K}{\partial h} = \alpha = \text{constant} \tag{4.46}$$

As a consequence, the exponential conductivity model satisfies several interesting properties examined below.

4.3.2.1 Kirchhoff Transform

Following Kirchhoff (1894), an integral transform has been widely used to simplify the task of solving unsaturated flow equations analytically (Philip, 1969; Raats, 1971; and others) as well as numerically (Brandt et al., 1971; Vauclin et al., 1979; Ababou, 1981). The Kirchhoff transform is defined by:

$$U(h) = \int_{-\infty}^{h} K(h')\,dh' \tag{4.47}$$

With the exponential model, this yields for $h \leq h_b$:

$$U(h) = \frac{1}{\alpha} K(h) \tag{4.48}$$

For steady flow, this transform leads to a particularly attractive, fully linear equation:

$$\nabla^2 U - \alpha \vec{\nabla} U \cdot \vec{\nabla} z = 0 \tag{4.49}$$

which can be solved analytically. Unfortunately, the transient flow equation is nonlinear. Furthermore, a one-to-one Kirchhoff transform cannot be defined for the case of a spatially variable relative conductivity curve in multidimensional space (which is the case of interest in this report).

4.3.2.2 Gravity-Driven Advection and Peclet Number

Ababou (1990b) indicates that the θ-based equation can be cast in the form:

$$\frac{\partial \theta}{\partial t} + \vec{V} \cdot \vec{\nabla} \theta = \vec{\nabla}(D \vec{\nabla} \theta) \tag{4.50}$$

where $\vec{V}$ represents the velocity of moisture disturbances, given by:

$$\vec{V} = -\frac{\partial K}{\partial \theta} \cdot \vec{\nabla} z \tag{4.51}$$

But, using Eqns. (4.40), (4.42), and (4.46), it turns out that $\vec{V}$ can be expressed alternatively as:

$$\vec{V} = -\alpha D \vec{\nabla} z \tag{4.52}$$

Therefore, the log-conductivity slope has the form:

$$\alpha = -\frac{\vec{V} \cdot \vec{\nabla} z}{D |\vec{\nabla} z|^2} \tag{4.53}$$

where $\vec{V}_z = (0,0,1)$ if the chosen coordinate system coincides with the natural system (x,y,z, with z vertical upwards). Equation (4.53) shows that α indicates the magnitude of gravity-driven advection relative to diffusion. Advection can also be characterized by a dimensionless Peclet number (actually a vector), $\vec{Pe} = \vec{V} L/D$, where L is a characteristic length scale. Inserting (4.52) yields

$$\vec{Pe} = -\alpha L \vec{\nabla} z \tag{4.54a}$$

On the other hand, going back to Eqn. (4.53), it can be seen that the moisture diffusion coefficient D is proportional to "velocity" times a length scale equal to the inverse of α. By analogy with dispersive transport, this suggests that:

$$\lambda_c = \frac{1}{\alpha} \tag{4.54b}$$

is a *capillary dispersivity* length scale. Intuitively, this is the length scale of dispersion of moisture around a moving moisture disturbance traveling at velocity $\vec{V}$. For alternative interpretations of λ_c, see White and Sully (1987, 1988).

4.3.2.3 Correlation of Unsaturated Log-Conductivity Slope with Other Parameters

Ababou (1981) investigated the relation between unsaturated log-conductivity slope (α) and saturated conductivity (K_s) among different types of soils. The results for nine soils are reported in Table 4-2 and Figure 4-3 (modified from Ababou, 1981, Table II and Figure 4). See also Bresler (1978) for a list of α-values from repacked laboratory soils and granular media. Figure 4-3 depicts a semi-log plot of α versus ϕ, the fine granulometry fraction (0 to 50 microns). An empirical relation:

$$\alpha \ (\mathrm{cm}^{-1}) \approx 0.104 \ x \ 10^{-1.313\phi} \tag{4.55}$$

was obtained by linear semi-log regression, with a correlation coefficient of 0.94. However, this empirical relation correlates α and ϕ values sampled from different sites, rather than within-site. For a given site, it is expected on physical grounds that α is in fact a function of pore size distribution, as well as pore structure (topology). This seems to be supported by the results of White and Sully (1987, 1988). These authors obtained a nearly linear relation between α and particle size among several repacked soils having narrow particle size distributions. In the case of fissured or fractured rocks, the effective (bulk) value of α would also be a function of fracture aperture distributions and fracture network topology, and would also depend on the direction of flow. Auxiliary models describing these relations would lead to a reduction of data collection requirements.

On the other hand, Ababou (1988, 1991) proposed a random field model of unsaturated conductivity with partial correlation between $\ln K$-slope (α) and saturated conductivity (K_s), thereby generalizing previous stochastic models by Yeh et al. (1985a,b,c), Mantoglou and Gelhar (1987a,b,c) and Yeh (1989). It may be instructive to examine whether such a correlation exists in an idealized model of fissured rock. Briefly, consider the case of a single set of parallel fractures having different apertures (b_i) and spacings (ℓ_i). Based on parallel plate theory [see Eqn. (4.12)], the saturated conductivity parallel to the fracture set is given by:

$$K_s = \frac{B^3}{12L} \frac{g}{\nu} \tag{4.56}$$

Table 4-2. Comparison of grain size distributions and log-conductivity slope for nine soils (modified after Ababou, 1981)

Soil	Sources	Clay Fraction (A) 0 - 2μ	Fine Particles Fraction (ϕ)	α (cm^{-1})
Dieri Sand (S.Di) 0-130 cm	Vachaud et al., 1978	0.014	0.05	.1124
Grenoble Sand (S.G.) (disturbed)	Touma, 1981 (personal communication)	0.000	0.01	.0989
Rabat Sand (S.R.) 0-50 cm	Ababou, 1982	0.075 ± .015	0.16 ± 0.03	.09
Dek Sand (S.De) 0-150 cm	Hamon, 1980	0.08 ± 0.01	0.18	.073
Nahal Sand (S.Na)	Brandt et al., 1971 Bresler, 1975	0.01	0.03	.065
Troup Loamy sand (TLS) Horizon Ap (0-24 cm)	Dane, 1980	0.032	0.165	.05
Yolo Fine Sandy Loam (YFSL) (disturbed)	Moore, 1939 Mualem, 1976	0.177	0.49	.025
Gilat loam (G.L.) (disturbed)	Brandt et al., 1971 Bresler, 1975	0.20	0.52	.025
Loess MC 4 0-50 cm (disturbed)	Freslon, 1980	0.105	0.61	.0128

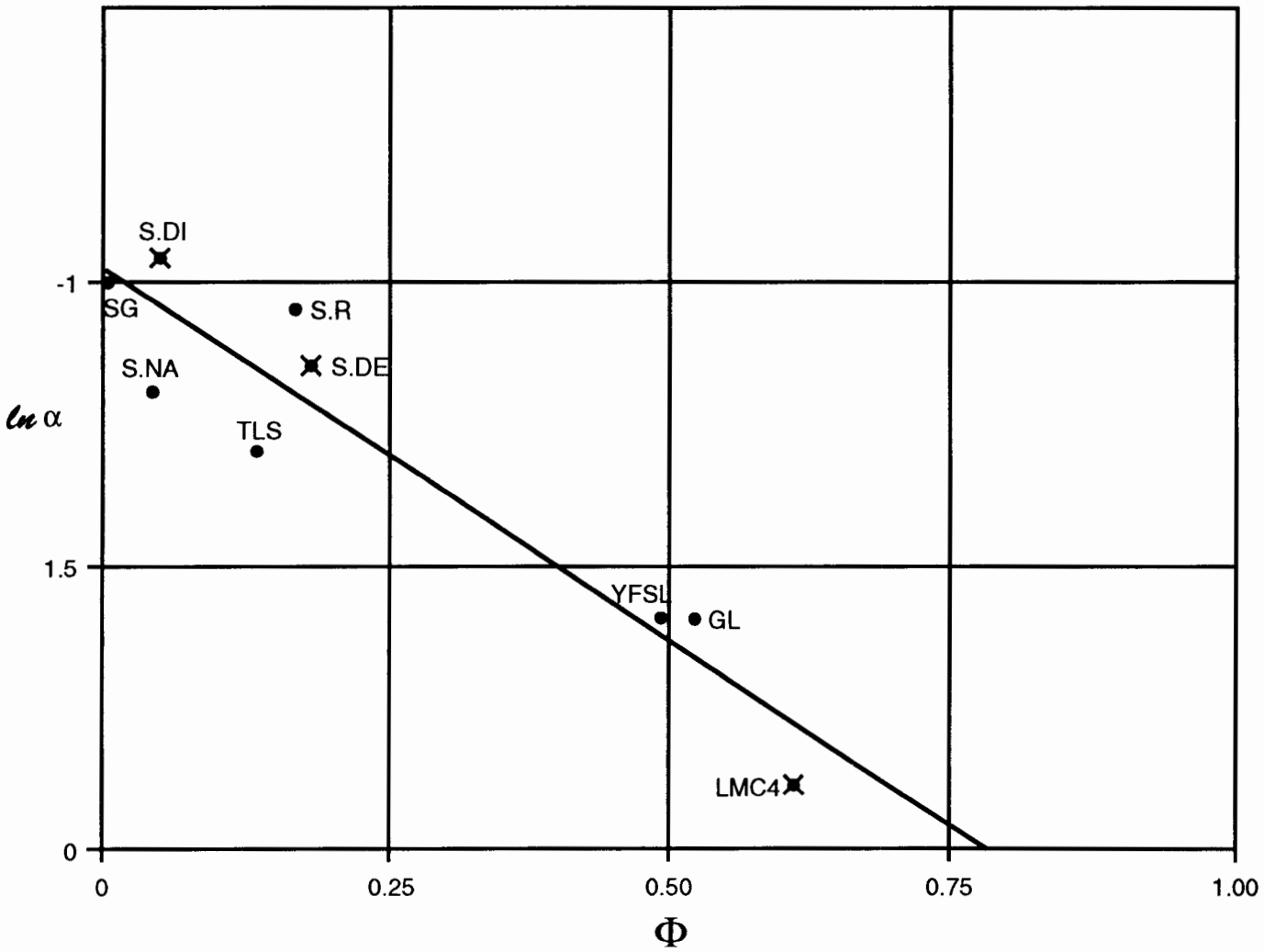

Figure 4-3. Relation between parameter log-conductivity slope α, and fraction Φ of fine particles (0-50 μ), for the soils listed in of Table 4-2

where B^3 is the cubic-mean aperture and L the mean aperture spacing: $B^3 = E(b^3)$ and $L = E(\ell)$. It is assumed here that the embedding matrix is impervious. With this proviso, capillary theory indicates that an individual parallel plate fracture will drain all its water if its aperture is larger than a threshold that depends on pressure. Therefore, only the tightest fractures will contribute to flow. By the Laplace formula, assuming perfectly wettable solid, the contributing fractures are such that:

$$b_i \leq \frac{2\sigma}{\rho g h} = b_o(h) \tag{4.57}$$

where σ is surface tension. A simple averaging calculation shows that the overall conductivity of the fracture set is now of the form:

$$K(h) = \frac{g}{\nu} \frac{1}{12L} \cdot \int_0^{b_o(h)} b^3 f(b)\,db \tag{4.58}$$

where $f(b)$ is the probability density function of the apertures. Assuming for instance an exponential distribution $f(b) = \lambda \exp(-\lambda b)$ where $\lambda = 1/E(b)$, yields an expression of the form:

$$K(h) = \frac{g}{\nu} \frac{[E(b)]^3}{6L} F\left(\frac{E(b)\rho g}{2\sigma} h\right) \tag{4.59}$$

where $F(x)$ is an increasing function of x such that $F(-\infty) = 0$ and $F(0) = 1$. The form of Eqn. (4.59) indicates, at least qualitatively, that the log-conductivity slope must be related to the group inside function F, that is:

$$\alpha \sim \frac{E(b)\rho g}{2\sigma} \tag{4.60}$$

At the same time, $F(0) = 1$ yields:

$$K_s \sim \frac{[E(b)]^3}{6L} \frac{g}{\nu} \tag{4.61}$$

Note that $E(b^3) = 2[E(b)]^3$ for the exponential distribution. In this particular instance, it appears that K_s and α are related by:

$$\alpha \sim (L \cdot K_s)^{1/3} \tag{4.62}$$

Equivalently, noting that the specific area of the fracture set is given by $\sigma_o = 2/L$, this relation takes the form:

$$\alpha \sim \left(\frac{K_s}{\sigma_o}\right)^{1/3} \tag{4.63}$$

But, by the previously derived Kozeny-Carman relation for saturated fractured media, we have $K_s \sim p^3/\sigma_o^2$. Combining this relation with Eqn. (4.63) gives:

$$\alpha \sim \left(\frac{K_s}{p}\right)^{1/2} \tag{4.64}$$

In summary, this idealized model of capillary flow through fractures indicates that the unsaturated log-conductivity slope α increases with K_s and decreases with porosity p. For fixed porosity, there is a perfect correlation between $\ln \alpha$ and $\ln K_s$. In practice, that correlation may be masked by variations in porosity. So far, there is no concrete evidence to either accept or refute the hypothesis of a three-way correlation between porosity, saturated conductivity, and log-conductivity slope. Mishra and Parker (1989), using the van Genuchten-Mualem model (van Genuchten, 1980), suggest that K_s is proportional to $(\theta_s - \theta_r)^{5/2}a^2$ where a is an inverse capillary length scale in the water retention curve. Wang and Narasimhan (1988, Appendix A) examined $\ln K_s$ versus $\ln \alpha$ from tuff matrix data, and concluded that the correlation was weak or non-existent. However, their slope parameter was evaluated for convenience only at large suctions; also, porosity was not included in the analysis, and the small-scale data used in their analysis concern the porous matrix rather than the fracture system.

With some refinements as indicated above, it may be possible to develop auxiliary models correlating *bulk* hydrodynamic parameters of fractured porous rocks. This would lead to a reduction of data requirements. Data collection could then be focused on spatial variability of a few single parameters such as saturated conductivity, texture, and structure of porous fractured rock. Some of the constitutive models discussed below can also help reduce data requirements.

4.3.3 Functional Conductivity Models of Burdine and Mualem

Burdine (1953), and later Mualem (1976), obtained the unsaturated conductivity of idealized porous media as a *functional* of the water retention curve $\theta(h)$, or its reciprocal $h(\theta)$. Their semi-empirical models are based essentially on capillary tube representations of pore structure. See also Bear (1972), and Dullien (1979) for other capillary network models, and more recently Gvirtzman et al. (1990) for an attempt at generalizing the Kozeny-Carman relation to unsaturated conductivity. The conductivity model of Burdine (1953) expresses the relative conductivity versus degree of saturation as follows:

$$K_r(S) = S^2 \frac{\int_0^S h^{-2}(s)\,ds}{\int_0^1 h^{-2}(s)\,ds} \tag{4.65}$$

The model of Mualem (1976) is similar in form, namely:

$$K_r(S) = S^{1/2}\left\{\frac{\int_0^S h^{-1}(s)\,ds}{\int_0^1 h^{-1}(s)\,ds}\right\}^2 \tag{4.66}$$

It is clear that these models, if accurate, provide a link between the water retention curve, which can be measured under hydrostatic conditions, and the conductivity curve, which must be measured under non-static conditions (therefore with greater difficulty). Good fits have been obtained for a number of soils (Mualem, 1976; van Genuchten, 1980). In what follows, we insert specific parametric curves $S(h)$ in Eqns. (4.65) and (4.66) in order to obtain a complete description of both constitutive relations with a small number of parameters (after van Genuchten, 1978 and 1980).

4.3.4 Brooks-Corey and van Genuchten Parametrization of Water Retention Curves

Brooks and Corey (1964, 1966) studied a relatively large number of porous media (including repacked and sieved soils) and concluded that the water retention curve is reasonably well approximated by a piecewise power law of the form:

$$\begin{aligned} S(h) &= \left(\frac{h}{h_b}\right)^{-\lambda} && \text{if } h \le h_b \\ S(h) &= 1 && \text{if } h \ge h_b \end{aligned} \tag{4.67}$$

Van Genuchten (1978, 1980) later refined this model to better fit the continuous S-shaped curves over the whole range of negative pressures, as observed experimentally. The van Genuchten retention curve is:

$$S(h) = [1 + (-ah)^n]^{-m} \tag{4.68}$$

where a is a characteristic inverse length scale (denoted α by van Genuchten) and n and m are two real exponents, or shape factors, as yet unrelated. It should be noted that Eqn. (4.68) reduces to:

$$S(h) \approx (-ah)^{-mn} \tag{4.69}$$

asymptotically as $(ah) \to -\infty$. Therefore, the Brooks-Corey and van Genuchten curves match in the dry range if $a = 1/h_b$ and $mn = \lambda$.

4.3.5 Combining Brooks-Corey and van Genuchten Retention Curves with Functional Conductivity Models of Burdine and Mualem

Van Genuchten (1978) inserted the Brooks-Corey curve (4.67) and the van Genuchten curve (4.68) in the functional conductivity models of Burdine (4.65) and Mualem (4.66). However, in the case of the van Genuchten curve, closed form expressions of conductivity could only be obtained by restricting the parameters m and n as follows:

$$m = 1 - 1/n \qquad 0<m < 1,\ n > 1 \qquad \text{(Van Genuchten - Mualem)}$$
$$m = 1 - 2/n \qquad 0 < m < 1,\ n > 2 \qquad \text{(Van Genuchten - Burdine)} \tag{4.70}$$

With these provisions, the relative conductivity curve predicted by the van Genuchten - Mualem model takes the form:

$$K_r(S) = S^{1/2}[1 - (1 - S^{1/m})^m]^2 \tag{4.71}$$

While the van Genuchten - Burdine model takes the form:

$$K_r(S) = S^2[1 - (1 - S^{1/m})^m] \tag{4.72}$$

We now focus on the van Genuchten - Mualem model which has been most widely used in the recent years, including Wang and Narasimhan (1988) and Smoot and Sagar (1990) for Yucca Mountain tuff matrix data, and Wierenga et al. (1986a, 1986b, 1989) for the three-dimensional strip-source trench site of Jornada near Las Cruces, New Mexico (INTRAVAL*, 1991). In particular, it will be useful to characterize the two-parameter relative conductivity curve (4.71) with a view to relating it to the one-parameter exponential conductivity model analyzed earlier. Indeed, most analytical solutions of unsaturated flow available to date have been obtained with the exponential models, not with the van Genuchten - Mualem model: see Philip (1969), for deterministic solutions; and Yeh et al. (1985a,b,c) and Mantoglou and Gelhar (1987a,b,c) for stochastic solutions.

Figure 4-4 depicts a typical water retention curve and the associated relative conductivity curve, following the parametric form proposed by van Genuchten. The inflection point characterizes uniquely the storage properties of the porous medium, as it corresponds to the point of maximum moisture capacity. Straightforward, but tedious, calculations lead to single expressions for the degree of saturation (S_o), suction head ($\Psi_o = -h_o$), and moisture capacity (C_o) at the point of maximum capacity.

$$S_o = \left(\frac{1}{m + 1}\right)^m \tag{4.73a}$$

$$\Psi_o = a^{-1} m^{1/n} \tag{4.73b}$$

---

*INTRAVAL - An International Project to Study Validation of Geosphere Transport Models. Unsaturated Zone Test Cases, in Phase I Final Report. T.J. Nicholson, ed. To be published by Swedish Nuclear Power Inspectorate. Stockholm, Sweden.

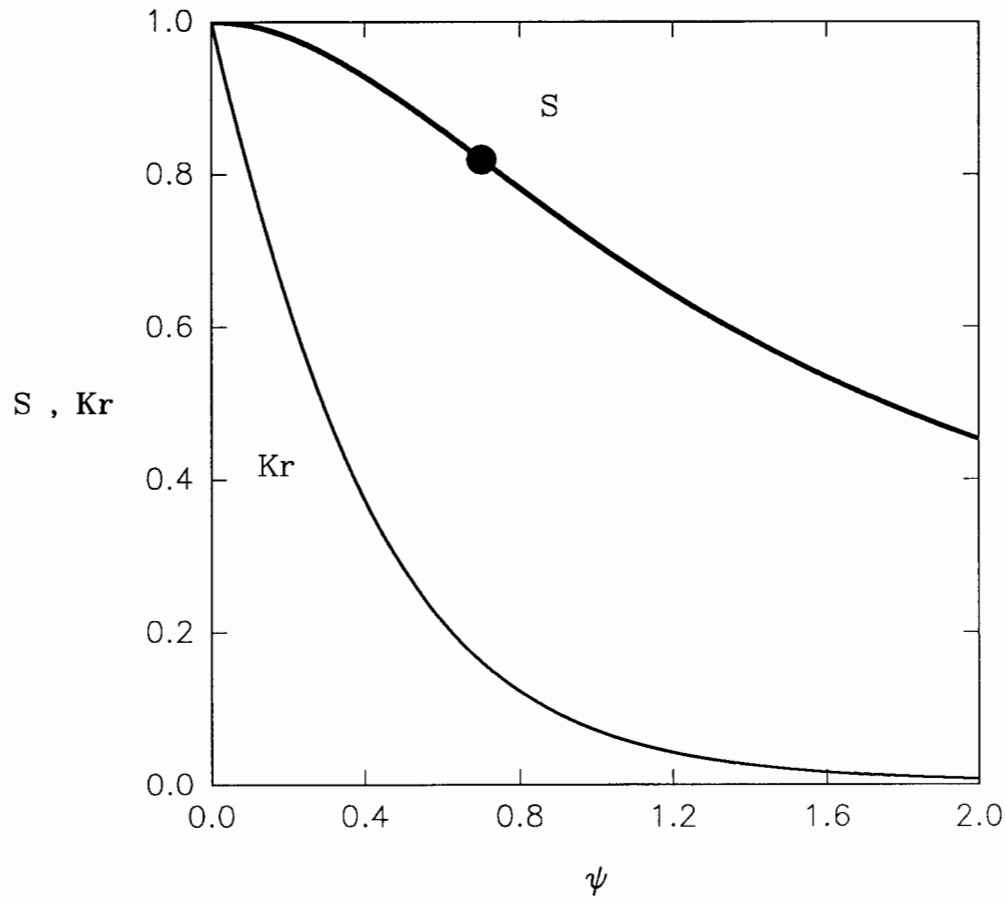

Figure 4-4. **Water retention curve (degree of saturation S) and relative conductivity curve (K_r) versus dimensionless suction ($\psi = a\Psi$) according to the Van Genuchten-Mualem model. Parameters from the Las Cruces-Jornada trench soil were used (m = 0.4955). The solid circle indicates the inflection point of the water retention curve.**

$$C_o = amn(\theta_s - \theta_r)\frac{(m)^m}{(m+1)^{m+1}} \tag{4.73c}$$

The physical significance of the state of maximum moisture capacity is that the *energy* required to add or extract a fixed quantity of water to or from the porous medium is minimal. Therefore, it seems appropriate to single out this particular state for evaluating the characteristic slope of log-conductivity, that is:

$$\alpha_o = \frac{\partial \ln K}{\partial \Psi}\Big|_{\Psi=\Psi_o} \tag{4.74}$$

Inserting the van Genuchten - Mualem conductivity model in (4.74), and making use of Eqns. (4.73), and skipping some tedious calculations, the final result is:

$$\alpha_o = a\frac{m^m}{2(1-m)(1+m)}\left\{\frac{4m^m}{[(1+m)^m - m^m]} - m\right\} \tag{4.75}$$

By way of example, the mean parameter values for the Las Cruces-Jornada trench soil were (Wierenga et al., 1986a; Ababou, 1988, Chapter 7):

$a = 0.0334$ cm^{-1}
$n = 1.982000$
$m = 0.495459$
$\theta_s = 0.368$
$\theta_r = 0.102$

Applying the previous relation, the state of maximum moisture capacity is found to be $\Psi_o = 21.0$ cm, and the log-conductivity slope at this point is $\alpha_o = 0.078055$ cm^{-1}. In comparison, note that the slope obtained at larger suction is smaller, e.g. $\alpha = 0.0494$ cm^{-1} for $\Psi = 80$ cm (value used in the three-dimensional simulation of Ababou, 1988, Chapter 7).

Equation (4.75) may provide a means to correlate the van Genuchten parameters (a,m) to structural/textural properties of spatially variable and fractured porous media. This has not been fully developed yet, but some indications can be given along these lines. Assume that the two van Genuchten parameters are spatially random and statistically independent. Furthermore, assume that $\langle m \rangle \sim 1/2$, which is typical of a number of porous media, such as the Las Cruces-Jornada soil. Perturbation analysis of (4.75) suggests, roughly:

$$\delta \ln \alpha_o(\vec{x}) \approx \delta \ln a(\vec{x}) - \delta m(\vec{x}) \tag{4.76}$$

Given Eqn. (4.76) and the assumed independence of $(a(\vec{x}), m(\vec{x}))$, it follows that:

$$\mathrm{var}(\ell n\, \alpha_o) \approx \mathrm{var}(\ell n a) + \mathrm{var}(m) \tag{4.77}$$

However if (a,m) are not independent, Eqn. (4.77) is no longer valid. In this case, we obtain instead:

$$\mathrm{var}(\ell n\, \alpha_o) = \mathrm{var}(\ell n a) + \mathrm{var}(m) - 2\mathrm{cov}(\ell n a\ ,\ m) \tag{4.78}$$

For the Jornada trench site, statistical data have been extracted by G. Wittmeyer (personal communication) from the Las Cruces database described in Wierenga et al. (1988), and INTRAVAL (1991). The statistics shown in Table 4-3 correspond to 562 cores collected at the site. Further calculation of the covariance cov($\ell n\ a$, m) will give the variance of log-conductivity slope directly from Eqn. (4.78).

Table 4-3. Partial list of single-point moments of hydrodynamic parameters for the Las Cruces-Jornada trench site from 562 cores

	θ_s	θ_r	a	$\ell n\ a$	m
Mean	0.322	0.0891	0.0538	-3.16	0.384
Standard Deviation σ	0.0348	0.0204	0.0758	0.608	0.0749

4.3.6 Scaling Factors in Similar Media Theory

Besides the scaling parameters encountered earlier, such as the log-conductivity slope α or the capillary scaling parameter a of the water retention curve, a systematic approach to scaling of constitutive relations (Miller and Miller, 1955, 1956), has been used to reduce the description of soil variability to that of one or two scaling factors (Sharma et al., 1980; Simmons et al., 1979; Russo and Bresler, 1980; Warrick et al., 1977).

Briefly, Miller and Miller's "similar media theory" is based on:

- Similitude analysis of the microscopic governing equations (Laplace equation for surface tension, and Stokes equation for viscous flow),
- Assumption of similarity of grain and pore structure, i.e. differences or spatial variations in geometric structure are restricted to similarity transformations (e.g. isotropic magnification).

At the macroscopic scale, the implication of the theory is that any porous medium property or state variable $Y(\vec{x})$ can be scaled to a standard value Y_o that does not vary in space, as follows: The theory predicts that:

$$\lambda^p(\vec{x})\ Y(\vec{x}) = Y_o \tag{4.79}$$

- $p = 1$ for pressure head ($Y = h$)
- $p = -2$ for conductivity ($Y = K$)
- $p = 0$ for water content ($Y = \theta$)

However, in practice, the spatially variable scaling factor $\lambda(\vec{x})$ is not unique, i.e. it depends on the particular variable being scaled. Recognizing this shortcoming of the theory leads to replace Eqn. (4.79) by:

$$\lambda_Y^p(\vec{x})Y(\vec{x}) = Y_o \tag{4.80}$$

In particular, for the two constitutive relations of porous media, this gives a scaling of the form:

$$\begin{aligned} K(h,\vec{x}) &= \lambda_K^2(\vec{x})\ K_o(\lambda_H^{-1}(\vec{x})h_o) \\ \theta(h,\vec{x}) &= \theta_o(\lambda_H^{-1}(\vec{x})h_o) \end{aligned} \tag{4.81}$$

where $K_o(h)$ and $\theta_o(h)$ represent the standard curves or scaled mean curves for the similar medium at hand. In the above-mentioned field studies, both $\lambda_K = \lambda_H$ and $\lambda_K \neq \lambda_H$ were tested. The scaling is generally better in the latter case, but the number of spatially variable parameters is increased, which somewhat weakens the value of the whole approach. In agricultural fields, the coefficient of variation of $\lambda(\vec{x})$ is typically on the order of 100 percent.

4.4 UNSATURATED HYDRAULIC PROPERTIES OF FRACTURED POROUS ROCKS

The parallel plate model of fractures was used in Section 4.2 to obtain the effective saturated conductivity tensor of a fractured rock with impervious matrix. In Section 4.3.2, the same parallel plate model was used again to evaluate the longitudinal unsaturated conductivity for a parallel set of fractures embedded in an impervious matrix [Eqn. (4-58)]. In reality, however, flow in relatively dry unsaturated rock may occur predominantly through the porous matrix, depending on the ambient flow rate and moisture content. More realistic constitutive models taking into account matrix/fracture interactions are therefore needed in order to predict the bulk hydraulic properties of the unsaturated fractured medium. Furthermore, it is expected that the bulk hydraulic conductivity, besides being pressure-dependent, must also be direction-dependent. The precise approach to effective constitutive relations should be consistent with the scales of simulation and the degree of resolution allowed by the global (large-scale) flow model. Alternative approaches to large-scale modeling are reviewed in Chapter 6, along with various methods of including fracture/matrix flow and medium heterogeneity. Ongoing laboratory experiments on fractured tuff at the Apache Leap Site aim at characterizing fracture and matrix conductivity on unsaturated blocks of size 20x50x50 cm. So far, only blocks with a single vertical fracture have been considered, and the conductivities parallel and orthogonal to fracture have not been measured. For more details, see Chuang et al. (1990), Haldeman et al. (1991), Rasmussen et al. (1990) and INTRAVAL (1991, Appendix B).

5. HYDROGEOLOGIC HETEROGENEITY AND SPATIAL STRUCTURE: FIELD DATA AND STOCHASTIC MODELS

5.1 INTRODUCTION

Chapter 3 focused on field experiments and observations of water flow and tracer transport in heterogeneous environments. Chapter 4 formulated and reviewed local hydraulic properties and constitutive relations. The emphasis here is on quantitative characterization of spatially variable hydrodynamic coefficients, such as those needed for implementing large-scale three-dimensional simulation models. Many field experiments have been undertaken on various scales to quantitatively characterize the naturally heterogeneous saturated/unsaturated properties of soils, sedimentary formations, and rocks. What follows is a general review of field measurements of hydrogeologic heterogeneity, which includes some observations of aquifer transmissivities, and gradually focuses on items more directly relevant to the Yucca Mountain site. In some cases, investigators represented the formation as a porous continuum, whose bulk properties reflect implicitly the granular and fissured nature of the medium. However, this simplified view cannot always be sustained in the case of fractured rocks. Accordingly, measurements and data on the hydraulic properties of fractures and fracture networks, as opposed to continuum characterization, will be treated separately.

5.2 STATISTICAL CONTINUUM HETEROGENEITY OF WATER-BEARING FORMATIONS

This section examines the hydraulic properties of heterogenous aquifers from data published in the literature. In the case of saturated groundwater flow, the hydraulic properties of interest are the saturated conductivity K (m/s) and the specific storativity S_s (m^{-1}), or their two-dimensional equivalents, the transmissivity T (m^2/s) and the storage coefficient or specific yield S_y (dimensionless). The following discussion will focus on conductive properties rather than storage coefficients. For completeness, however, note the papers by Clifton and Neuman (1982) and Hoeksema and Kitanidis (1985) concerning the spatial variability of specific storativity. In particular, the first-quoted authors found a positive correlation between log-transmissivity and log-storativity, with a slope close to unity.

The spatial variability of hydraulic conductivity and transmissivity has been the object of intensive experimental studies, in an effort to characterize natural variability in a statistical rather than purely descriptive fashion. Gelhar (1986) reviewed some of the available field data. Many experimental studies of aquifer variability were limited to horizontal variability of the transmissivity or depth-averaged conductivity as determined from well pumping tests (Delhomme, 1979; Binsariti, 1980; Devary and Doctor, 1982; Hoeksema and Kitanidis, 1985). Their statistical data could be summarized as follows: the standard deviation of log-transmissivity ($\ln T$) ranged between 0.6 (sandstone aquifer of Hoeksema and Kitanidis) to 2.3 (limestone aquifer of Delhomme), with correlation ranges on the order of one kilometer to several tens of kilometers. The domain sizes were on the order of five kilometers to several hundred kilometers.

In other studies, borehole data were used to investigate vertical variability. Figure 5-1 (top) from Gelhar (1976) depicts the vertical fluctuations of the log-saturated conductivity of small cores

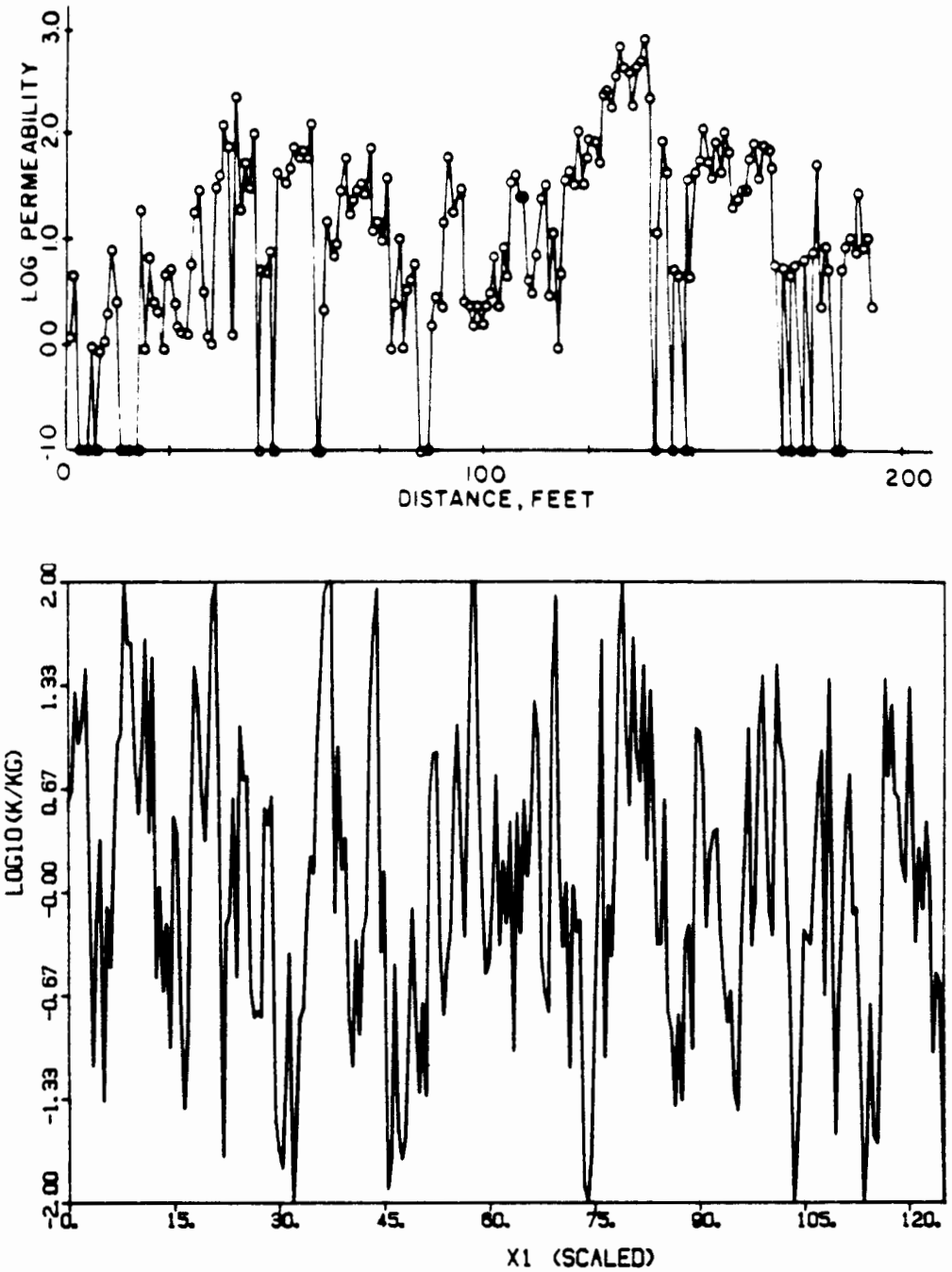

Figure 5-1. Log-conductivity records $\ln K(x)$ in one spatial dimension. Top: Mount Simon borehole data (from Gelhar, 1976). Bottom: Synthetic random function (from Ababou, 1988).

taken from a borehole in the Mount Simon sandstone aquifer in central Illinois. The conductivity at this borehole appears to fluctuate randomly over a broad range, approximately four orders of magnitude (this is also indicated by data from several other boreholes in Bakr, 1976). It is instructive to compare the available log-conductivity record to a synthetic log-conductivity record obtained by taking a transect of a three-dimensional realization of a stationary Gauss-Markov random function as shown in Figure 5-1 (lower part, from Ababou, 1988).

The mean, variance, correlation scale and Markovian correlation function of the synthetic random function in Figure 5-1 (below) were selected to fit the one-dimensional statistics of the observed record of Figure 5-1 (top), as interpreted by Bakr (1976) based on spectral analysis. There appear some qualitative discrepancies between the two records. The assymmetric appearance of the observed record, with sharp negative peaks at $\log K = -1.0$, are most likely due to lack of resolution at the low end of the conductivity range (a common problem). In addition, the observed record also appears to be generally smoother than the synthetic record. Indeed, the high-wavenumber range of spectral densities, where wavelengths are smaller than twice the measurement spacing, cannot be seen in the observed record, while such wavelengths are present in the (hypothetical) synthetic record. Finally, it is also possible that the low wavenumber spectral densities (used in generating the synthetic record) were underestimated. Indeed, large wavelength fluctuations are difficult to capture accurately given the inherent limitations of stationary spectral analysis and the finite length of observation (here about 200 feet or 65 meters). Ababou and Gelhar (1990) offered an alternative interpretation of the same data using a truncated self-similar spectral model based on the theory of fractal random functions. This alternative model of stochastic heterogeneity appears more flexible, as it can be made to depend explicitly on cut-off length scales related to scales of observation (discussed below).

In addition to Bakr (1976), other investigators have collected and analyzed the spatial distribution of local hydraulic conductivities from small scale measurements along multiple vertical boreholes (Hufschmied, 1985; Sudicky 1986). Combining the results of the three studies, the standard deviation of log-conductivity ($\ln K$) ranged from 0.6 to 2.2, with correlation ranges on the order of 0.1 to 1.0 meters in the vertical direction. The lengths of the vertical transects (boreholes) ranged from 20 to 100 meters. The data collected by Hufschmied (1985) and Sudicky (1986) are particularly remarkable because these authors actually determined, by different methods, the *three-dimensional* variability of the log-conductivity field. Hufschmied used a relatively sophisticated flowmeter measurement of conductivities in 16 wells, for twenty 1-meter thick layers in each well. The statistics of the point process $\ln K(\vec{x})$ in the vertical were then obtained by using statistical identities relating the point process to the local averaging process. Information obtained among different wells was used indirectly to infer the horizontal covariance structure of $\ln K(\vec{x})$. On the other hand, Sudicky (1986) measured the conductivities from small core samples along a number of vertical boreholes emplaced along two perpendicular planes. This particular choice allowed them to estimate the covariance structure of $\ln K$ in three-dimensional space.

The statistical results obtained by Hufschmied (1985) and Sudicky (1986) are summarized in Table 5-1. In addition, Figure 5-2 (top) shows the log-conductivity contours obtained by Sudicky (1986) along the vertical plane aligned with the natural hydraulic gradient at the Borden site. For comparison, the bottom part of Figure 5-2 (from Ababou, 1988) displays a synthetically

Table 5-1. Statistical properties of measured three-dimensional conductivities ($\ln K$) in saturated formations, from Hufschmied (1985) and Sudicky (1986)

	Hufschmied (1985)	Sudicky (1986)
Site	Aeflingen, Switzerland	Borden site, Ontario
Formation	20 m thick, sand and gravel	Outwash sand
Covariance	Anisotropic exponential	Anisotropic exponential
K_G	(6 10^{-3} m/s)	7.17 10^{-5} m/s
σ_f	1.92	0.54 - 0.62
λ_1	15 - 20 m	2.8 m
λ_2	15 - 20 m	2.8 m
λ_3	0.5 m	0.12 m

generated anisotropic random field obtained by the turning band method (Tompson et al., 1989). Note that both Hufschmied and Sudicky's data show a significant statistical anisotropy between the horizontal and vertical directions.

In summary, the aquifer data reviewed above indicates that the conductivities and transmissivities can vary over several orders of magnitudes in natural formations. In addition, the analyses of Hufschmied (1985) for the Aeflingen site, and Sudicky (1986) for the Borden site, clearly show that the conductivities follow a log-normal probability distribution more closely than a normal distribution. It is also clear that there is a relatively strong anisotropy in the vertical/horizontal correlation scales of the log-conductivity (Table 5-1). However, it should be cautioned that the anisotropy observed by these authors may be relative to the scales of observations, which were significantly larger horizontally than vertically, e.g. 12 m × 3 m in the Borden aquifer study (Sudicky, 1986). The sand formations at the Aeflingen and Borden sites are considered to be relatively homogeneous from a geological point of view. This translates as statistical homogeneity, which allows the use of stationary random field models of heterogeneity. However, Woodbury and Sudicky (1991) reported more recently the existence of a number of low conductivity outliers which had not been previously detected at the Borden site. The existence of such outliers (in a formation considered to be geologically homogeneous) creates conceptual difficulties in applying statistical estimation theories to the sample data. Woodbury and Sudicky conclude that the distribution of log-conductivity fits an exponential or a gaussian distribution, i.e. these two distributions are equally valid models in view of the sampling statistics.

Single-hole and cross-hole pumping tests were conducted to evaluate the three-dimensional variability and effective anisotropic conductivity of fractured granite at the Oracle site near Tucson, Arizona (Hsieh et al., 1983; Neuman and Depner, 1988). While the previously mentioned studies indicated horizontal/vertical aquifer anisotropy due to natural stratification of deposits, the results of Neuman and Depner indicate a more complex three-dimensional anisotropy with inclined axes, due mostly to preferential flow through diversely oriented

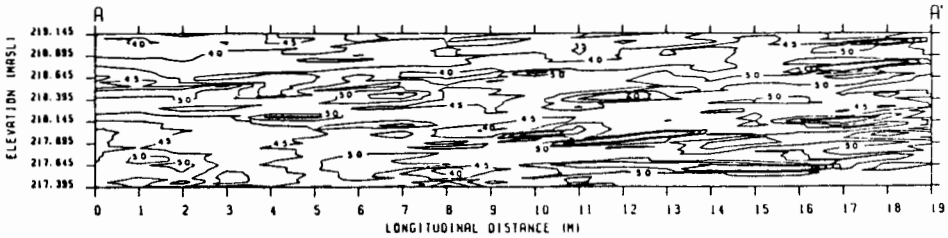

Location of measurements and distribution of -ln(K) along A-A' (contour interval = 0.5; vertical exaggeration = 2; K < 10^{-3} cm/s in stippled zones).

(a): Measured

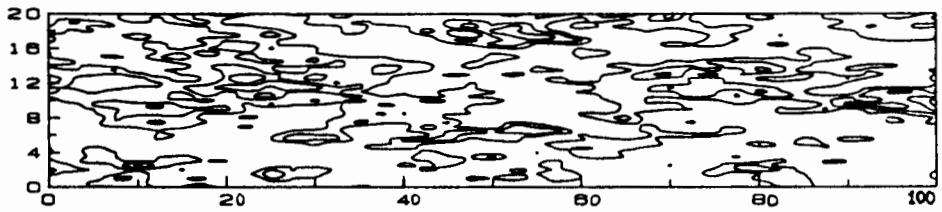

(b): Simulated by the Turning Band Method

Figure 5-2. Log-conductivity contours in a vertical plane. (a) from Sudicky (1986) (measured at the Borden Tracer Site). (b) by simulation, using the turning band method with an anisotropic spectrum.

fractures. An additional comment is warranted: the probability distribution function of ℓnK from single-hole packer tests was not found to be bimodal, as would be expected for fracture-matrix flow, even though fractures are known to exist. There are two possible causes for this: (1) permeability of intact porous rock is negligible, and scale of measurement is large (here, one meter vertically and perhaps more horizontally) relative to fracture density and connectivity; (2) there is a broad distribution of relatively fine fissures down to very small scales, such that the rock behaves on the whole like a porous medium. However, the macroscale anisotropy observed by Neuman and Depner (1988) was probably dominated by a sparse network of larger scale fractures rather than fine-scale fissures. See Ababou (1990a) for an alternative identification of macroscale anisotropy at the Oracle site based on new closed-form expressions of effective conductivity tensor.

Other studies, among those previously mentioned, indicate that the presumed stationary correlation structure of porous formations is not well defined for certain sites and/or for certain scales of observation. This is suggested for instance by the statistics of aquifer transmissivities compiled and analyzed by Hoeksema and Kitanidis (1985). They found, for a number of sites, that the best-fit correlation scale was either very small, on the order of measurement spacing, or very large, on the order of domain size. In addition, other studies suggest that the correlation structure and the degree of variability appear to be strongly influenced by certain subjective choices, such as empirical detrending (an example can be found in Devary and Doctor, 1982).

These difficulties suggest that the measured statistical properties of supposedly homogeneous conductivity fields may be in fact scale-dependent in certain situations. This is not necessarily an obstacle to the application of stochastic concepts, as long as the fact is recognized, and that adequate methods are developed to transfer information from one scale of analysis to another. For instance, going back to the Mount Simon record of borehole log-conductivity (Figure 5-1 above), an alternative scale-dependent interpretation of heterogeneity was developed by Ababou and Gelhar (1990). The first step of this approach was to re-examine the data in a new light. A fractional Brownian motion process (Mandelbrot and van Ness 1968; Mandelbrot and Wallas 1969) was fitted to the spectral density data, which are essentially the Fourier-space version of the 200 foot record of Figure 5-1 (above). The log-log plot shown on Figure 5-3 is a comparison of (1) the sampled spectral density function inferred from borehole data by Bakr (dots), (2) the Markov spectral density model fitted by Bakr, and (3) the fractional Brownian motion spectrum with unit slope ($1/f$-noise). The latter model seems to fit the spectral data rather well, except at the very low and high ends of the observable wavenumber range, where both the estimated spectral densities *and* the estimated confidence interval become unreliable.

The second step of the Ababou-Gelhar approach consisted in assuming that the formation "at large" satisfies the random fractal model within some range of wavelength scales. The scale of observation L was assumed to lie within this range. The scale-dependent effects of formation heterogeneity were then explicitly accounted for by separating the spectrum of heterogeneity in two parts, a high wavenumber part contributing to mixing and homogenization in flow and transport processes, and a low wavenumber part conditioning the smaller scale processes and acting as uncertainty. These concepts are illustrated in Figure 5-4 in terms of spectral density (upper part) and spatial record (lower part). Specifically, the lower portion of the figure illustrates what would happen if the scale of observation were smaller than the available 200-foot record. First, the estimated mean value would be different from the mean of the larger region;

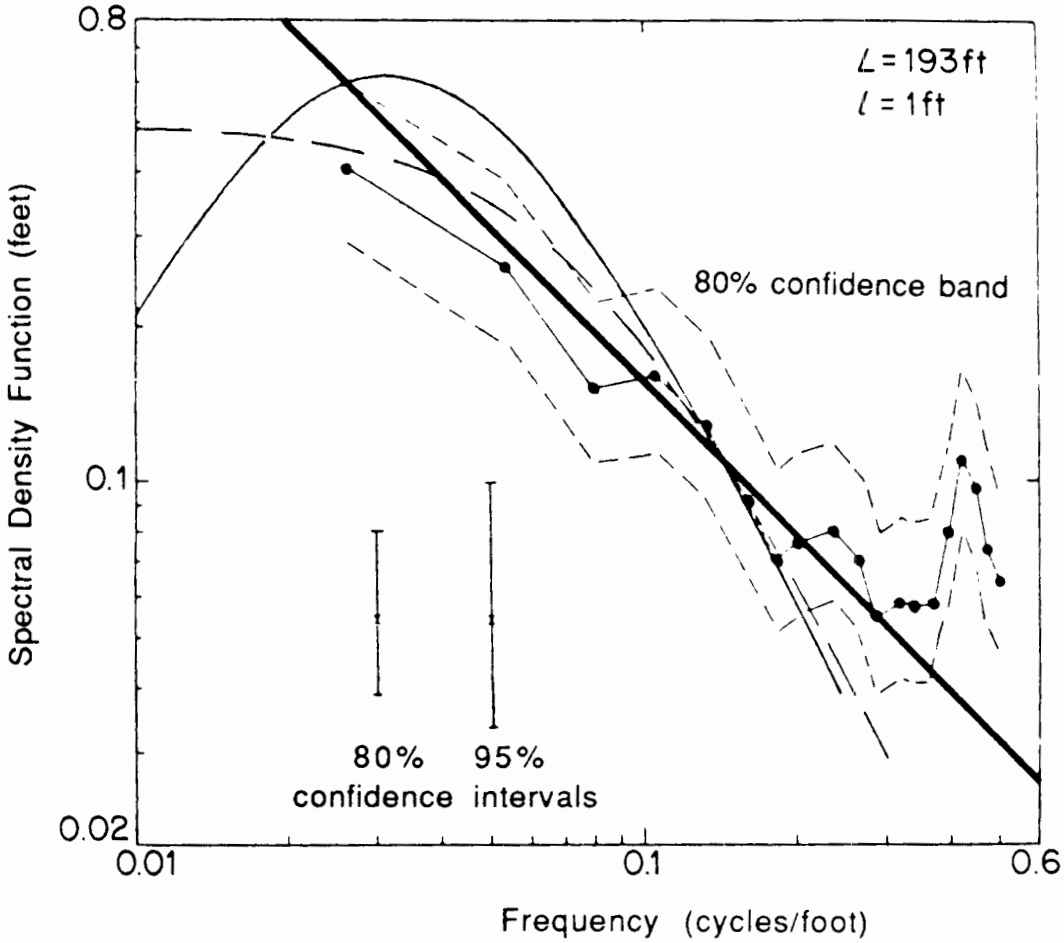

Figure 5-3. **One-Dimensional spectral density of measured log-conductivity in a vertical borehole (black circles) and fitted spectral density functions (from Ababou and Gelhar, 1990).**

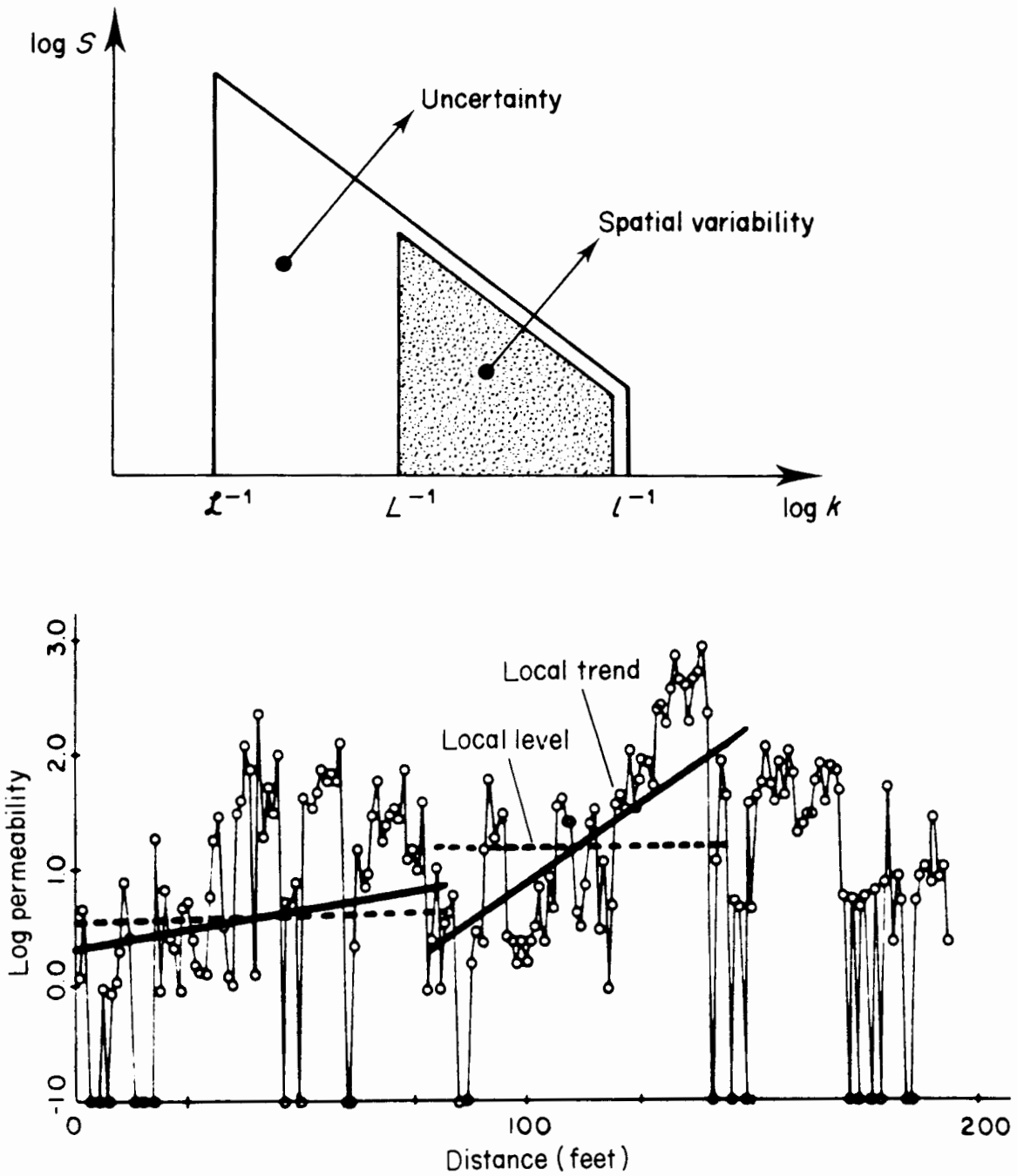

Figure 5-4. Illustration of the spectral conditioning method after Ababou and Gelhar (1990): log-spectral density versus log-wavenumber (above); sample function of log-conductivity process (below)

secondly, a trend would also appear; and thirdly, both the mean level and the mean trend would depend on the specific location of the sampled domain within the larger 200-foot region. These intuitive concepts can be formulated more precisely for quantitative analysis of stochastic flow systems. For more details on spectral conditioning, uncertainty, and stochastic solutions for self-similar heterogeneity, see Ababou and Gelhar (1990).

5.3 STATISTICAL CONTINUUM HETEROGENEITY OF UNSATURATED MEDIA

5.3.1 General Considerations

The hydraulic properties of unsaturated media such as soils and rock formations also exhibit random-type heterogeneity. In this case, however, spatial variability is more difficult to characterize because the hydraulic coefficients are a function of the state of the system (water pressure). In order to model both transient and steady flow systems in heterogeneous unsaturated media, two spatially variable constitutive relations need to be determined (Chapter 4):

- the water retention curve $\theta(h,x)$ which relates volumetric moisture content to pressure head; and

- the unsaturated conductivity curve $K(h,x)$ which relates hydraulic conductivity to pressure head.

Specific functional relationships for $\theta(h,x)$ and $K(h,x)$ can be selected by inserting spatially variable parameters in the functional models of Gardner, Mualem and van Genuchten, Brooks and Corey, etc. (Chapter 4). These functions are empirical or, at best, semi-empirical. In the absence of a consensus on appropriate theoretical relationships, experimental investigators have used a wide variety of functional shapes $\theta(h)$ and $K(h)$ in their statistical analyzes of spatial variability. In addition, data are obtained at various scales of measurement (measurement resolution), generally either on small core samples in the laboratory (rocks and soils), or from in-situ experiments on small field plots (soils) with areal resolution on the order of 1-10 m^2 and vertical resolution on the order of 0.1-1 m. This makes it difficult to synthesize the available pool of data in a compact form. Some data on natural soil variability are summarized in Table 5-2, while others not shown in the table are discussed in the text.

5.3.2 Field Data

Table 5-2 gives information on the probability distribution function and the correlation structure of the hydraulic parameters intervening in the constitutive relationships $\theta(h)$ and $K(h)$. It should be repeated that these results correspond to different scales of analysis and different schemes of data collection, so they are not always directly comparable. However, some common features seem to emerge as a whole. First of all, it should be emphasized that only one author (Russo, 1983) analyzed the correlation structure of the whole conductivity curve $K(h)$, including in particular the correlation structure of the saturated conductivity $K_s(x)$ as well as that of the slope parameter:

Table 5-2. Summary of statistical data on the in-situ spatial variability of unsaturated soils from the literature

Y	$\bar{Y}$	CV_Y	$\sigma_{\ln Y}$	γ_Y	λ_Y	Ref. and Remarks
K_o (cm/h)	1.96	0.71	0.64	2.49	a = 38 m λ = 17 m Spherical variogram	Russo (1983): Hamra Red Mediterranean soil $K(h) = K_o e^{-\alpha h}$ A = 2 + 2.5 ha
α (cm^{-1})	0.286	0.43	0.41	1.36	a = 51 m λ = 72 m Exponent. variogram	N = 25 + 6 plots; 1 plot = 3m x 3m n = 5 depths; a = range of variogram λ = integral correlation length
θ_s	.338	0.08	0.08	(0.23)	76 m	Russo and Bresler (1981): Hamra Red Mediterranean soil
θ_r	0.030	0.30	0.29	(0.93)	39 m	$(\theta-\theta_r)/(\theta_s-\theta_r) = (h_w / h)^\beta$
K_o (cm/h)	22.0	0.41	0.39	(1.2)	34 m	$(K/K_o) = (h_w/h)^\eta$
β	1.160	0.68	0.62	2.35	23 m	$\eta = 2\beta + 2$; A = 0.8 ha
h_w (cm)	-7.2	0.22	0.22	(0.7)	48 m	N = 30 locations; n = 4 depths (depth z=0 shown here)
θ_s	.397	0.10	0.10	(0.29)	----	Nielsen et al. (1973): Panoche soil
K_o (cm/h)	0.85	1.06	0.87	4.37	----	A = 150 ha; N = 20 plots n = 6 depths; (depth z=30 cm shown here)
K_o (cm/h)						Scisson and Wierenga (1981) A = 40 m^2 3 sets of infiltration rings:
						Diameter / Number
(1)	0.27	0.70	0.63	2.45	0.13 m	ϕ_1 = 5 cm / N_1 = 625
(2)	0.35	0.54	0.51	1.79	----	ϕ_2 = 25 cm / N_2 = 125
(3)	0.36	0.22	0.22	0.68	----	ϕ_3 = 127 cm / N_3 = 25
K_o (cm/h)	0.70	0.40	0.38	(1.26)	50 m (10-50 m)	Vieira et al. (1981): A = 0.88 ha; N = 1280 plots 160 plots / transect 55 transects
K_o (cm/h)	1.46	0.60	0.56	2.02	----	Sharma et al. (1980): watershed A = 9.6 ha N = 26 plots
K_o (cm/h)	0.13	1.02	0.84	4.10	0-2 m	Luxmore et al. (1981): A = 192 m^2 N = 48 plots

$$\alpha(x) = \left.\frac{\partial \ell n K}{\partial h}\right|_x \tag{5.1}$$

Russo's results indicate that both α and K_s are log-normally distributed, and that the correlation range of $\ell n\alpha(x)$ is significantly larger than that of $\ell n K_s(x)$.

The log-normality of K_s, α, and other inherently positive unsaturated soil parameters, seems to be confirmed by other authors. For convenience, we have listed in Table 5-2 the skewness coefficient γ. When indicated in parenthesis, the skewness was computed by us based on the assumption of *log-normality* instead of the normal distribution assumed by the authors (references are given in the right-most column). Thus, in all cases, the skewness γ_Y was computed from the classical identity:

$$\gamma_Y = 3CV_Y + (CV_Y)^3 \tag{5.2}$$

where CV_Y is the coefficient of variation of the log-normal random variable Y. In addition, we also used the following identities:

$$(CV_Y)^2 = \frac{\sigma_Y^2}{(\overline{Y})^2} = \exp(\sigma_{\ell n Y}^2) - 1 \tag{5.3}$$

$$\overline{Y} = Y_G \exp(\sigma_{\ell n Y}^2/2) \tag{5.4}$$

where Y_G is the geometric mean defined by:

$$Y_G = \exp(\overline{\ell n Y}) \tag{5.5}$$

Relations (5.2) through (5.4) can be found for instance in Vanmarcke (1983). They were used to compute the ℓnY-statistics in Table 5-2, when not provided by the authors themselves.

It appears that a number of authors adopted the normality assumption precisely in those cases where the variability was too mild to be able to distinguish a normal from a log-normal distribution. Overall, we conclude that all the parameters listed in the table were in fact more or less positively skewed, and are presumably better represented by log-normal distributions. Figure 5-5 illustrates the difference between a normal and a log-normal random function (artificially generated for illustration). Note the sharp maxima and smooth minima typical of a positively skewed random function.

Another feature that emerges from Table 5-2 is that the unsaturated conductivity curve seems *in general* to have greater variability than the water retention curve (although this is not always verified for a given site). The coefficient of variation of K_s was larger than unity in four cases, whereas the coefficient of variation of parameters involved in the $\theta(h)$ relation was always below or at most equal to 0.6.

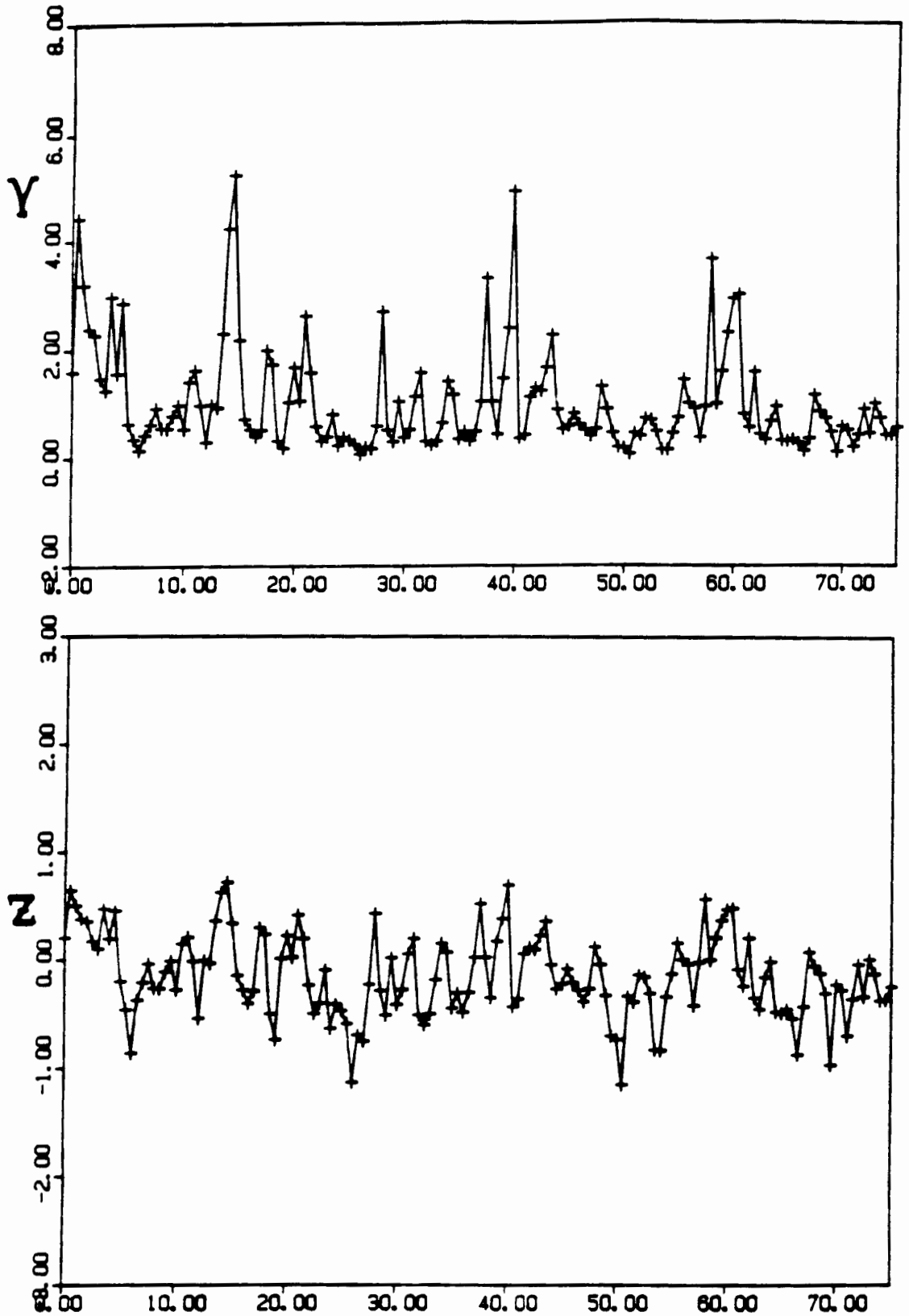

Figure 5-5. Synthetic realization of a 1D gauss-markov process with exponential covariance function (log-normal above, Gaussian below)

The data of Table 5-2 do not contain any information on the correlation structure of soil properties in the vertical direction. The horizontal correlation scales range from 10 cm to a few tens of meters. These numbers should be taken "with a grain of salt", as the apparent correlation scales are most probably influenced by the density and size of the measurement networks. In addition, the results of Scisson and Wierenga (1981) indicate that the scale of the instrument (infiltration ring) has a definite effect on variability. Finally, it should also be noted that the correlation structures were only determined for relatively small domains, on the order of one hectar for Russo and Bresler (1981), Vieira et al. (1981), and Russo (1983). The largest domain of investigation was the 150 ha site of Nielsen et al. (1973); however these authors did not determine any correlation structures.

More detailed two- and three-dimensional soil data are available in the Las Cruces Trench Database for the on-going strip-source trench experiment at the Jornada site near Las Cruces, New Mexico. These are reported in detail in Wierenga et al. (1986a,b), Wierenga et al. (1989), and INTRAVAL (1991, Appendix C). See also Jacobson (1990) for a variogram analysis of the Las Cruces soil, layer by layer. These data are currently being analyzed and processed in three-dimensional model validation activities of INTRAVAL Phase I and Phase II using the BIGFLO code (see section 6.6).

To summarize, the relatively large amount of data available for soils indicate that hydrodynamic parameters such as porosity, saturated conductivity, and certain shape factors of the conductivity and water retention curves, are all log-normally distributed (or more generally positively skewed). Precisely, it appears that investigators always arrived at this conclusion when variability was high enough to distinguish a skewed distribution from a symmetric one. Experimental evidence supporting this can be found in Nielsen et al. (1973), Warrick et al. (1977), Sharma et al. (1980), Gelhar et al. (1982), and Russo (1983). Data concerning the degree of spatial correlation and the multidimensional correlation structure of unsaturated flow properties are scant. In some experimental studies, the correlation scale was presumed to be negligible. In the comprehensive field measurements collected by Nielsen et al. (1973), spatial correlations were ignored altogether. In other studies like those of Scisson and Wierenga (1981), and Gajem et al. (1981), the investigators found a significant sensitivity of the observed variances and correlation scales with respect to the scale and spacing of measurements (e.g. from infiltration rate data on a network of infiltration rings of different sizes).

5.3.3 Auxiliary Hydrodynamic Models and Cross-Correlations

The statistical data summarized in Table 5-2, although collected with great efforts, are too scant to completely characterize the spatial variability of unsaturated soils hydraulic properties in terms of three-dimensional random field parameters. In the case of the Las Cruces Database evoked above, for instance, there are no data characterizing the spatial structure of relative unsaturated conductivity curves. Part of the missing information could be recovered by using models correlating readily accessible parameters (such as K_s and θ_s) to other less accessible parameters.

Several possibilities can be advanced in view of the literature, although no single approach is widely accepted: capillary tube models, leading for instance to Mualem's relation between conductivity curve and retention curve (Mualem, 1976); classical Kozeny-Carman relation and

its extension to unsaturated flow; similar media hypothesis; etc. Some of these concepts, which are derived from microscopic analyses of porous medium hydrodynamics, were reviewed earlier in Chapter 4. However, the conductivity curve cross-correlation model may also be applicable to large-scale analyses of effective conductivity based on stochastic concepts, as explained below.

5.3.3.1 Conductivity Curve Cross-Correlation

One possible approach toward reducing data requirements is to seek a correlation between the spatially variable slope α and intercept $\ln K_s$ of the $\ln K(h)$ curve. This amounts to correlating the saturated conductivity K_s to the capillary dispersivity length scale $\lambda_c=1/\alpha$. The latter is thought to be related to the width of the pore size distribution, but also could be influenced by micro-fissuration or fracture density, depending on the scale of measurement.

Figure 5-6 reproduces the unsaturated conductivity curves obtained by Nielsen et al. (1973) on the Maddock sandy loam. Note that both the saturated conductivity and the overall slope of the $\ln K(h)$ curve are fairly variable from one curve to another (spatial variability in the horizontal direction). The figure does not clearly indicate a strong degree of correlation between these two parameters, although some correlation could be expected to exist, as coarser soils, which are more permeable at saturation, also have (generally) a steeper $\ln K(h)$-slope. This fact was illustrated earlier in Section 4.3.2, Figure 4-3 and Table 4-2 using representative soil types from different sites (from Ababou, 1981).

In the case of variably fissured rocks, although direct evidence is lacking, it is suspected that a significant correlation should exist between the bulk saturated conductivity and the rate of decay of unsaturated conductivity with suction. This correlation would be directly due to fissuration, provided however that the density of fissuration be high enough or the scale of measurement large enough to average out individual fissures. Numerical experiments of three-dimensional moisture plume migration (Ababou, 1988, Chapter 7) and one-dimensional infiltration (Yeh, 1989) in statistical continuum soils revealed that the presence or absence of cross-correlation can have significant effects on the macroscale behavior and heterogeneity of the flow system. A new stochastic model that accounts for both spatial correlation and local cross-correlation has been developed and is being refined (Ababou, 1991). Figure 5-7 gives a schematic representation of one of the findings of the model: conductivity anisotropy is minimized for suction such that the local conductivity curves intersect at that point. The model makes a similar statement in the case of many random curves, rather than just two conductivity curves. In addition, a statistical upper bound to the composite conductivity curves is obtained. These results and their interpretation will be presented in future reports.

5.3.3.2 Similar Media Hypothesis

This approach expresses the spatially variable $K(h,x)$ and $\theta(h,x)$ curves in terms of reference curves $K(h)$ and $\theta(h)$ multiplied by spatially variable scaling parameters. In its original form, the similar media model reduces the characterization of spatial variability of $\theta(h)$ and $K(h)$ to that of just one random scaling factor. However, because of failure to satisfy the hypothesis, investigators have relaxed the theoretical requirement and adopted two distinct scaling factors, one for $\theta(h,x)$, and one for $K(h,x)$. More details are given in Section 4.3.5. For experimental data and procedures, see Warrick et al. (1977), Simmons et al. (1979), Russo and Bresler (1980),

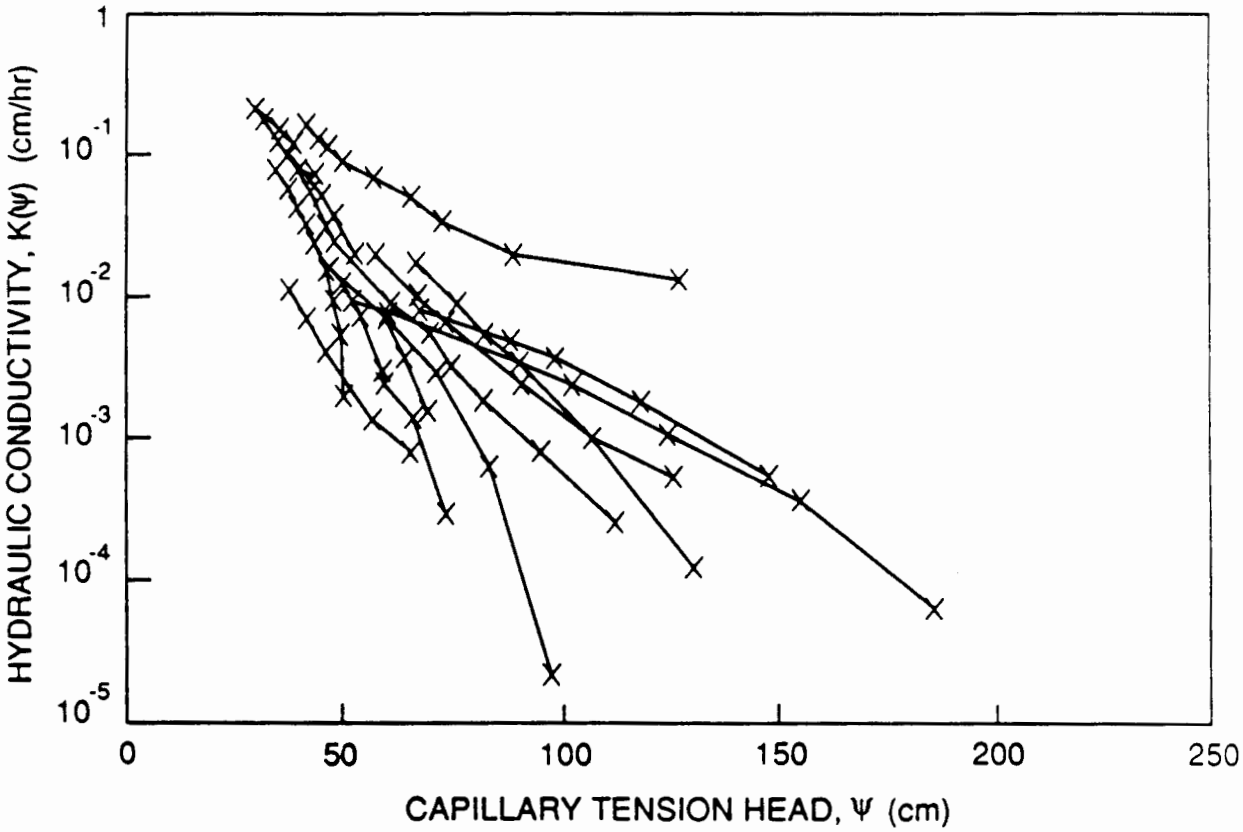

Figure 5-6. **Unsaturated hydraulic conductivity versus capillary tension head for the maddock sandy loam (from Mantoglou and Gelhar, 1987a, and Polmann et al., 1988).**

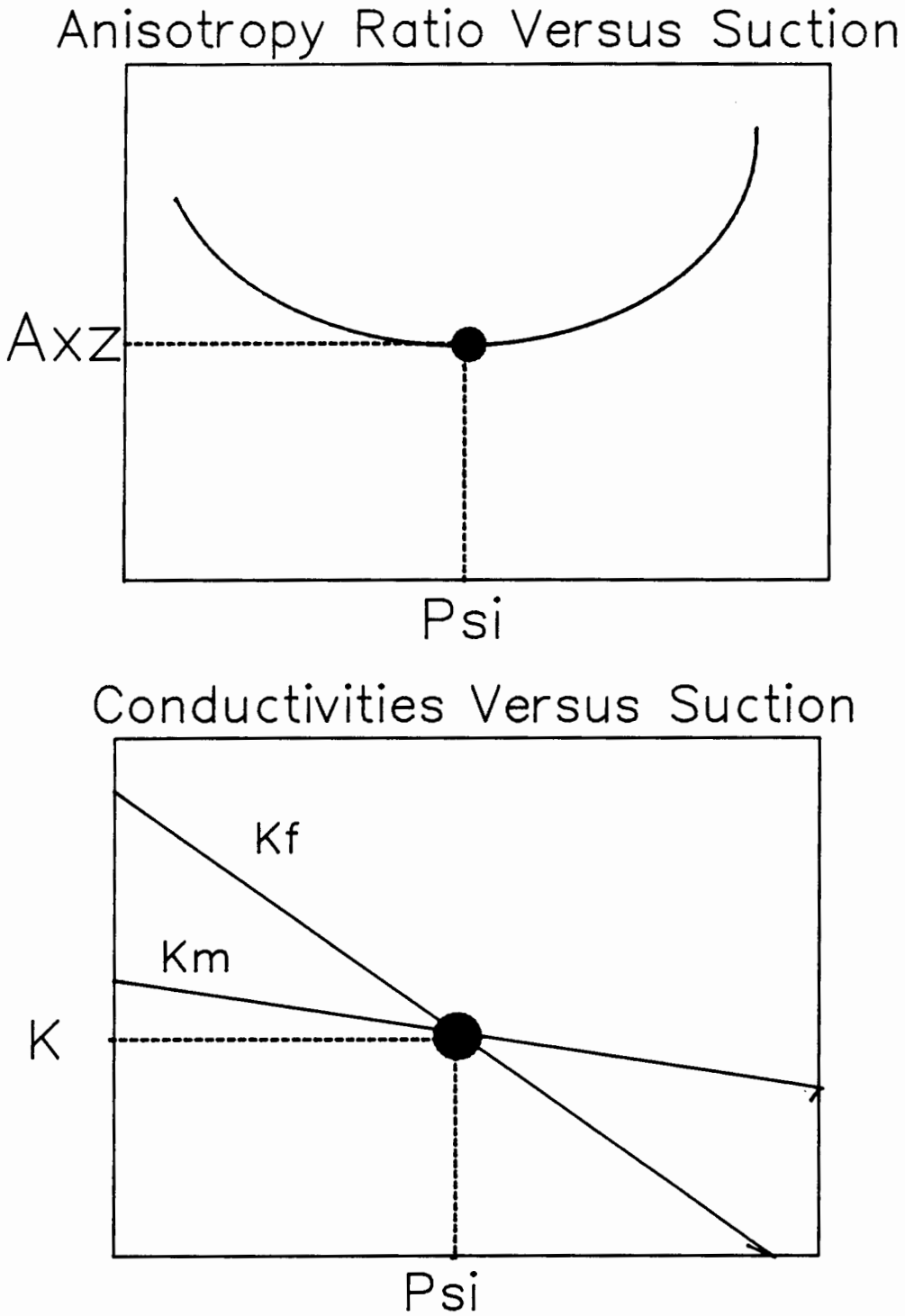

Figure 5-7. **Schematic representation of suction-dependent anisotropy of conductivity, and crossing point of fracture-matrix conductivity curves**

Vauclin et al. (1981), Sharma et al. (1980), and Claustnitzer et al. (1990).

In conclusion, future research should focus on the development and assessment of such correlations or similarity assumptions, as a means of characterizing in a more comprehensive fashion the spatial variability of the nonlinear constitutive relations of unsaturated porous media. New models of the kind reviewed above need to be developed specifically for fissured rocks.

5.4 FIELD CHARACTERIZATION OF FRACTURED ROCKS AND FRACTURE NETWORKS

5.4.1 Hydraulic Characterization and Mapping of Fracture Networks

In addition to the Yucca Mountain fracture data compiled in the Site Characterization Plan (1988) and those available from the Nevada Test Site G-Tunnel (INTRAVAL*, 1991), two possible sources of data have been identified concerning the multidimensional geometry of rock fracture networks: (1) fracture traces and three-dimensional fracture network at the inclined borehole site of the Apache Leap tuff site (Rasmussen et al., 1990, and INTRAVAL, 1991, Appendix B); (2) statistical data on two- and three-dimensional fracture orientations at the uranium mine drift site of Faney-Augères, France (after Long and Billaux, 1987; Cacas et al., 1990a,b; and references therein).

A stereonet projection of fracture strikes and dips observed at the Apache Leap Inclined Borehole site is shown in Figure 5.8, from Yeh et al. (1988, Figure 8). These data were collected from oriented cores during the drilling of the boreholes. The three-dimensional domain covered by the boreholes is on the order of 10 m^3. In addition, fracture trace data were also collected and analyzed. Figure 5.9 shows a large-scale map of fracture traces at Apache Leap, and Figure 5.10 shows a smaller scale map in the vicinity of the Borehole Site and Heater Site [INTRAVAL, 1991, Appendix B (to be published)]. The principal axes of fracture orientations were determined by Thornberg (1990) using the Bingham distribution method (Cheeney, 1983). Approaches to deal with the recovery of three-dimensional fracture orientations and densities from one- or two-dimensional intersections and traces are discussed in Andersson et al. (1984) and Long and Billaux (1987), among others.

A stereonet of fracture orientation data collected at the Faney-Augères Drift site is given in Figure 5.11 (Long and Billaux, 1987, Figure 5). The Faney Augères drift wall where fracture traces were observed was 180 m long by 2 m high. In addition, ten 50 m long radiating boreholes were used for core analysis, fracture logging, and in-situ permeability packer tests. The five fracture sets depicted on Figure 5.11 were identified in an ad-hoc manner. Long and Billaux noted that sixty percent of the observed fractures do not fall into any of the seven tectonic classifications proposed elsewhere. For aperture distributions, they used the results of over 200 packer tests, along with some direct observations of core aperture, to infer the probability distribution of fracture apertures within each set. Long and Billaux analyzed also the

*INTRAVAL - An International Project to Study Validation of Geosphere Transport Models. Unsaturated Zone Test Cases, in Phase I Final Report. T.J. Nicholson, ed. To be published by Swedish Nuclear Power Inspectorate. Stockholm, Sweden.

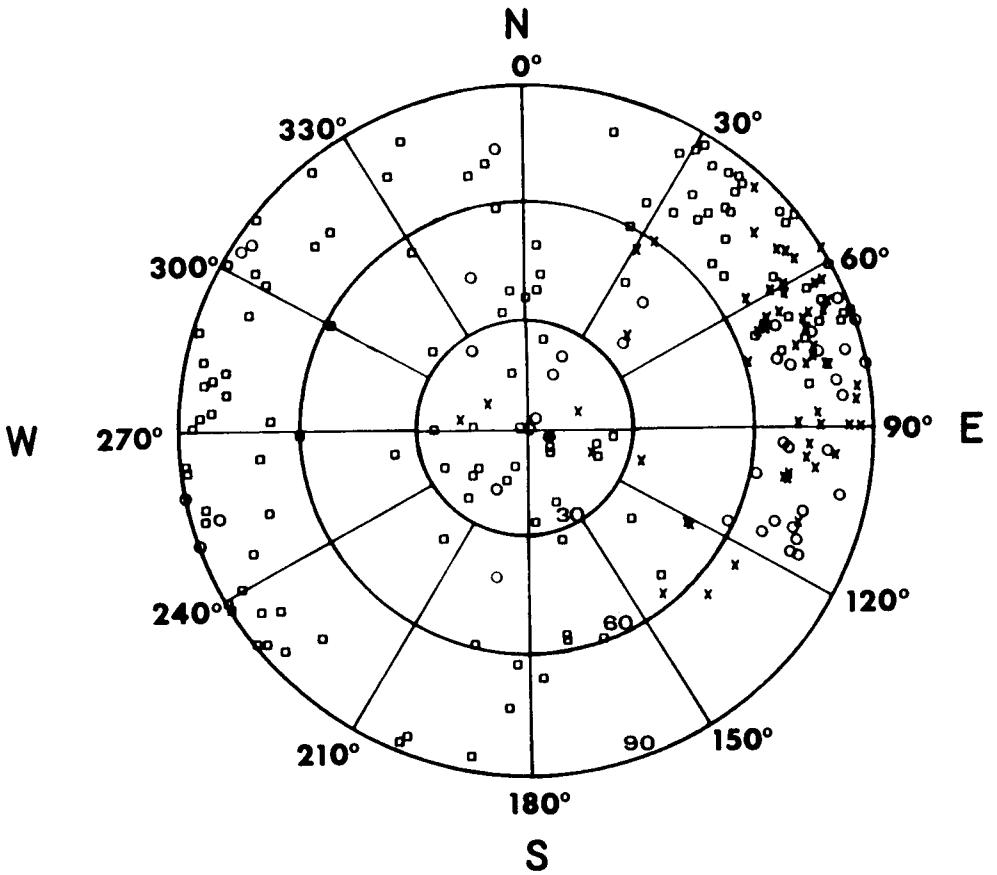

Figure 5-8. **Lower stereonet projection of fracture orientations observed at Apache Leap Tuff site, from X-series boreholes (crosses), Y-series boreholes (circles), and Z-series boreholes (squares) [from Yeh et al., 1988].**

Figure 5-9. **Line interpretation of structural lineaments in the Apache Leap Tuff. Fractures were traced from an aerial photo scaled at 1:14,350. The area bounded by registration marks has been studied in detail (Thornburg, 1990).**

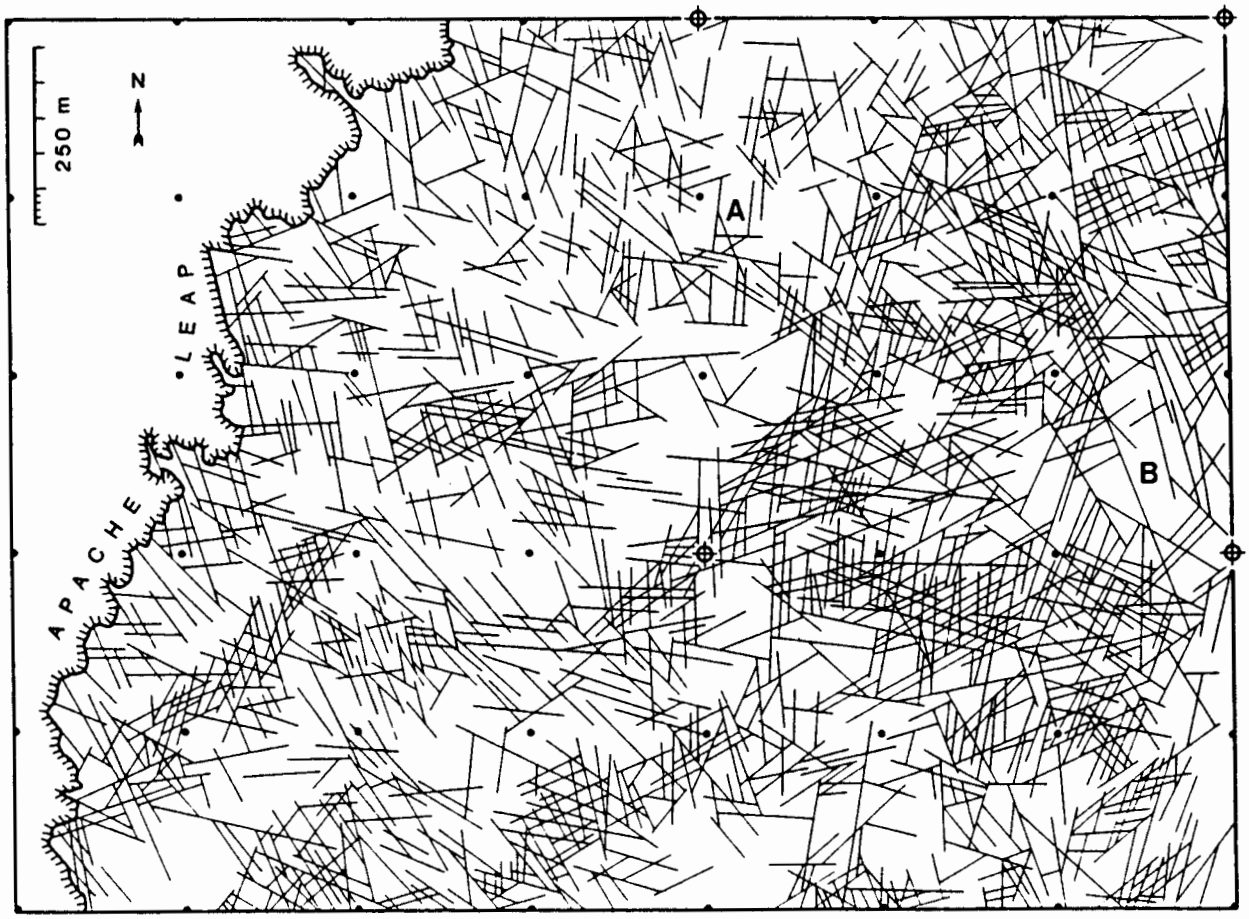

Figure 5-10. Line interpretation of structural lineaments in the Apache Leap Tuff. Fractures were traced from an aerial photo scaled at 1:7,180. The University of Arizona field sites are located: [A] Rock Knoll Heater Site, and [B] Inclined Boreholes Site. The area bounded by registration marks has been studied in detail (Thornburg, 1990).

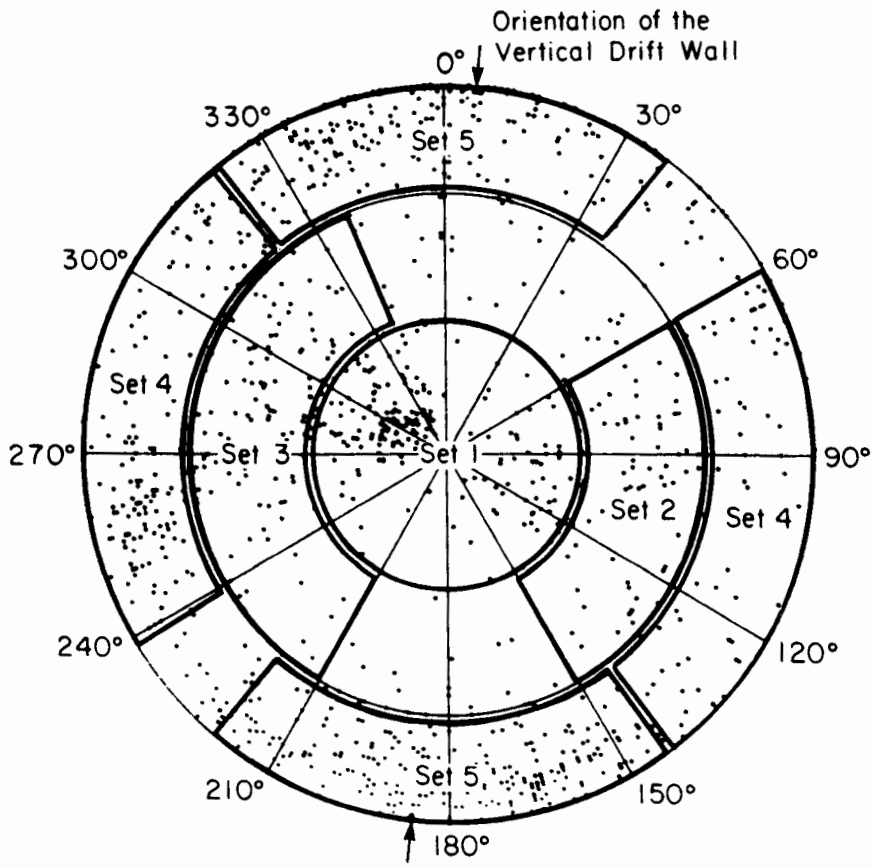

Figure 5.11. Definition of sets and poles of fractures mapped in the 80m section of the drift wall at the Faney-Augères mine (from Long and Billaux, 1987).

distributions (mean and variance) of orientation angles and fracture lengths. In all, about 7000 fractures were analyzed for either orientation, location, and permeability or aperture characteristics.

Long and Billaux used a single random network model to generate a two-dimensional synthetic fracture network comprising 65,470 fractures. This synthetic network is reproduced in Figure 5.12, from Long and Billaux (1987, Figure 9). The generation procedure is relatively straightforward conceptually. Each of the five sets was generated separately, and all five fracture sets were then superimposed in space. For each set, the generation procedure was as follows: (1) fracture centers were generated randomly based on measured fracture density; (2) fracture orientations were randomly assigned to each center based on measured fracture density; (3) fracture lengths were randomly assigned based on log-normal or exponential distribution; and (4) fracture apertures were randomly assigned based on log-normal distribution. Each random parameter was generated independently, e.g. without correlations between fracture aperture and orientation, etc. The procedure can be applied to subdomains, in order to allow for large-scale variations of fracture network statistics such as density, mean aperture, mean orientation, etc.

In Hestir et al. (1989), the same site of Faney-Augères was modelled in three dimensions using instead a parent-daughter fracture generation model. Parent-fractures were generated according to a doubly stochastic Poisson process, while daughter-fractures were distributed around each parent according to a simple Poisson process. Other fracture generation models could conceivably be fitted to the same data.

Although the fracture densities, orientations, and apertures at the Faney-Augères site are not expected to be directly analogous to the Yucca Mountain site, screening of these statistical data will provide valuable information for constraining statistical models of fracture networks in preliminary simulations of the Yucca Mountain flow system. This will be discussed in a future report.

5.4.2 Hydraulic Characterization of Unsaturated Fractured Rocks

Several controlled field experiments are presently being conducted in unsaturated fractured tuff at the Apache Leap site near Tucson, Arizona (Evans and Nicholson, 1987; Rasmussen and Evans, 1987; Rasmussen et al. 1990). It should be noted that the Apache Leap experiments appear to be unique, in that they are geared specifically towards in-situ hydrodynamic characterization of unsaturated fractured rock on relatively large three-dimensional scales (on the order of ten meters, large relative to laboratory scales). In addition, the rock formations at Apache Leap are analogous, albeit not identical, to those of Yucca Mountain (fractured tuffs). The Apache Leap multiple experiments (ongoing or planned) include, in particular, in-situ gas pumping tests for assessing, somewhat indirectly, the hydraulic permeability of the rock and the associated fracture system. Gas pumping tests can be interpreted by using suitable inverse methods, or type-curve methods, based on single-phase compressible flow models. To actually *measure* the relative permeability at low saturation of the moving fluid (gas), would require forcing some water into the rock before pumping the gas, assuming furthermore that the water phase remains immobile during gas pumping even at high moisture content. However, this approach would yield the relative permeability for the non-wetting phase, rather than that for the

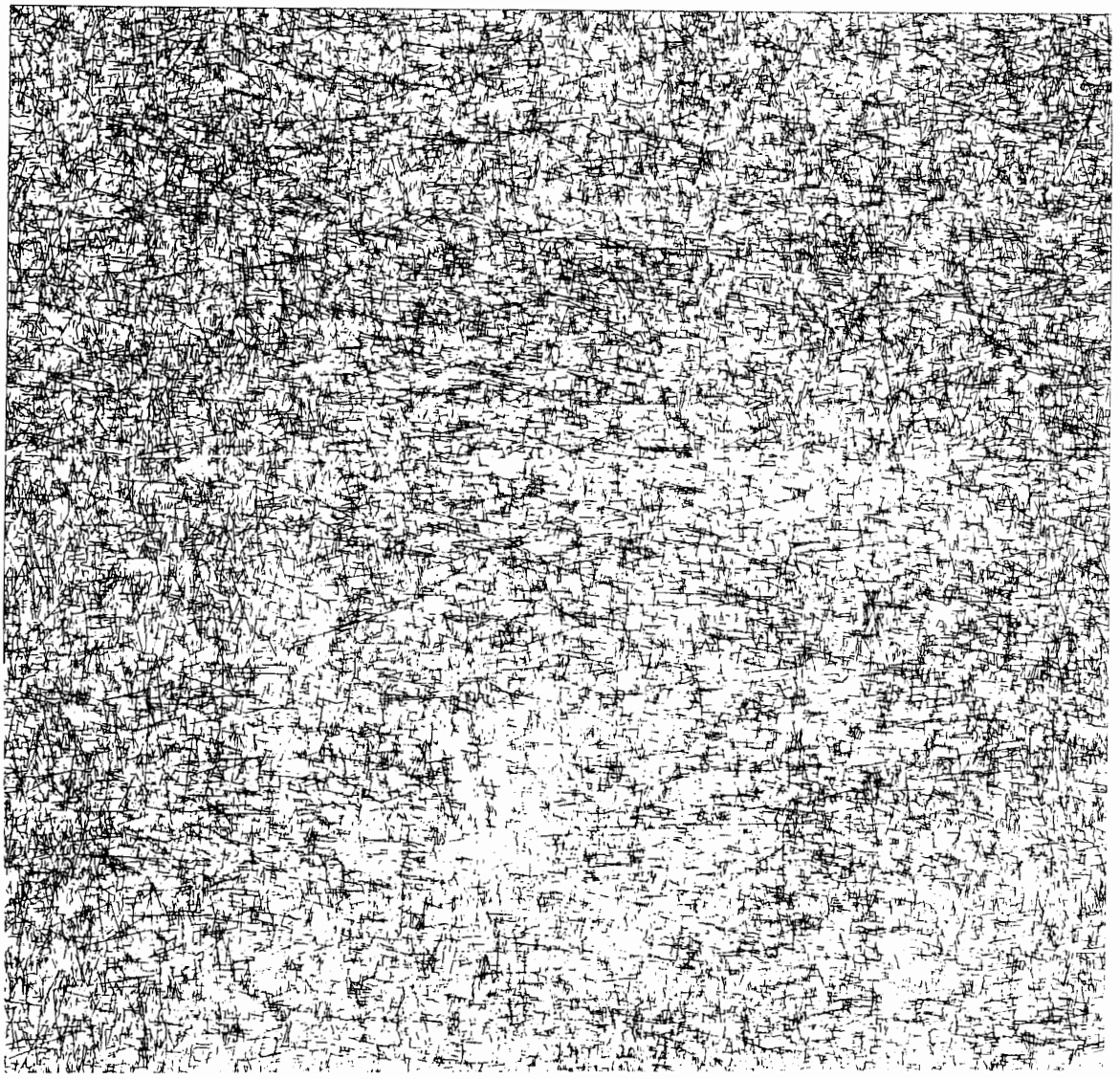

Figure 5-12. Synthetic two-dimensional fracture network in a 100m × 100m domain, where each 10m × 10m subdomain was generated independently. The total number of fractures is 65,740 (from Long and Billaux, 1987).

wetting phase. A model relating these two constitutive relations would be needed in order to obtain the relative permeability with respect to water.

CHAPTER 6. OUTLOOK OF FIELD-SCALE FLOW MODELING FOR HETEROGENEOUS AND FRACTURED UNSATURATED MEDIA

6.1 GENERAL CONSIDERATIONS

Modeling involves essentially three stages: defining physically identifiable variables and parameters for the hydrogeologic setting at hand formulating the conceptual model and governing equations; and actually solving equations for prescribed values of model parameters. In the case at hand, this last step is to be implemented numerically, since we do not expect to obtain analytical solutions except under highly idealized conditions. It is, however, important to keep in mind the distinction between the conceptual model and its numerical implementation (sometimes dubbed "numerical model"). Both aspects will be examined in this chapter.

The advantages and disadvantages of alternative modeling approaches to subsurface flow should be assessed, in our view, on the following criteria:

(1) *Equations:* The governing equations and auxiliary models should be physically-based and generic, rather than empirical. In other words, the model and submodels should be based on as much physics as possible, with minimal use of empirical coefficients and adjustment parameters.

(2) *Simplifying Assumptions:* The necessary simplifications introduced at various stages should form a self-consistent set of assumptions, should be consistent with the objectives of modeling, and should capture the known characteristics of the field site. In the case at hand, for instance, assumptions aimed at simplifiying the three-dimensionality, discontinuity, fracturation, stratification, anisotropy, and nonlinearity of hydraulic coefficients, may not be justifiable if the objective is to identify the entire distribution of travel times and/or to identify the fastest flow paths. In addition, it may not be consistent to proceed with a fine representation of heterogeneities in less than three dimensions, as this would artificially limit the degree of freedom of fluid and contaminant pathways. The steady state assumption may be justifiable provided that it does not conflict with the imposed boundary conditions. Indeed, steady solutions can be either unbounded or unstable under certain conditions; the former case is usually obvious, but not the latter. At any rate, transient simulations may be needed to back up (or even validate) steady state calculations.

(3) *Model Inputs:* The model should be as parsimonious as possible in terms of input parameters, particularly in the absence of high-quality data. This requirement puts a bound on the allowed degree of sophistication of the model. In the direct simulation approach to stochastic modeling, a few statistical parameters are used to generate a large number of hydrogeologic coefficients. The statistical parameters need not be precisely evaluated; they should be estimated by combining site-specific data with indirect, non-specific information from related experiments and sites. In this way, relatively parsimonious stochastic models can be used to simulate highly heterogeneous flow systems in detail. This could also be achieved in principle by

purely descriptive models, but only at the exorbitant cost of collecting a very large quantity of data in-situ. On the other hand, the selected model should not be so parsimonious as to ignore significant and singular features of the subject site.

(4) *Computational Feasibility:* Finally, it should be demonstrated that the numerical solution of model equations is computationally feasible with current computing hardware, such as workstations and supercomputers. Computational feasibility depends, of course, on the efficiency of specific solution algorithms selected for numerical implementation of the model. New conceptual models may require new algorithms for their solutions. Owing to the complexity of unsaturated flow processes in highly heterogeneous and fractured media, it is expected that the numerical implementation of any realistic model of these processes will be non-trivial. Therefore, the judicious selection or development of efficient algorithms may be key to the whole modeling approach.

6.2 CONCEPTUAL APPROACHES TO FIELD-SCALE FLOW MODELING

As observed earlier, it is now increasingly recognized that accurate modeling of hydrogeologic flow and transport systems over large space-time scales requires adequate representation of a whole hierarchy of natural heterogeneities, discontinuities, and/or fractures having many sizes and shapes. See for instance Cushman (1990) for a recent collection of works in this area. Moreover, in the case of partially saturated or unsaturated flow, the complex spatial features of the geologic medium must be represented through nonlinear matrix/fracture hydrodynamic properties according to Richards equation (4.38). Therefore, the difficulty in modeling heterogeneous processes is compounded by the nonlinear nature of the governing equations, owing to the nonlinear pressure-dependence of unsaturated moisture content and hydraulic conductivity.

Based on the current literature, scientific approaches to field-scale flow modeling can be broadly classified in two types. The first type of approach is essentially a direct simulation of the detailed hydrodynamics based on classical Darcy-Richards equations. This requires an explicit representation of fine-scale heterogeneities, stratification, and/or fracturation of the geologic medium, e.g., based on a combination of geostatistical models and hydrogeologic data. The second type of approach, coarse-scale or effective modeling approach, makes use of auxiliary sub-scale models, more or less physically-based, for describing in a simplified way the detailed hydrodynamics processes not explicitly accounted for in the coarse-scale simulation model. Combinations of these two approaches are also conceivable, as will be explained below.

6.2.1 Direct Simulation Approach

A clear advantage of the direct simulation approach is that, in principle, it requires only basic phenomenological equations to model the flow system, such as the classical Darcy-type equations, and additional constitutive relations for fractures, if any. However, while fine-scale spatial variations of groundwater velocity are known to play a significant role in radionuclide transport and dispersion (Gelhar and Axness, 1983; Winter et al., 1984; Dagan, 1987), there are obvious limits to how extensively and explicitly the broad spectrum of geologic heterogeneities can be represented in a flow model. In the first place, site-specific data are not likely to be

available with the required degree of detail, so that much effort must be put in auxiliary analyses - e.g., statistical interpolation and conditioning, use of soft information, statistical continuum models of heterogeneous porous media, random fracture network models, and so on. Secondly, the computational demands are likely to be high, which requires an informed evaluation of computational feasibility and a careful selection of advanced solution methods and supercomputer resources. The computational demands in the case of fractured porous media, with both continuum and discontinuum-type heterogeneity, are likely to be even higher owing to the extreme disparity of active fluctuation scales - from fracture aperture up to the largest identifiable geologic features.

6.2.2 Indirect Simulation Approaches

Alternatives to the direct simulation approach utilize auxiliary hydrodynamic models in order to alleviate part of the above-mentioned demands. The main idea behind this indirect modeling approach is to simplify the overall flow model by subsuming certain spatial features and processes in simplified black-box models. For instance, all heterogeneities and fractures would be subsumed in various submodels. Typically, these auxiliary models express effective constitutive relations, matrix/fracture transfer relations, and other conceptual relations, in a quasi-analytical fashion:

(1) *Single Equivalent Continuum:* The heterogeneous and/or fractured medium is treated as a single homogeneous continuum with unique effective coefficients, e.g. with specific moisture capacity and hydraulic conductivity tensor depending nonlinearly on pressure through known spatial-statistical properties of the medium (for an equivalent continuum treatment of non-fissured stratified media, see Polman et al., 1988). This type of approach captures the pressure-dependent anisotropy due to stratification, but not that due to fractures.

(2) *Dual Equivalent Continuum (Double Porosity):* The fractured medium is treated as a mixture of two distinct continua of unspecified geometry, a homogeneous matrix (tight porosity) and a homogeneous fracture continuum (coarse porosity). Each continuum is characterized by distinct pressure, flux, and hydrodynamic parameters; an effective transfer term is added to keep track of transfers between the two continua (Barenblatt et al., 1990; Shapiro, 1987). This type of approach requires refinements in modeling the transfer terms and defining the (anisotropic) conductivity of the so-called "fracture continuum".

(3) *Combination of Single and Dual Equivalent Continua:* The dual equivalent continuum model has been traditionally implemented assuming spatially uniform properties for each continuum. However, if effective flow models are made available for each type of equivalent continuum, then it may be possible to improve the overall model by combining (1) and (2) above. For instance, Mantoglou and Gelhar (1987a,b,c) may provide an acceptable equivalent model for randomly stratified porous matrix. This may possibly be extended to anisotropic rock matrix containing microfissures. Concerning fractures, the hydrodynamic transfer term between matrix and fractures as proposed in the literature, may have to be seriously reconsidered.

6.2.3 Combination of Direct and Indirect Modeling

In fact, the indirect approach to heterogeneous flow modeling can be used in combination with explicit modeling of certain types of heterogeneities that are either not accounted for by the auxilary models, or too important to be treated implicitly. This is obviously indicated in the case of major (mesoscale to macroscale) geologic features such as faults, extensive fractures, bedding sequence of geologic units, and large-scale trends in hydraulic parameters (e.g. due to increasing overburden with depth). Besides explicit modeling of site-specific large scale geologic discontinuities and trends, auxiliary models such as reviewed above would be used to deal with smaller scale heterogeneity in a simplified manner.

In conclusion, when indirect modeling methods are implemented with a view to obtain representative field-scale simulations of site-specific processes, direct representation of heterogeneities is still needed to capture essential features. As a consequence, only a limited part of the modeling effort can be transferred from the global model to the submodel(s). In addition, there are pending questions regarding the conceptual/empirical basis of the submodels, their consistency with the global model, their intrinsic range of validity, and the identifiability of their internal parameters. The physical basis of effective continuum and double-porosity continuum models needs to be better ascertained, particularly for the case of unsaturated flow. These questions ought to be fully answered before indirect simulation models can be used with confidence for the subject site. Specific modeling approaches are now being reviewed and discussed.

6.3 SINGLE EQUIVALENT CONTINUUM MODELS

Equivalent media models, based on effective moisture retention and effective conductivity curves, have been previously developed for stratified, but continuous, random media (Yeh et al., 1985a,b,c; Mantoglou and Gelhar, 1987a,b,c) and have been tested numerically (Ababou, 1988; Yeh, 1989). In spite of the many approximations involved, these equivalent models have the advantage of being clearly derived from the microscale governing equations (Darcy-Buckingham and mass conservation). Unfortunately, no comparable unsaturated flow equivalent model is available for a *discontinuum* such as fractured porous rock. Instead, empirical equivalent models have been used.

One notable semi-empirical model for representing the unsaturated fracture/matrix system as a single equivalent continuum, was proposed and tested by Pruess et al. (1986). In their effective continuum approximation, the unsaturated conductivity of fractured rock is approximated by the simple arithmetic sum:

$$K(h) = K_m(h) + K_f(h) \tag{6.1}$$

A similar isotropic conductivity for composite fracture/matrix medium was also employed by Peters and Klavetter (1988, Eqns. 18-21). Pruess et al. (1986) recognized and demonstrated that this approximation is based on hypothetical equilibrium between fracture and matrix pressures, and breaks down in the presence of fast transients. More recently, Pruess et al. (1990a,b) tested their effective continuum approximation under various conditions involving near-field nonisothermal, two-phase flow in the vicinity of a hot waste package. They concluded again that

the approximation breaks down for very tight rock matrix, large fracture spacings, and/or rapid transients.

Another potential shortcoming of Eqn. (6.1) is that the effective conductivity of the fractured medium is assumed to be isotropic. This appears to be in contradiction with other models such as Wang and Narasimhan (1985), reviewed below. The derivation of the effective continuum approximation presented in Pruess et al. (1990b, Appendix) starts with isotropic Darcy equations for the matrix and the fractures, respectively. While the intact rock matrix can possibly be assumed isotropic as a first approximation, there is no physical basis for assuming isotropy of the fracture system, except in the very special case of continuous, uniform, and isotropic distribution of fracture orientations. It may be concluded that, although models based on Eqn. (6.1) have been successfully tested for near-field simulations focussing on coupled heat-fluid flow phenomena, they may not be strictly applicable to large-scale three-dimensional flow in the presence of non-isotropically distributed fractures and/or non-isotropic matrix properties.

6.4 DUAL CONTINUUM MODELS AND FRACTURE/MATRIX FLOW

For reviews of dual continuum approximations, see Shapiro (1987), Barenblatt et al. (1990), and Gureghian and Sagar(1991). Early proponents of the dual continuum approach were Barenblatt et al. (1960), Warren and Root (1963), and Streltsova (1976). The dual continuum approximation considers separate governing equations for the fluid in the fracture system (*f*) and the fluid in the porous matrix (*m*), with a coupling term to model transfers between the two systems. Note that this approach is similar to that required for modeling multi-phase immiscible fluids, except that the two fluid "phases" are not truly distinguishable here. The term "phase" is, therefore, a slight abuse of language.

In the case of transient saturated flow through a fractured porous rock, the postulated dual continuum equations are of the form:

$$\frac{\partial}{\partial t}(\rho\theta_m) = \rho C_m \frac{\partial h_m}{\partial t} = -\vec{\nabla}(\rho\vec{q}_m) - \rho\Gamma \tag{6.2a}$$

$$\frac{\partial}{\partial t}(\rho\theta_f) = \rho C_f \frac{\partial h_f}{\partial t} = -\vec{\nabla}(\rho\vec{q}_f) + \rho\Gamma \tag{6.2b}$$

where θ is the volume fraction (e.g. porosity), C is the specific capacity (e.g. specific storativity), $\vec{q}$ is the specific discharge rate or flux (related to velocity by $\vec{q} = \theta\vec{v}$), and ρ is the fluid density. All these quantities are defined for the matrix fluid and the fracture fluid, respectively, except for fluid density ($\rho = \rho_m \approx \rho_f$). Finally, $\rho\Gamma$ is the rate of exchange of fluid mass between the two continuum systems.

The main assumptions of the model are that (1) the flux $\vec{q}$ in each continuum is governed by a Darcy equation, and (2) the exchange term Γ is proportional to the local pressure difference between the two fluid "phases". The individual Darcy laws are given by:

$$\vec{q}_m = -K_m \vec{\nabla}(h_m + z) \tag{6.3}$$

$$\vec{q}_f = -\overline{\overline{K}}_f \vec{\nabla}(h_f + z) \tag{6.4}$$

Furthermore, Barenblatt and others assumed that the exchange term is proportional to $(h_m - h_f)$ times porous matrix conductivity divided by an areal scale A_f (m^2):

$$\Gamma = \frac{K_m}{A_f}(h_m - h_f) \tag{6.5}$$

Note the following limitation: matrix conductivity, unlike fracture conductivity, is required to be isotropic in order for Γ to be a scalar quantity. This is the reason for not using a tensor conductivityin Eqn. (6.3).

Several alternative interpretations of A are possible. One may consider that $A_f = \ell^2$, $A_f \sim \ell/\sigma$, or $A_f \sim 1/\sigma^2$, where σ is the specific area of fractures (m^2/m^3), and ℓ a typical block size (m). The exact interpretation depends on assumed representations of the actual porous/fracture system (see Warren and Root, 1963; Kazemi, 1969; Gilman and Kazemi, 1983; and Narasimhan, 1982). In Narasimhan (1982), it is shown that $A_f \sim \ell^2/4$ for a system of parallel fractures with spacing ℓ. In this particular case the specific fracture area is just $\sigma = 1/\ell$, so that $A_f = \ell^2/4 = \ell/4\sigma = (2\sigma)^{-2}$.

Equations (6.2) through (6.5) have been adapted for numerical simulations of matrix/fracture flow through *unsaturated* media. In the unsaturated case, θ represents volumetric moisture content rather than porosity, C represents specific moisture capacity rather than storativity, and K represents unsaturated conductivity rather than saturated conductivity. However, the mere formulation of Eqns. (6.2) through (6.5) is not sufficient to specify completely the dual continuum model for implementation in specific cases. In particular, it is not clear how the moisture retention curve $\theta_f(h_f)$ and the unsaturated conductivity tensor $\overline{\overline{K}}_f(h_f)$ should be determined from geometric and hydraulic fracture data. Furthermore, generalization of Eqn. (6.5) to the unsaturated case has not been critically examined by independent means, whereas some evidence of the correct form of Eqn. (6.5) exists for the case of saturated flow. For instance, mixture theory was used to obtain transfer terms similar to Eqn. (6.5) plus additional terms which were found negligible in the case of fast pressure propagation (see Shapiro, 1987, Section 3.2.2). In the nonlinear case of unsaturated flow, however, the celerity c of pressure disturbances can be slow or fast depending on ambient moisture conditions ($c = dK/d\theta$). Moreover the averaging operations used in mixture theory are more difficult to justify when the local coefficients are nonlinear functions of pressure. Another criticism of Eqn. (6.5) is that the transfer term Γ does not explicitly incorporate parameters that take into account the inherent anisotropy of fracture systems.

In the case of *saturated* flow, where the assumptions $K_m \ll K_f$ and $\theta_f \ll \theta_m$ can be justified, the dual continuum equations can be reformulated in a more attractive way for the fracture fluid alone. Indeed, neglecting matrix saturated conductivity and fracture porosity in Eqns. (6.2) and inserting the postulated transfer term Γ from Eqn. (6.5) yields:

$$\rho C_m \frac{\partial h_m}{\partial t} = -\rho \frac{K_m}{A_f}(h_m - h_f) \tag{6.6a}$$

$$0 = -\vec{\nabla}(\rho \vec{q}_f) + \rho \frac{K_m}{A_f}(h_m - h_f) \tag{6.6b}$$

The matrix pressure h_m can be eliminated by time-differentiating the second equation, substituting the first equation, and neglecting fluid compressibility (not a critical assumption). This yields:

$$C_m \frac{\partial h_f}{\partial t} = -\left\{\vec{\nabla} \cdot \vec{q}_f + \frac{A_f C_m}{K_m} \frac{\partial}{\partial t}(\vec{\nabla} \cdot \vec{q}_f)\right\} \tag{6.7}$$

But, since the matrix and fracture continua are assumed to be homogeneous, and since both media are assumed here to be fully saturated, the parameters A_f, C_m, and K_m are constant in space and time. This allows us to take the divergence operator out of the brackets, leading to:

$$C_m \frac{\partial h_f}{\partial t} = -\vec{\nabla} \cdot \left(\vec{q}_f + \frac{A_f C_m}{K_m} \frac{\partial \vec{q}_f}{\partial t}\right) \tag{6.8}$$

Equation (6.8) is similar to equations previously given by Barenblatt et al. (1990, Section 1.8.2) and by de Marsily (1986, Section 4.1). The latter author judiciously observed that an equation like (6.8) can be interpreted as a special time-dependent Darcy law for fractured porous media. Indeed, combining Darcy's equation (6.3) through (6.4) with Eqn. (6.8) gives:

$$C_m \frac{\partial h_f}{\partial t} = -\vec{\nabla} \cdot \vec{q}_{mf} \tag{6.9}$$

where $\vec{q}_{mf}$ is a composite flux incorporating both fracture flow and matrix/fracture exchanges, satisfying the generalized time-dependent Darcy equation:

$$\vec{q}_{mf} = -\overline{\overline{K}}_f \cdot \vec{\nabla}(h_f + z) - \frac{\overline{\overline{K}}_f A_f C_m}{K_m} \vec{\nabla}\left(\frac{\partial h_f}{\partial t}\right) \tag{6.10}$$

Note that the storage term on the left in Eqn. (6.9), C_m, is the storativity of the matrix while the conductivity tensor in the first term of the generalized Darcy law (6.10) is that of the fracture continuum. This reflects the assumptions noted earlier. Fracture storage effects are neglected, and matrix conductivity is neglected except for its role in regulating matrix/fracture exchanges (second term of the generalized Darcy law). Unfortunately, Eqns. (6.9) through (6.10) are not directly applicable to unsaturated flow, since flow through the unsaturated matrix continuum can

far exceed that occuring in the unsaturated fracture continuum, depending on the precise initial and boundary conditions, fracture apertures, and so on. Nevertheless, the time-dependent Darcy law (6.10) suggests a more fully tensorial law that takes into account the anisotropic structure of both matrix and fractures, and regulates the matrix/fracture transfers in a more realistic fashion. To formulate such a tensorial law, particularly in the nonlinear case of unsaturated flow, would require revising the postulated exchange term of Eqn. (6.5) based on detailed fluid flow equations with locally defined pressures and explicit fracture network geometry.

Special versions of the dual continuum equations have been formulated for the case of two-phase oil-water flow in fractured oil reservoirs. In spite of the analogy between water flow in an air-filled rock and water flow in an oil-filled rock, the simplifying assumptions used in these formulations do not appear to be adequate for the case of unsaturated flow in relatively dry rock. Briefly, Barenblatt et al. (1990, Section 5.4) developed a specialized dual continuum model for the case of immiscible displacement of oil by water under certain restrictive assumptions. In their model, the coarse porosity medium or fracture network is represented as a continuous and well-connected medium (No. 1), while the fine porosity medium is a disperse set of inclusions (No. 2). Furthermore, based on the contrast of saturated permeabilities, $k_2 \ll k_1$, the fluxes of oil and water are neglected in the fine porosity medium. In the case where the coarse-porosity medium No. 1 represents a fracture network, its porosity is also neglected. Several other ad hoc assumptions are used, notably for expressing the transfer terms of both fluids between the active coarse-porosity medium (No. 1) and the passive fine-porosity medium (No. 2). This enables the authors to recover, at the large-scale, the features predicted by the one-dimensional Buckey-Leverett theory, and to predict entrapment of the wetting phase (water) in low permeability inclusions.

It does not seem that the same type of approach can be used for modeling unsaturated water flow in a fractured porous rock under naturally dry hydrogeologic conditions. Indeed, the model described above ignores the case where a significant part of the flow is carried through the matrix. Under dry conditions, it is quite possible that part of the fracture system actually impedes flow. Ideally, a more flexible dual continuum model is needed in order to account for fast local fracture flow as well as significant matrix flow. The partition between fracture flow and matrix flow contributions should be allowed to depend on overall flow and moisture conditions, and on the relative distributions of *unsaturated* matrix/fractures conductivities.

On the other hand, Barenblatt et al. (1990, Section 5.4.3) specialized their matrix/fracture transfer term to model, explicitly, one-dimensional two-phase flow through a set of (say) parallel fractures separated by porous matrix. This model may be applicable to high rate infiltration (or ponded infiltration) on a fractured ground surface. Barenblatt et al. find that the asymptotic saturation front at infinite times has the form of a traveling wave $S=S(z-Vt)$, where the downward wave velocity V decreases with increased imbibition coefficients of porous matrix, and is proportional to the surface flow rate through outcropping fractures (surface infiltration through porous matrix is apparently neglected in their model). Other models have been devised specifically for unsaturated matrix-fracture infiltration, without using the dual continuum approximation. See for instance Buscheck and Nitao (1988 and 1991), Nitao and Buscheck (1989), and Nitao (1989), for the case of predominantly vertical infiltration on single vertical fractures or arrays of vertical fractures imbedded in a porous matrix. Part of their results is based on quasi-analytical solutions

for the advancement of water down a fracture with imbibing rock matrix (Nitao, 1989). In addition, Zimmerman and Bodvarsson (1990) proposed an analytical model of transient imbibition through unsaturated porous blocks bordered by fractures. These specialized infiltration and imbibition models could possibly be used as auxiliary inputs, or as boundary conditions, for larger scale three-dimensional simulations of the kind envisioned here.

Finally, the dual continuum approximation can be used in combination with explicit modeling of flow through major fractures, as was done in the two-dimensional steady saturated flow model of Shapiro and Andersson (1983). These authors used a boundary element method to solve the dual continuum equations within subdomains delimited by fractures. Narasimhan (1982) discusses the links between single-continuum, dual-continuum, and explicit fracture flow models within the framework of the Integrated Finite Differences method. Huyakorn et al. (1983) compared and tested numerically four conceptual models of saturated flow through fractured rocks: (1) explicit fracture flow, (2) dual continuum with equilibrium matrix/fracture transfer function, (3) dual continuum with nonequilibrium transient transfer function based on prismatic blocks idealization, and (4) same with nonequilibrium transient transfer function based on spherical blocks approximation. More recent developments improving or extending the dual continuum approach can be found in Dykhuizen (1990) and Liu and Chen (1990).

6.5 DIRECT MODELING OF PARTIALLY SATURATED FLOW IN FRACTURED ROCK

6.5.1 Direct Modeling of Flow through Variably Saturated Parallel Plate Fracture Networks

Rasmussen and Evans (1989, Chapter 3) adapted the Boundary Element Method for simulating steady water flow in partially saturated fractures without interactions with the embedding rock mass. They considered the case of single and multiple intersecting fractures, each individual fracture being modelled as a parallel plate of arbitrary shape partially filled with water. Figure 6.1 depicts a partially saturated parallel plate rectangular fracture (from Rasmussen and Evans, 1989, Figure 3.5). The particular shape of the air-water interface is due to flow conditions at the fracture boundaries, e.g. partial intersection with another fracture on the sides, rather than to variable fracture aperture.

In the Rasmussen-Evans model, the governing flow equations within each fracture are based on free surface flow theory, with specific storage and variable transmissivity coefficients analogous to these defined for unconfined aquifers. The effective retention curve of an individual dipping fracture is piecewise linear rather than linear, and the slope of the intermediate linear part gives the specific storage coefficient of the partially saturated fracture. The boundary element formulation solves first for pressures at fracture boundaries and fracture intersections, and recovers the solution in the interior domain via Greens function integrals. However, a special treatment is required for the air-water interface nodes. The position of the interface is updated iteratively using a Newton-Raphson scheme, and the standard boundary integral solution method is used at each iteration step. Although only steady state solutions were computed, the iteration procedure is somewhat analogous to time-marching. A simplified case involving a single vertical fracture connected to the atmosphere and intersected by two horizontal constant head fractures, is depicted in Figures 6-2 and 6-3 from Rasmussen and Evans (1989, Figures 3.13 and 3.17).

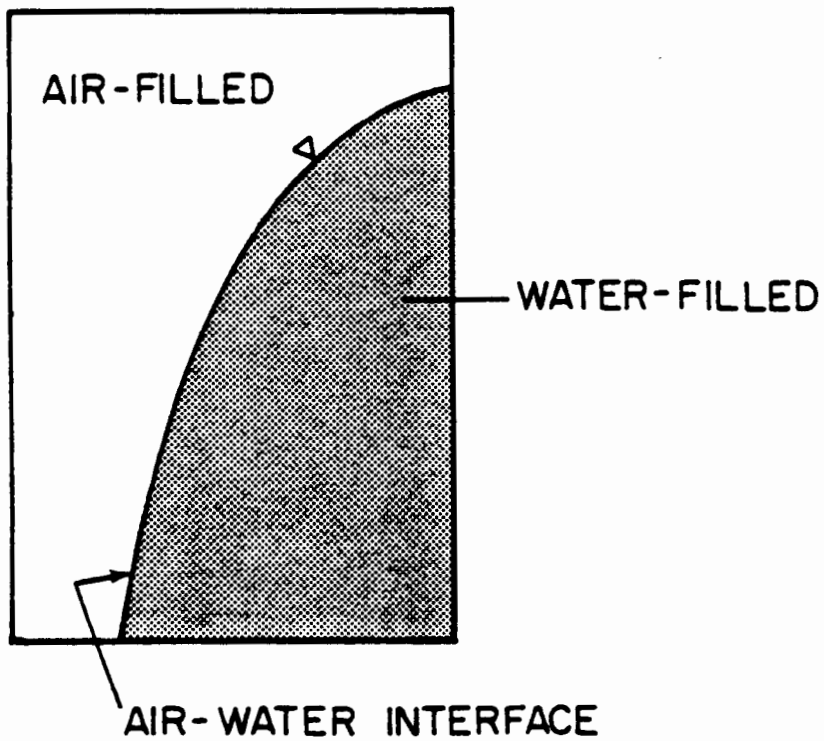

Figure 6-1. Conceptual model of partially saturated parallel plate fracture (after Rasmussen and Evans, 1989).

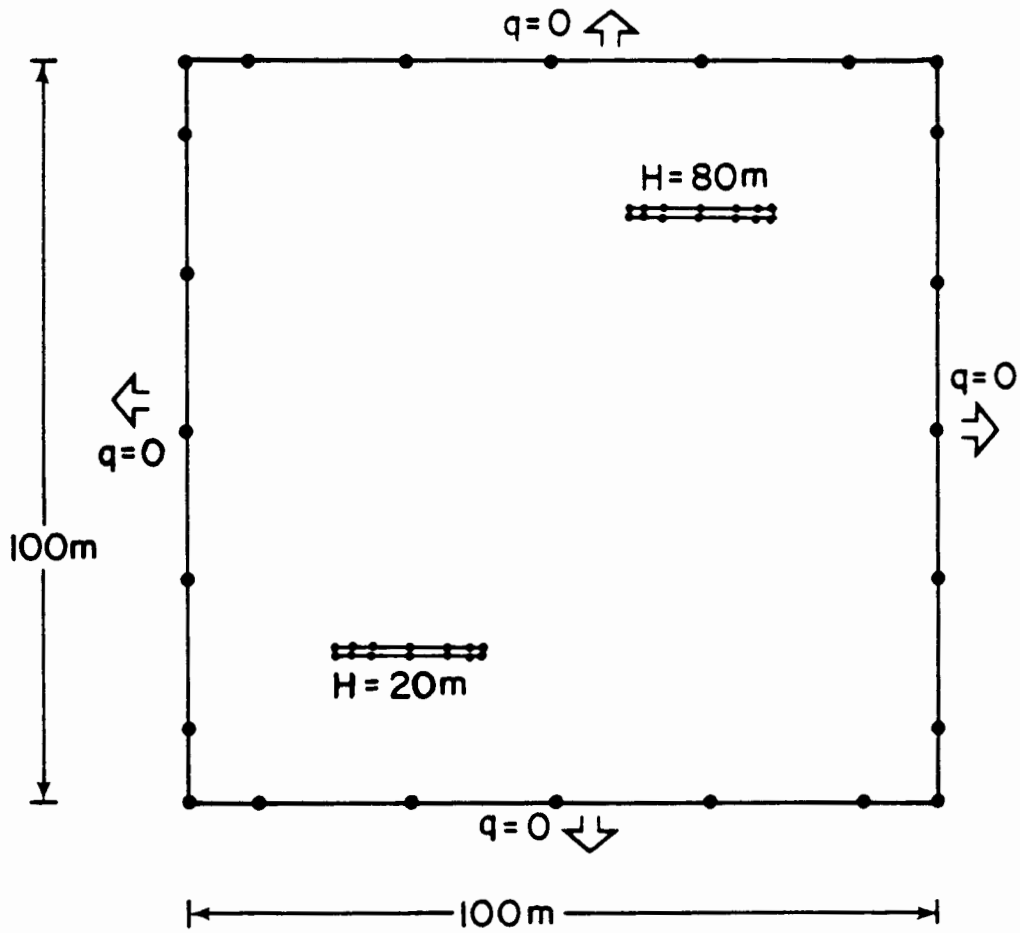

Figure 6-2. **Flow geometry and internal and boundary conditions for a vertical fracture intersected by two constant-head horizontal fractures (after Rasmussen and Evans, 1989).**

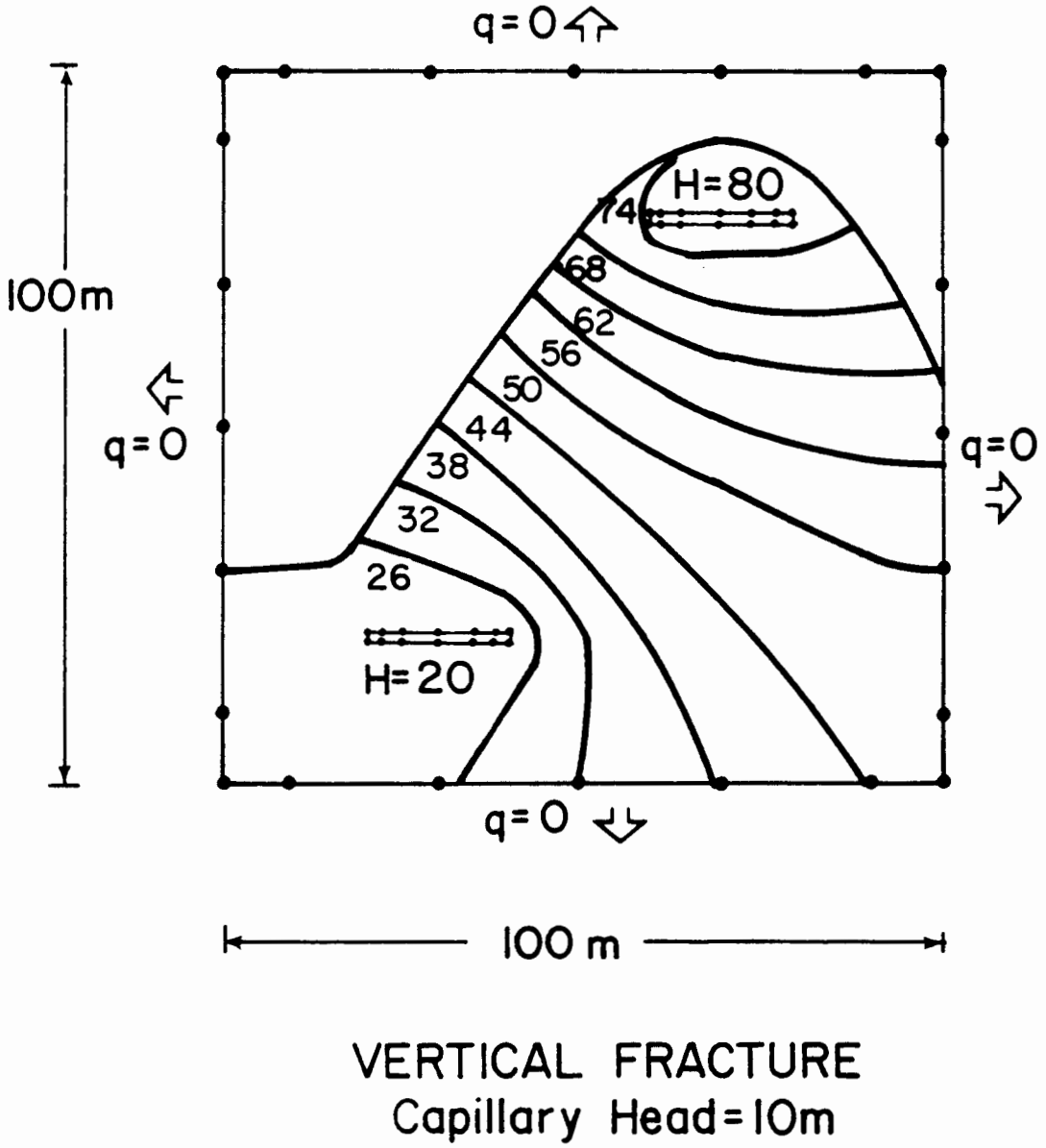

Figure 6-3. **Contours of total head and air-water interface within the plane of the vertical fracture described in Figure 6-2. A capillary head of 10m was used, and air entry was allowed (from Rasmussen and Evans, 1989).**

The main advantage of this model is that it allows for an explicit relationship of the detailed flow system across an arbitrary three-dimensional network of variably oriented fractures, including the detailed pressure and streamline fields within each individual fracture of the network. The latter is computed efficiently via boundary integrals, which require only one-dimensional discretization along fracture boundaries and intersections. However, the model assumes an impervious rock matrix, so that the rock mass itself is excluded from the computational domain. Under relatively low flow rate and saturation, matrix flow may not be negligible,and fracture aperture variations (contacts) may bypass the fracture system. The Rasmussen-Evans model of free surface fracture flow may be more applicable, if extended to transient flow, in the case of a partially saturated fracture network under relatively high flow rate and saturation, most of the water transits through the fracture network. Note that the same authors adapted the boundary element method to solve explicitly for both matrix and fracture flow under *saturated* conditions (Rasmussen and Evans, 1989, Chapter 2). The next section discusses an approach to coupled matrix-fracture flow in the case of unsaturated or partially saturated flow.

6.5.2 Direct Modeling of Unsaturated Matrix/Fracture Flow Based on Bulk Unsaturated Fracture Properties

A model combining explicit representation of fracture network with equivalent constitutive relations for a variable-aperture fracture embedded in a porous matrix was developed by Wang and Narasimhan (1985). The model was implemented numerically for the case of an orthogonal set of identical horizontal fractures, and identical vertical fractures based on an enhanced version of the Integrated Finite Differences TRUST code (Narasimhan et al., 1978). The effective moisture retention and conductivity curves of a single fracture surrounded by porous matrix were deduced from a random aperture model taking also into account the existence of contact areas. While fracture apertures were represented ideally by a gamma-distribution, an additional cut-off was introduced. The cut-off was determined separately by using a deterministic model of contact areas based on a regular array of discs (in spite of the randomness of the aperture distribution). Both the fracture/matrix retention curve, and the unsaturated conductivity orthogonal to fracture, were expressed as functiond of contact areas and ambient water pressure, given prescribed constitutive relations of the porous matrix. Figure 6-4 (from Wang and Narasimhan, 1985, Figure 1) illustrates the role of contact areas in transmitting water across fractures. Finally, the unsaturated conductivity parallel to fracture was expressed as a function of aperture distribution in a manner similar to Eqn. (4-58), and was also multiplied by a constriction factor to account for contact areas.

One of the main advantages of the Wang-Narasimhan model is that it allows for pressure-dependent anisotropic behavior of flow across a fracture. The model also takes into account possible contact areas by which matrix flow can by-pass the unsaturated (dry) fractures, and is well suited to simulation of transient storage-destorage effects. However, the model also has some shortcomings which leave room for improvement in at least two areas. Firstly, the contact area model should be reconciled with the random aperture model, as suggested earlier. Secondly, it may be necessary to modify the treatment of orthogonal versus parallel conductivities, especially for large-scale applications involving more realistic non-orthogonal fracture networks and anisotropic matrix. In the Wang-Narasimhan model, the orthogonal conductivity incorporates the conductivity of the embedding matrix, whereas the parallel conductivity does not [same as

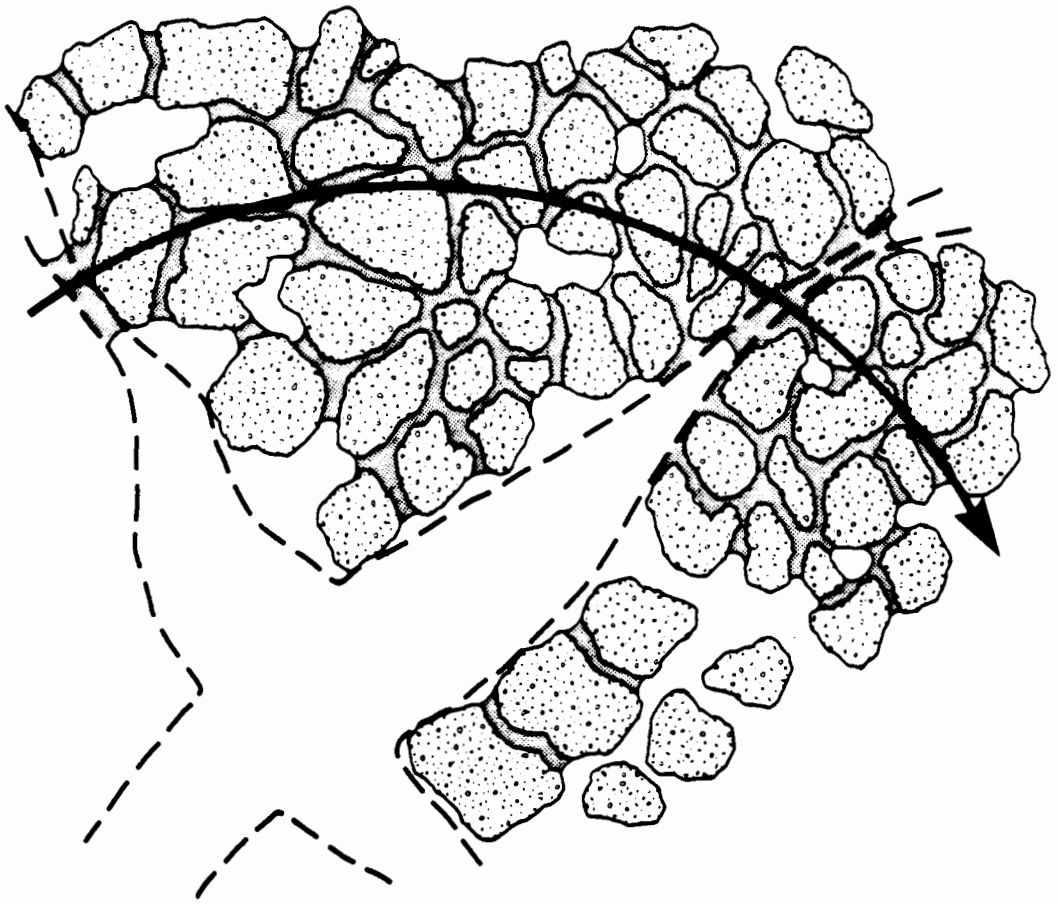

Figure 6-4. Conceptual model of partially saturated, fractured, porous medium showing schematically the flow line moving around the dry portions of the fractures (Wang and Narasimhan, 1985)

Eqn. (4-58)]. In contrast, a model based on clearly defined scale-averaged properties would incorporate both the matrix conductivity (possibly anisotropic) and the fracture conductivity (also anisotropic) in all directions. This type of approach may be required, in particular, when considering the effective flow behavior in the vicinity of fracture intersections (such as the one shown in Figure 6-4).

6.6 HIGH-RESOLUTION MODELING OF UNSATURATED FLOW IN RANDOMLY HETEROGENEOUS AND STRATIFIED CONTINUUM

6.6.1 Background, Simulation Results, and Analysis

As mentioned above, one possible modeling approach is to take into account the detailed geologic features, explicitly and directly, in the governing flow equations. These must then be solved numerically. A direct numerical simulation approach based on a continuum random field representation of heterogeneity was previously developed for saturated groundwater flow and transport (Ababou et al., 1989; Tompson and Gelhar, 1990), and for unsaturated flow systems as well (Ababou, 1988). Even in the absence of explicit fractures, the numerical model of spatially random *unsaturated* flow attains a high level of complexity. The simulation results require a good deal of auxiliary analysis, both experimental and theoretical, in order to be properly understood and interpreted (Ababou, 1988; Ababou and Gelhar, 1988). If more complex types of processes were included, e.g., multiphase and coupled hydro-thermomechanical processes, the overall model could become even more intricate. Although this project is concerned only with the case of partially saturated flow, it should be noted that the latter can be viewed as a special case of immiscible two-phase flow (water, plus a passive air phase). The results obtained so far without fractures are discussed below. Fractures will be introduced in future tasks of the project.

A high-resolution, three-dimensional finite difference model based on a mixed variable formulation of partially saturated/unsaturated flow has been previously used to model strip source infiltration and drainage in a randomly heterogeneous and imperfectly stratified soil (Ababou, 1988; Ababou and Gelhar, 1988). The flow regime, soil properties, and boundary conditions were selected to mimic (albeit with some differences) the first Las Cruces strip source experiment, one of the test cases of INTRAVAL (INTRAVAL, 1991). The nonlinear behavior and statistical properties of the soil were inferred, in part, from preliminary hydrodynamic data collected at the trench site. The 15 m x 15 m x 5 m computational domain was discretized into 300,000 cells, each with its own distinct unsaturated conductivity curve.

As part of our involvement in the validation exercise of INTRAVAL, the transient moisture plume simulation data were processed and visualized on an IRIS 4D workstation at the CNWRA, with the aid of three-dimensional isosurface and volumetric color graphics software (Figures 6-5 and 6-6). This approach provided direct evidence of moisture-dependent horizontal spreading, which lends credence to a previous theoretical finding based on linearized spectral perturbation solutions of stochastic unsaturated flow (Mantoglou and Gelhar, 1987a,b,c and Polmann et al. 1991). Thus, it can be seen from the color plates shown on Figures 6-5 and 6-6 that the marginally wet outer shell of the plume (blue) exhibits more horizontal spreading than the wet core of the plume (purple). In the case at-hand, moisture-dependent anisotropy due to the imperfect, random layering of hydraulic soil properties. Such imperfect stratification is a

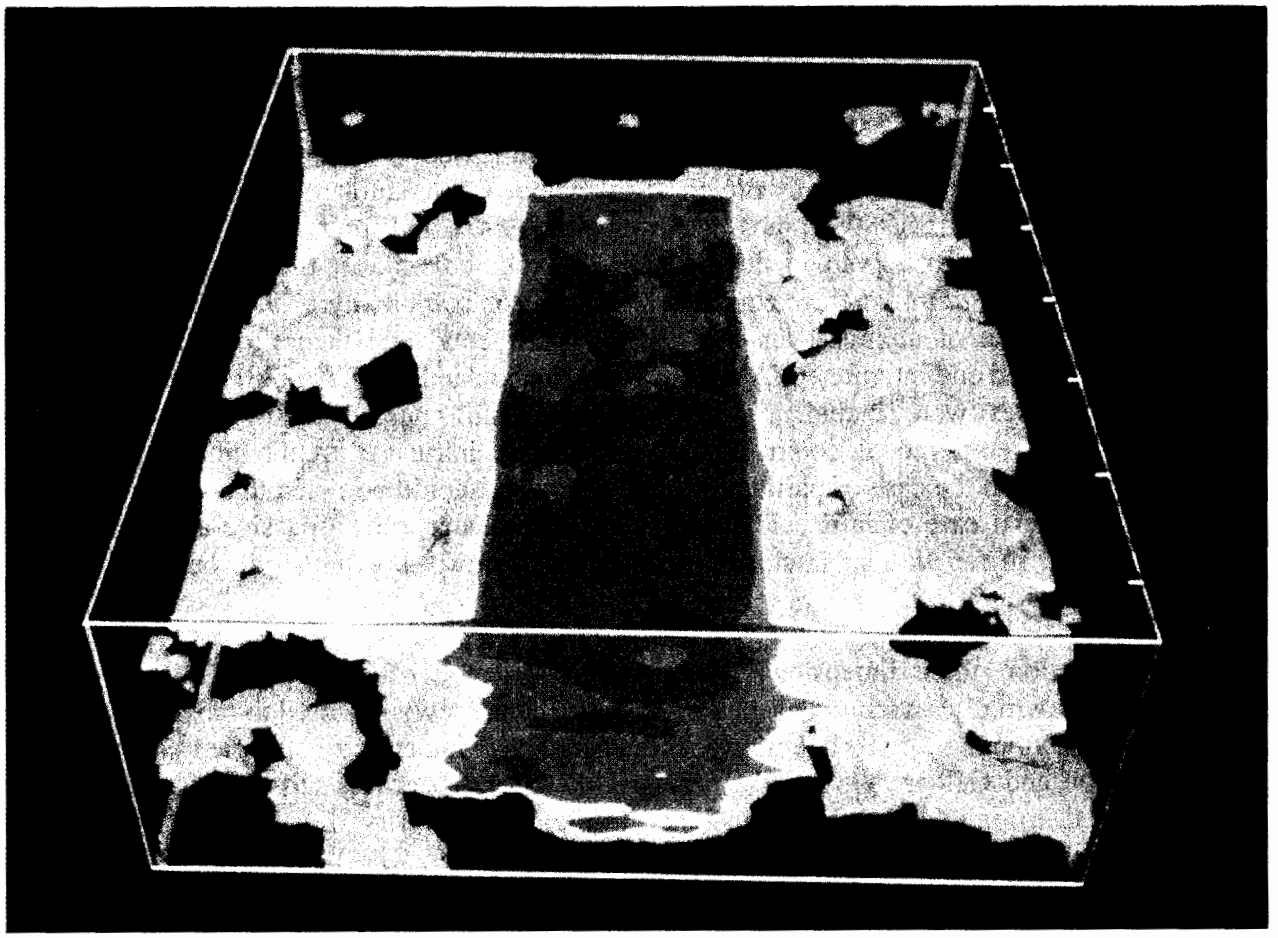

Figure 6-5. Front view of peeled-off three-dimensional moisture plume from stochastic flow simulations

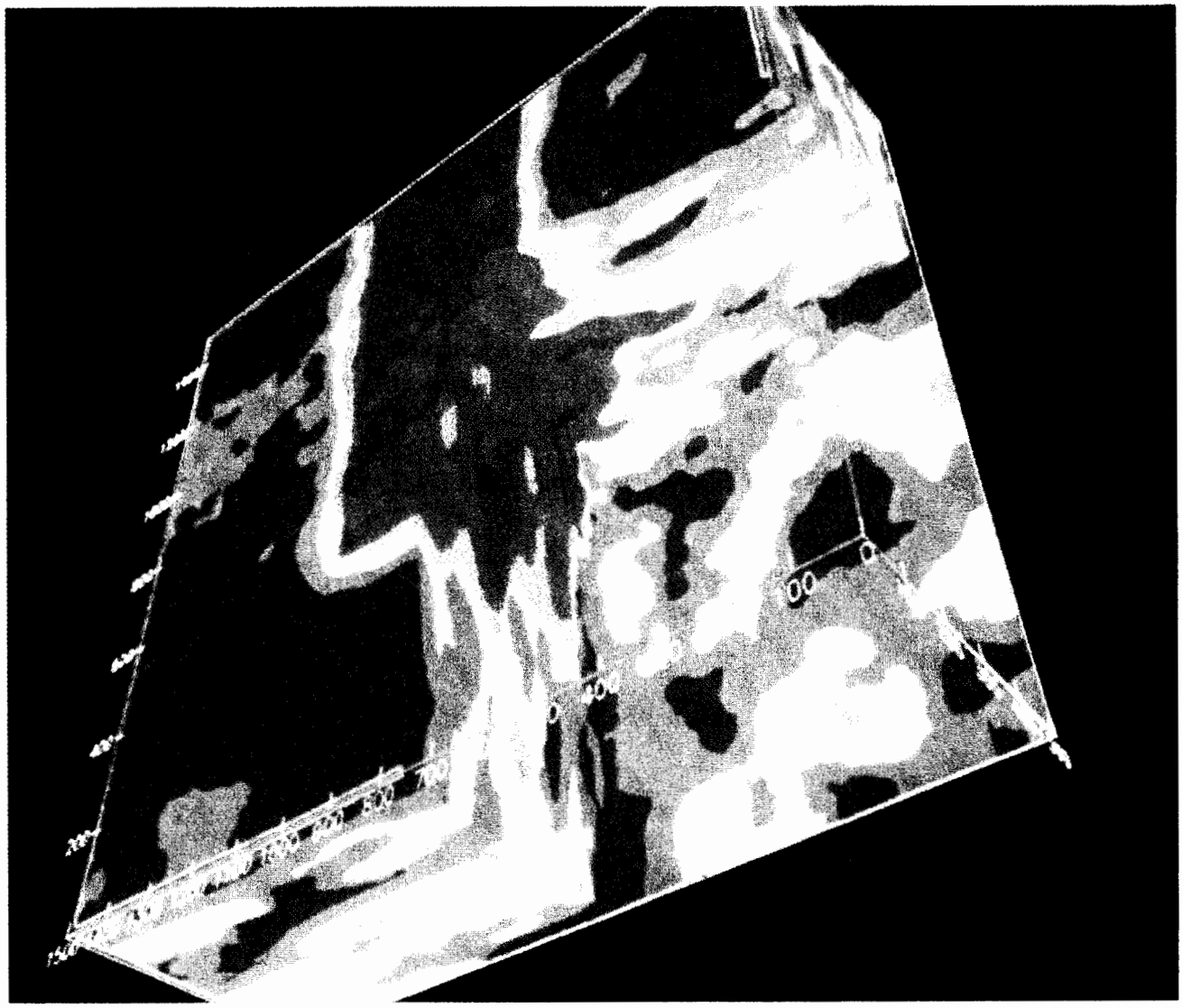

Figure 6-6. Back view of three-dimensional moisture pattern from stochastic flow simulations; the cut-off moisture plume is visible in purple and blue

pervasive feature of both consolidated and unconsolidated geologic media, including the tuff formations of Yucca Mountain.

6.6.2 Computational Aspects of Direct High-Resolution Simulations

6.6.2.1 Numerical Analysis of Nonlinear Unsaturated Flow

In an initial effort to evaluate certain aspects of the unsaturated flow modeling problem from a numerical viewpoint, a study was recently developed to examine the effects of nonlinearity on the stability and accuracy of numerical solutions, the interplay between capillary-driven and gravity-driven flow, and the convergence of nonlinear solution schemes in the case of homogeneous media (Ababou, 1990b). The findings of this study outline the role of gravitational flow, which is expressed through a dimensionless Peclet number ($Pe = \alpha\Delta z$) proportional to the slope α of the log-conductivity/pressure curve. Based on the form of the unsaturated flow equation, $\lambda_c=1/\alpha$ is essentially the length scale of *capillary dispersivity*, not to be confused with the moisture diffusion coefficient D.

In order to avoid instabilities, Ababou (1990) indicates that the vertical mesh size of a numerical flow model should be no larger than λ_c, which typically lies in the range 10-100 cm for sandy to clayey soils, but could be smaller for a fractured rock mass, and larger for the tight porous matrix of intact rock. This rule of thumb was based on approximate stability analysis. Specifically, for a one-dimensional flow system, the stability constraint obtained by Ababou (1990b) is:

$$Pe = |\alpha g \Delta z| \le 2\sqrt{1 + \left(2\,\frac{Ki}{Ci}\,\frac{\Delta t}{\Delta z^2}\right)^{-1}} \tag{6.11}$$

This inequality can be formulated equivalently as a space-time stability condition, of the form:

$$\text{either} \quad Pe = |\alpha g \Delta z| \le 2 \quad \text{or else} \quad \frac{Ki}{Ci}\,\frac{\Delta t}{\Delta z^2} \le \frac{2}{(Pe-2)(Pe+2)} \tag{6.12}$$

In these equations, Pe represents the grid Peclet number, K_i the nodal conductivity, C_i the nodal moisture capacity, and g the projection onto axis z of the unit gravity vector (a unit vector parallel to gravity). Note that the direction of flow need not be vertical.

6.6.2.2 Effects of Heterogeneity on Numerical Accuracy

The stability condition given here emphasizes the advective role of gravity, and it can be generalized to three dimensions by defining a Peclet number for each coordinate axis (x,y,z). The possible effects of material heterogeneity are however more difficult to capture, particularly in the case of spatial variability of parameter α or its inverse λ_c (the capillary dispersivity). Ababou indicates that instabilities will be triggered in zones of small capillary dispersivity (λ_c small), and will grow faster in zones where the moisture diffusion coefficient is largest ($D=K/C$ large). Generally, these worst case conditions are met in wet regions of coarse porosity (e.g. preferential

flow along fracture zone). See Ababou (1990b) for additional analyses on truncation error and on convergence of nonlinear unsaturated flow equations.

Let us consider, from a new vantage point, the question of numerical accuracy for a model that explicitly incorporates detailed three-dimensional features of the heterogeneous geologic medium. In the case of a continuum porous matrix with random heterogeneity, numerical experiments with transient flow systems (Ababou, 1988; Ababou and Gelhar, 1988) indicate that the effects of nonlinearity and heterogeneity are inextricably intertwined. This makes it difficult to analyze not only the simulation results, but also the accuracy of numerical discretization and solution schemes. Nevertheless, the accuracy of solutions can be evaluated a posteriori using mass balance checks. The rate of change of total mass of water is compared to the algebraic sum of discharge rates through all boundaries. The approximations used to compute fluxes, to integrate fluxes over two-dimensional boundaries, and to integrate moisture over the three-dimensional domain, must all be consistent with those used in the numerical solution procedure (Ababou, 1988, Chapter 5). Discrepancies in mass balance can be due either to inaccurate (coarse) discretization in space and time, or to numerical errors in solving the discretized nonlinear system, or to a combination of both.

6.6.2.3 Algebraic System Solvers

In the type of numerical flow model envisioned here, the solution of large sparse algebraic systems constitutes the computationally intensive part (computational kernel) of the numerical code. Moreover, in the case of three-dimensional high-resolution field-scale models of unsaturated flow, the systems to be solved will be large, nonlinear, and poorly conditioned due to high conductivity contrasts. See Ababou et al. (1985), Ababou (1988) and Ababou et al. (1989) for analyses of the effects of system size and material heterogeneity on the condition number of the linearized conductivity matrix.

Although the preferred discretization algorithms have not been selected yet, the development of a series of iterative sparse matrix solvers (modules) that exploit the particular diagonal data structure of the three-dimensional Finite Difference unsaturated flow equations has been pursued. The initial focus was on symmetric matrix solvers, based on the observation that unlike Newton methods, Picard-type linearization schemes generate sequences of symmetric matrix systems (Ababou, 1988). The preconditioned iterative solvers are based on SIP (Strongly Implicit Procedure) and Conjugate Gradients iterations with various types of preconditioning. It already appears that speed-ups of a factor 20/1 are achieved on vector supercomputers with some of the Conjugate Gradient solvers. Their efficiency will be tested extensively in the next Task of this Project and will be reported in future.

6.7 OTHER REVIEWS OF MODELING APPROACHES IN THE LITERATURE

For completeness, other sources of information on both numerical and conceptual modeling approaches, mainly review works, are noted here without further comments. Some of these sources are currently being exploited for assessing conceptual and numerical models proposed in the literature. These sources include: Ababou (1988, Chapter 5) for saturated/unsaturated statistical continuum models and numerical flow solvers; Yeh et al. (1988) for unsaturated flow codes; Shapiro (1987) for dual continuum approaches; Gureghian and Sagar (1991) for review

of a dual-porosity flow code; Milly (1988) and Nielsen et al. (1986) for unsaturated flow modeling; Parker (1989) for a review of multiphase flow-transport processes; Gelhar (1986), Dagan (1986), and Mantoglou and Gelhar (1987a,b,c) for statistical continuum approaches to field heterogeneity; Barry (1990) for a review of solute transport; Wang et al. (1983) for a review of hydro-thermo-mechanical flow codes for fractured rock; and Mangold and Tsang (1991) for a review of hydrochemical transport models.

7. SUMMARY AND CONCLUSIONS

Realistic far-field modeling of radionuclide transport in the vadose zone at Yucca Mountain will require incorporating the effects of natural heterogeneity, stratification, and fracturing in modeling the unsaturated flow system. A review of field-scale observations from several vadose zone contamination sites (Section 2.1) and unsaturated transport experiments (Chapter 3) provides evidence for both preferential flow pathways through vertical root channels, fissures, or fractures, and extensive lateral spread along horizontal or dipping strata. The specific hydrogeologic setting of Yucca Mountain (Section 2.3) exhibits both aspects, owing to the presence of two near-vertical fracture sets, as well as horizontal dipping stratification and bedding.

Because the hydraulic properties of unsaturated geologic media are pressure-dependent (Chapter 4), the response of the natural system at Yucca Mountain may be highly sensitive to the choice of hydraulic parameters and to their assumed spatial distribution. There is relatively clear evidence of nonuniformity as well as anisotropy of in-situ fracture network properties (orientations, density, and apertures), and of highly variable rock matrix properties (core permeabilities and porosities). However, data characterizing unsaturated rock constitutive relations over broad ranges of pressures are generally scant, and will likely be confined to a few "representative" locations. Realism dictates that the spatial structure of the least accessible material properties, such as relative conductivity curves, be analyzed indirectly through correlations with more easily measured parameters. Therefore, auxiliary models need to be developed and tested in order to correlate the parametrized conductivity curves with, say, void structure, porosity, and saturated conductivity (Sections 4.3.2 through 4.3.5).

Furthermore, parsimonious models are required in order to capture three-dimensional heterogeneity and anisotropy over a broad range of scales, as occurs in the field. The view adopted here is that stochastic models, based on geometric probability and random functions, are most appropriate to achieve these goals (Chapter 5). A review of statistical continuum interpretations of available aquifer data (Section 5.2) and of unsaturated soil properties (Section 5.3) generally confirms this view, although some problems of nonstationarity and scale-dependence are encountered. Section 5.2 discusses scale-dependence and uncertainty as consequences of the self-similar or fractal nature of heterogeneity. The availability and nature of fracture data is also discussed in Section 5.4.

Overall, the reviewed statistical data can help constrain stochastic models of spatial variability and anisotropy at Yucca Mountain. However, more work is required towards a screening of available databases for (1) hydraulic fracture properties, and (2) multidimensional fracture network geometry. For the latter, it is suggested that statistical databases available from other sites can help constrain random network models of the fracture system at Yucca Mountain. In addition, site-specific features can be introduced in stochastic models by conditional simulation techniques.

Chapter 6 presented a preliminary screening of global modeling approaches for large-scale (say mountain-scale) unsaturated flow through heterogeneous, stratified, and fractured geologic media. Criteria to assess the advantages and disadvantages of alternative modeling approaches were discussed in Section 6.1. The key criteria concern the nature of the governing equations

(maximize physical basis and minimize fudge factors), the underlying assumptions (maintain consistency with objectives and with physical principles), the model inputs (minimize the required quantity of information while satisfying certain objectives), and computational feasibility (demonstrate feasibility and/or develop new algorithms). Alternative approaches were introduced in Section 6.2. Three main categories were distinguished: direct simulation based on microscale equations with explicit representation of heterogeneity, indirect simulation based on effective flow submodels, and various combinations of the above. Sections 6.3 through 6.5 review more specifically a sparse selection of such approaches from the literature, including single- and dual-continuum models (Section 6.3), explicit fracture flow models (Section 6.3) and matrix/fracture flow models with explicit fracture geometry (Section 6.4), and a case study of direct high-resolution simulation for a three-dimensional stratified statistical continuum (Section 6.5).

One conclusion to be drawn from this review is that current equivalent media models are probably not able at this stage to capture the dominant geologic features present at Yucca Mountain, such as dipping stratification, near vertical fracturing, and other features which combine to form inherently three-dimensional broad-band patterns of variability. On the other hand, while direct simulations of detailed unsaturated flow processes appear to be computationally feasible in the case of randomly stratified continua, detailed simulations of coupled fracture-matrix flow have only been implemented for simplified fracture network geometry and uniform isotropic matrix.

For more realistic simulations of large-scale flow processes infractured formations, the preferred approach may be a compromise between direct high-resolution simulation of fine-scale details, and the indirect simulation approach based on uniform equivalent media models. A hybrid approach would be less computationally demanding for a prescribed scale of simulation, yet it would capture a broad range of fine-scale to large-scale phenomena either directly (explicitly) and indirectly (implicitly). Advanced numerical algorithms would still be needed to resolve high contrasts and nonlinearities in material properties, and new auxiliary models would need to be developed from existing ones in order to correctly capture subgrid phenomena within the global model. It is also important to keep in mind that auxiliary hydrodynamic models of the type envisioned here may take the form of nonlinear, anisotropic constitutive relations (unlike the form assumed in most flow codes). In addition, the three-dimensional geometry of material properties required in such a model may be fairly complex, e.g. in the likeness of a fracture network pattern combined with rock stratification. This type of geometry will require discretization schemes that are particularly flexible, while at the same time maintaining a reasonable degree of sparsity in the algebraic systems. Finally, some processes, such as short and long time-scale fluctuations of hydroclimatic inputs, can be addressed separately via numerical and analytical modeling using simplified matrix/fracture geometries. In this way, it may be possible to achieve mountain-scale predictions of vadose zone flow while taking into account a broad range of potential flow paths and/or flow barriers throughout the mountain.

8. REFERENCES

Ababou, R. 1981. *Modeling of Soil Water Transfers for Localized Irrigation*, Docteur-Ing. Thesis, Institut de Mecanique de Grenoble, Université Scientifique et Institut National Polytechnique de Grenoble, France. 218 pp. (in French).

Ababou, R. 1982. *Measurement of Soil Water Transfers: Evaporation and Percolation Through a Sandy Soil of Rabat.* Proceedings, Scientific Meeting of the International Commission on Irrigation Drainage, Lisbon, Portugal. March 1982. Published in "Hommes, Terre et Eaux," Special Issue II. v12(47). Rabat, Morrocco. 45-58. (in French).

Ababou, R., D. McLaughlin, L.W. Gelhar, and A.F.B. Tompson. 1985. Numerical simulation of saturated flow fields in randomly heterogeneous porous media. *The Stochastic Approach to Subsurface Flow.* International Symposium, A.I.R.H., Montvillargennes, France. Preprints. 20pp.

Ababou, R. 1988. *Three-Dimensional Flow in Random Porous Media.* PhD Thesis. Department of Civil Engineering, Massachusetts Institute of Technology. Cambridge, Massachusetts. 2 volumes, 833pp.

Ababou, R. and L.W. Gelhar. 1988. A high-resolution finite difference simulator for 3D unsaturated flow in heterogeneous media. *Computational Methods in Water Resources.* Elsevier and Computational Mechanics Publications. 1: 173-178.

Ababou, R., D. McLaughlin, L.W. Gelhar, and A.F. Tompson. 1989. Numerical simulation of three dimensional saturated flow in randomly heterogeneous porous media. *Transport in Porous Media.* 4: 549-565.

Ababou, R. 1990a. Identification of effective conductivity tensor in randomly heterogeneous and stratified aquifers. *Proceedings of the Fifth Canadian-American Conference on Hydrogeology: Parameter Identification and Estimation for Aquifers and Reservoirs.* Calgary, Alberta, Canada. S. Bachu, ed. Published by National Water Well Association, Dublin, Ohio. 155-157.

Ababou, R. 1990b. Numerical analysis of unsaturated flow equations. *Proceedings VIIIth Conference on Computational Methods in Water Resources.* G. Gambolati et al., eds. Venice, Italy: Computational Mechanics Publications and Springer-Verlag: A: 151-160.

Ababou, R. and L.W. Gelhar. 1990. Self-similar randomness and spectral conditioning: analysis of scale effects in subsurface hydrology. *Dynamics of Fluids in Hierarchical Porous Media.* J. Cushman, ed. New York, NY: Academic Press. 505pp.

Ababou, R. 1991. Modeling heterogeneous unsaturated flow systems. *Proceedings of the Fifth Workshop on Flow and Transport Through Unsaturated Fractured Rock - Related to High-Level Radioactive Waste Disposal.* January 7-10, 1991. Tucson, Arizona. D.D. Evans and T.J. Nicholson (eds.). NUREG/CP-0040. U.S. Nuclear Regulatory Commission. Washington D.C.

Anderson, L.A. 1981. Rock Property Analysis of Core Samples from the Yucca Mountain UE25a-1 Borehole, Nevada Test Site, Nevada. USGS-OFR-81-1338, Open File Report. U.S. Geological Survey. Denver, Colorado.

Andersson, J., A.M. Shapiro, and J. Bear. 1984. A stochastic model of a fractured rock conditioned by measured information. *Water Resour. Res.* 20:79-88.

Bachu, S. (ed.). 1991. Parameter identification and estimation for aquifer reservoir characterization: *Proceedings of the Fifth Canadian-American Conference on Hydrogeology*, September 18-20, 1990. Calgary, Alberta, Canada. Published by the National Water Well Association, Dublin, Ohio. 453pp.

Bakr, A.A. 1976. *Stochastic Analysis of the Effect of Spatial Variations of Hydraulic Conductivity on Groundwater Flow.* PhD Thesis, New Mexico Institute of Mining and Technology. Socorro, New Mexico.

Barenblatt, G.I., Y.P. Zheltov, and I.N. Kochina. 1960. Basic concepts in the theory of seepage of homogeneous liquids in fissured rocks. *J.Appl. Math. & Mech.* 24:1286-1303.

Barenblatt, G.I., V.M. Entov, and V.M. Ryzhik. 1990. *Theory of Fluid Flows Through Natural Rocks.* Dordrecht, The Netherlands: Kluwer Academic Publishers.

Barr, G.E. 1985. *Reduction of the Well Test Data for Test Well USWH-1, Adjacent to Nevada Test Site, Nye County, Nevada.* SAND84-0637. Sandia National Laboratories. Livermore, California.

Barry, D. A. 1990. *Supercomputers and their Use in Modeling Subsurface Solute Transport.* Reviews of Geophysics. 28(3).

Barton, C.C. 1986. Fractal geometry of two-dimensional fracture networks at Yucca Mountain, southwestern Nevada. *Proceedings of International Symposium on Fundamentals of Rock Joints.* Bjorkliden, Lapland, Sweden.

Bear, J. and Y. Bachmat. 1966. A generalized theory on hydrodynamic dispersion in porous media. *I.A.S.H. Symp. Artificial Recharge and Management of Aquifers.* Haifa, Israel. IASH, P.N. 72: 7-16.

Bear, J. and Y. Bachmat. 1967. A generalized theory on hydrodynamic dispersion in porous media. *I.A.S.H. Symp. Artificial Recharge and Management of Aquifers.* Haifa, Israel. IASH P.N. 72:7-16.

Bear, J. 1972. *Dynamics of Fluids in Porous Media.* New York, NY: American Elsevier. 746pp.

Binsariti, A.A. 1980. *Statistical Analyses and Stochastic Modelling of the Contaro Aquifer in Southern Arizona.* PhD dissertation, Dept. of Hydrology and Water Resources, University of Arizona. Tucson, Arizona.

Bonano, E.J., R.M. Cranwell, and P.A. Davis. 1989. Performance assessment methodologies for the analysis of high-level nuclear waste repositories. *Radioactive Waste Management and the Nuclear Fuel Cycle*. 13(1-4): 229-239.

Borg, I.Y., R. Stone, H.B. Levy, and L.D. Ramspott. 1976a. *Information Pertinent to the Migration of Radionuclides in Ground Water at the Nevada Test Site. Part 1. Review and Analysis of Existing Information*. Lawrence Livermore Laboratory Report No. UCRL-52078 (Pt. 1). 221pp.

Borg, I.Y., R. Stone, H.B. Levy, and L.D. Ramspott. 1976b. *Information Pertinent to the Migration of Radionuclides in Ground Water at the Nevada Test Site. Part 2. Annotated Bibliography*. Lawrence Livermore Laboratory Report No. UCRL-52078 (Pt. 2), 114pp.

Bowman, R.S., D.P. Grabka, J.F. Gibbens and D.B. Stephens. 1990. Three-dimensional solute transport in a heterogeneous vadose zone. *Am. Geophys. Union Spring Meeting Abstracts*. EOS. 514.

Box, G.E.P. and G.M. Jenkins. 1976. *Time Series Analysis, Forecasting, and Control*. Revised Edition. San Francisco, CA: Holden-Day Publishers.

Brandt, A., E. Bresler, N. Diner, I. Ben-Asher, J. Heller, and D. Goldberg. 1971. Infiltration from a trickle-source, II. experimental data and theoretical predictions. *Soil Sci. Soc. Am. Proc.* 35: 683-689.

Bresler, E. 1975. Two-dimensional transport of solutes during nonsteady infiltration from a trickle-source. *Soil Sci. Soc. Am. Proc.* 39: 604-612.

Bresler, E. 1978. Analysis of trickle irrigation with application to design problems. *Irrigation Science*. 1(1): 3-17.

BRGM (Bureau de Recherches Géologiques et Minierès). 1987. *Etude des Ecoulements sur le site de Fanay-Augères: Conception et réalization du dispositif expérimental, détermination des caracteristiques structurales et hydrauliques du massif*. Final Report Part 1. Rep. 87 SGN502STO, European Economic Community.

Brooks, R.H. and A.T. Corey. 1964. *Hydraulic Properties of Porous Media*. Hydrology Paper No. 3. Civil Engineering Department, Colorado State University. Fort Collins, Colorado.

Brooks, R.H. and A.T. Corey. 1966. Properties of porous media affecting fluid flow. *J. Irrig. Drain. Div. Am. Soc. Civil Eng.* 92(IR2): 61-88.

Brown, S.R. 1989. Transport of fluid and electric current through a single fracture. *J. Geophys. Res.* 94(B7):9429-9438.

Buckingham, E. 1907. *Studies on the Movement of Soil Moisture*. U.S. Dept. Agric. Bureau of Soils. Bulletin No. 8.

Burdine, N.T. 1953. Relative permeability calculations from pore-size distribution data. *Petr. Trans. Am. Inst. Mining Metall. Eng.* 198: 71-77.

Buscheck, T.A. and J.J. Nitao. 1988. *Estimates of the Width of the Wetting Zone Along a Fracture Subjected to an Episodic Infiltration Event in Variably Saturated, Densely Welded Tuff.* Lawrence Livermore National Laboratory report UCID-21579. Livermore, California.

Buscheck, T.A. and J.J. Nitao. 1991. Non-equilibrium fracture-matrix flow during episodic infiltration events in Yucca Mountain. *Proceedings Workshop V: Flow and Transport Through Unsaturated Fractured Rock - Related to High-Level Radioactive Waste Disposal.* January 7-10, 1991. Tucson, Arizona. D.D. Evans and T.J. Nicholson, (eds.), NUREG/CP-0040. U.S. Nuclear Regulatory Commission. Washington, D.C.

Cacas, M.C., E. Ledoux, G. de Marsily, B. Tillie, A. Barbreau, E. Durand, B. Feuga, and P. Peaudecerf. 1990a. Modeling fracture flow with a stochastic discrete fracture network: calibration and validation, 1: the flow model. *Water Resour. Res.* 26(3): 479-489.

Cacas, M.C., E. Ledoux, G. de Marsily, A. Barbreau, P. Calmels, B. Gaillard, and R. Margritta. 1990b. Modeling fracture flow with a stochastic discrete fracture network: calibration and validation, 2: the transport model. *Water Resour. Res.* 26(3): 491-500.

Carr, M.D. and J.C. Yount (ed.). 1988. *Geologic and Hydrologic Investigations of a Potential Nuclear Waste Disposal Site at Yucca Mountain, Southern Nevada.* U.S. Geological Survey, Bulletin No. 1790. Denver, Colorado. 156pp.

Cheeney, R.F. 1983. *Statistical Methods in Geology.* George Allen & Unwin. London.

Chuang, Y., W.R. Haldeman, T.C. Rasmussen, and D.D. Evans. 1990. *Laboratory Analysis of Fluid Flow and Solute Transport Through a Variably Saturated Fracture Embedded Inporous Tuff.* NUREG Report CR-5482, U.S. Nuclear Regulatory Commission. Washington, DC.

Claustnitzer, V., J.W. Hopmans, and D.R. Nielsen. 1990. Simultaneous scaling of soilwater retention and unsaturated conductivity curves. *Fall Meeting of the Amer. Geophys. Union.* October 23. Abstract. EOS Tranactions. 71(43).

Clifton, P.M. and S.P. Neuman. 1982. Effects of kriging and inverse modeling on conditional simulation of the Avra Valley aquifer in southern Arizona. *Water Resour. Res.* 18(4): 1215-1234.

Code of Federal Regulations, Title 10 Part 60. 1-1-89. Disposal of High-Level Radioactive Wastes in Geologic Repositories. NRC.

Code of Federal Regulations, Title 40 Part 191. 7-1-87. Environmental Radiation Protection Standards for Management and Disposal of Spent Nuclear Fuel, High-Level and Transuranic Radioactive Waste. EPA.

Craig, R.W. and J.H. Robison. 1984. *Geohydrology of Rocks Penetrated by Test Well UE-25p#1, Yucca Mountain Area, Nye County, Nevada.* USGS-WRI-84-4248, Water Resources Investigations Report. U.S. Geological Survey. Denver, Colorado.

Cushman, J. 1990. *Dynamics of Fluids in Hierarchical Porous Media.* J. Cushman, ed. New York, NY: Academic Press: 505.

Czarnecki, J.B. 1984. *Simulated Effects of Increased Recharge on the Groundwater Flow System of Yucca Mountain and Vicinity, Nevada-California.* U.S. Geological Survey Water Resources Investigation report 84-4344. 33pp.

Dagan, G. 1986. Statistical theory of groundwater flow and transport: pore to laboratory, laboratory to formation, and formation to regional scale. *Water Resour. Res.* 22(9): 120S-134S.

Dagan, G. 1987. Solute transport in groundwater. *Annual Review of Fluid Mechanics.* 19.

Daily, W., W. Lin, and T. Buscheck. 1987. Hydrological properties of Topopah Spring Tuff - laboratory measurements. *Journal of Geophysical Research.* 92(B8): 7854-7864.

Daily, W. and A. Ramirez. 1987. *An Experiment To Determine Drilling Water Imbibition by In-Situ Densely Welded Tuff.* Lawrence Livermore National Laboratories. Report No. UCID-21249-Rev. 1. Contract W-7405-ENG-48. 8pp.

Dane, J. 1980. Comparison of field and laboratory determined hydraulic conductivity values. *Soil Sci. Soc. Am. Journal.* 44(2): 228-231.

Darcy, H.P.G. 1856. *Les Fontaines Publiques de la Ville de Dijon, Exposition et Application des Principes à Suivre et des Formules à Employer dans les Questions de Distribution d'Eau.* Paris: Victor Dalmont.

Delhomme, J.P. 1979. Spatial variability and uncertainty in groundwater flow parameters: a geostatistical approach. *Water Resour. Res.* 15: 269-280.

deMarsily, G. 1986. *Quantitative Hydrogeology (Groundwater Hydrology for Engineers).* Academic Press. New York. 440 pp.

DePoorter, G.L., A.V. Abeele, B.W. Burton, T.G. Hakonson and B.A. Perkins. 1982a. *Novel Experiments for Understanding the Shallow-Land Burial of Low-Level Radioactive Wastes.* Report LA-UR-82-1078. Los Alamos National Laboratory, New Mexico.

DePoorter, G.L., A.V. Abeele, B.W. Burton, T.G. Hakonson and B.A. Perkins. 1982b. *Shallow Land Burial Technology in Development - Arid.* Report LA-UR-82-2535. Los Alamos National Laboratory, New Mexico.

Devary, J.L. and P.G. Doctor. 1982. Pore velocity estimation uncertainties. *Water Resour. Res.* 18(4): 1157-1164.

DOE Site Characterization Plan. 1988 (Vol. II, Part A, Chap. 3.9: Site Hydrogeologic System), Nuclear Waste Policy Act, Section 113. DOE/RW-0199, U.S. Department of Energy.

Duffy, C.J. and S. Al-Hassan. 1987. Time and frequency domain analysis of tracer migration in crushed tuff. *Workshop on Modeling of Solute Transport in the Unsaturated Zone*. Los Alamos, New Mexico. NUREG/CR-4615. 2: 82-116.

Dullien, F.A.L. 1979. *Porous Media: Fluid Transport and Pore Structure*. New York, NY: Academic Press. 396pp.

Dykhuizen, R.C. 1988. *Transport of Solutes Through Unsaturated Fractured Media: Nevada Nuclear Waste Storage Investigations Project*. Sandia National Laboratories report SAND-86-0940. Albuquerque, New Mexico. 16pp.

Dykhuizen, R.C. 1990. A new coupling term for dual-porosity models. *Water Resour. Res.* 26(2): 351-356.

Eaton, R.R. and N.E. Bixler. 1986. *Analysis of a Multiphase, Porous-Flow Imbibition Experiment in Fractured Volcanic Tuff*. Sandia National Laboratories report SAND86-1679C. Albuquerque, New Mexico. 18pp.

Eaton, R., K.S. Udell, and M. Kaviany. 1988. Drying of an initially saturated fractured volcanic tuff. *Multiphase Transport in Porous Media*. American Society of Mechanical Engineers: 55-60.

Elabd, H.I., I. Porro, and P.J. Wierenga. 1988. Estimation of field transport parameters using the convection dispersion equation. *Validation of Flow and Transport Models for the Unsaturated Zone*. P.J. Wierenga and D. Bachelet, eds. Conference Proceedings.

Erickson, J.R. and R.K. Waddell. 1985. *Identification and Characterization of Hydrologic Properties of Fractured Tuff Using Hydraulic and Tracer Tests: Test Well USW H-4, Yucca Mountain, Nye County, Nevada*. U.S. Geological Survey Water Resources report 85-4066. 30pp.

Evans, D.D. and Th.J. Nicholson (eds.). 1987. *Flow and Transport Through Unsaturated Fractured Rock*. Geophysical Monograph 4-2. Washington, DC: American Geophysical Union. 187pp.

French, R.H. 1986. *Daily, Seasonal, and Annual Precipitation at the Nevada Test Site, Nevada*. U.S. Department of Energy. DOE/NV/10384-01. 64pp.

French, R.H. 1987. *Effects of the Length of Record on Estimates of Annual and Seasonal Precipitation at the Nevada Test Site, Nevada*. U.S. Department of Energy. DOE/NV/10384-18. 50pp.

Freslon, M. 1980. *Transferts d'eau et de Solutés dans un Loess Sous Climat Mediterranéen*. Doctoral thesis. Univ. Paris VI and I.N.R.A. Montfavet, France.

Freyberg, D.L. 1986. A natural gradient experiment on solute transport in a sand aquifer, 2: spatial moments and the advection and dispersion of non-reactive tracers. *Water Resour. Res.* 22(13):2031-2046.

Gajem, Y.M., A.W. Warrick, and D.E. Myers. 1981. Spatial dependence of physical properties of a typic torrifluvent soil. *Soil Sci. Soc. Am. J.* 45: 709-715.

Gelhar, L.W. 1976. Stochastic analysis of flow in aquifers. *Advances in Groundwater Hydrology.* Proceedings, 1976 Symposium of the Amer. Water Resour. Assoc., Minneapolis, Minnesota.

Gelhar, L.W., P.J. Wierenga, K.R. Rehfeldt, C.J. Duffy, M.J. Simonett, T.-C. Yeh, and W.R. Strong. 1982. *Irrigation Return Flow Water Quality Monitoring, Modeling, and Variability in the Middle Rio Grande Valley, New Mexico.* EPA Report 600/2-83-072. New Mexico Institute of Mining and Tech. Socorro, New Mexico.

Gelhar, L.W. and C.L. Axness. 1983. Three dimensional stochastic analysis of macrodispersion in aquifers. *Water Resour. Res.* 19(1): 161-180.

Gelhar, L.W. 1984. Stochastic analysis of flow in heterogeneous porous media. *Selected Topics in Mechanics of Fluids in Porous Media.* Proceedings NATO Symposium, J. Bear and M.Y. Corapcioglu, eds. Dordrecht, The Netherlands: Martinus Nijhoff Publishers: 673-718.

Gelhar, L.W., A. Mantoglou, C. Welty, and K. Rehfeldt. 1984. *A Review of Field Scale Subsurface Solute Transport Processes Under Saturated and Unsaturated Conditions.* Report RP-22485-05. Electrical Power Research Institute.

Gelhar, L.W. 1986. Stochastic subsurface hydrology from theory to applications. *Water. Resour. Res.* 22(99): 135S-145S.

Gilman, J.R. and H. Kazemi. 1983. Improvements in simulation of naturally fractured reservoirs. *Soc. Pet. Eng. J.* pp. 695-707.

Gureghian, A.B. and B. Sagar. 1991. Evaluation of DCM3D - a dual continuum, 3-D groundwater flaw code for unsaturated fractured, porous media, Section 8.2 in "Report on Research Activities for Calendar Year 1990," CNWRA 90-01A, W. Patrick ed. Center for Nuclear Waste Regulatory Analyses. San Antonio, Texas.

Gutjahr, A.L., C.T. Kincaid, J.W. Mercer, I.P. Murarka, M.D. Siegal, and P.J. Wierenga. 1987. Panel summary report. *Workshop on Modeling of Solute Transport in the Unsaturated Zone.* Los Alamos, NM. NUREG/CR-4615. 2: 174-199.

Gvirtzman, H., M. Magaritz, Y. Kanfi, and I. Carmi. 1988. Matrix and fissure water movement through unsaturated calcareous sandstone. *Transport in Porous Media.* 3: 343-356.

Gvirtzman, H., J. Dvorkin, and A. Nur. 1990. Revising Kozeny equation for partly saturated porous media. *Fall Meeting Amer. Geophys. Union.* October 23, 1990. EOS Transactions. 71(43).

Haldeman, W.R., Y. Chuang, T.C. Rasmussen, and D.D. Evans. 1991. Laboratory analysis of fluid flow and solute transport through a fracture embedded in porous tuff. *Water Resour. Res.* 27(1):53-65.

Hamon, G. 1980. *Mise en euvre et Critique de Methods de Caracterisation Hydrodynomique de la Zone Non Saturee du Sol (application aux sols de culture du Senegal).* Doctoral Thesis. Univ. of Grenoble (I.M.G.) France.

Hestir, K., J. Long, J.-P. Chilès, and D. Billaux. 1987. *Some techniques for stochastic modeling of three-dimensional fracture networks.* Geostatistical, Sensitivity, and Uncertainty Methods for Groundwater Flow and Radionuclide Transport Modeling. B.E. Buxton ed. Battelle Press. Columbus, Ohio. pp. 495-519.

Hoeksema, R.J. and P.K. Kitanidis. 1985. Analysis of the spatial structure of properties of selected aquifers. *Water Resour. Res.* 21(4): 563-572.

Hoffman, D.C., W.R. Daniels, K. Wolfsberg, J.L. Thompson, R.S. Rundberg, S.L. Fraser, and K.S. Daniels. 1983. *Review of a Field Study of Radionuclide Migration from an Underground Nuclear Explosion at the Nevada Test Site.* Los Alamos National Laboratory report LA-UR-83-493. 17pp.

Hsieh, P.A., S.P. Neuman and E.S. Simpson. 1983. *Pressure-Testing of Fractured Rocks - A Methodology Employing Three-Dimensional Cross-Hole Tests.* U.S. Nuclear Regulatory Commission. Topical Report NUREG/CR-3213. 176pp.

Hufschmied, P. 1985. Estimation of three dimensional statistically anisotropic hydraulic conductivity field by means of single well pumping tests combined with flowmeter measurements. *The Stochastic Approach to Subsurface Flow.* pre-prints International Symposium, A.I.R.H., Montvillargenne, France.

Huyakorn, P.S., B.G. Jones, J.C. Parker, T.D. Wadsworth, and H.O. White Jr. 1987. Finite element simulation of moisture movement and solute transport in a large caisson. *Workshop on Modeling of Solute Transport in the Unsaturated Zone.* Los Alamos, New Mexico. NUREG/CR-4615. 2: 117-173.

INTRAVAL. 1990. INTRAVAL - An International Project to Study Validation of Geosphere Transport Models. Progress Report No. 4. Period March-October 1989. Published by Swedish Nuclear Power Inspectorate. Stockholm, Sweden.

Jacobson, E.A. 1990. Investigation of the spatial correlation of saturated hydraulic conductivities from a vertical wall of a trench. *Proceedings of the Fifth Canadian-American Conference on Hydrogeology: Parameter Identification and Estimation for Aquifers and Reservoirs.* Calgary, Alberta, Canada. S. Bachu, ed. Published by National Water Well Association, Dublin, Ohio. 189-198.

Jacobson, R.L., M.S. Henne, and J.W. Hess. 1986. *A Reconnaissance Investigation of Hydrogeochemistry and Hydrology of Rainier Mesa.* U.S. Department of Energy. DOE/NV/10384-05. 62pp.

Johnston, C.D., D.H. Hurle, D.R. Hudson and M.I. Height. 1983. *Water Movement Through Preferred Paths in Lateritic Profiles of the Darling Plateau, Western Australia.* Groundwater Research Paper No. 1, Commonwealth Scientific and Industrial Research Organization, Australia.

Kazemi, H. 1969. Pressure transient analysis of naturally fractured reservoirs with uniform fracture distribution. *Soc. Pet. Eng. J.* pp. 451-462.

Kent, B.C., C.R. Mauldin, and M.W. Cooper. 1982. *Evaluation of Subsurface Migration from Solar Ponds.* Underground Resource Management Report, Austin, Texas.

Khaleel, R. 1990. Porous medium models for advective transport through colonnade networks. *Fall Meeting Amer. Geophys. Union.* October 23, 1990. EOS Transactions. 71(43).

Kirchhoff, G.R. 1894. *Vorlesungen uber die Theorie der Warme.*

Klavetter, E.A. and R.R. Peters. 1986. *Estimation of Hydrologic Properties of an Unsaturated, Fractured Rock Mass.* Sandia National Laboratories report SAND84-2642. Albuquerque, New Mexico. 49pp.

Lahoud, R.G., D.H. Lobmeyer, M.S. Whitfield. 1984. *Geohydrology of Volcanic Tuff Penetrated by Test Well UE-25b#1, Yucca Mountain, Nye County, Nevada.* USGS-WRI-84-4253, Water Resources Investigations Report. U.S. Geological Survey. Denver, Colorado.

Lin, W. and W. Daily. 1984. *Transport Properties of Topopah Spring Tuff.* Lawrence Livermore National Laboratory report UCRL-53602. Livermore, CA. 20pp.

Liu, M.-X. and Z.-X. Chen. 1990. Exact solution for flow of slightly compressible fluids through multiple-porosity, multiple-permeability media. *Water Resour. Res.* 26(7): 1393-1400.

Long, J.C.S., and D.M. Billaux. 1987. From field data to fracture network modeling: an example incorporating spatial structure. *Water Resour. Res.* 23(7): 1201-1216.

Luxmoore, R.J., B.P. Spaulding, and I.M. Munro. 1981. Areal variation and chemical modification of weathered shale infiltration characteristics. *Soil Sci. Soc. Am. J.* 45: 687-691.

Mandelbrot, B.B. and J.W. Van Ness. 1968. Fractional Brownian motions, fractional noises and applications. *SIAM Review.* 10(4): 422-437.

Mandelbrot, B.B. and J.R. Wallis. 1969. Some long-run properties of geophysical records. *Water Resour. Res.* 5(2): 321-340.

Mangold, D. C. and C.-F. Tsang. 1991. *A Summary of Subsurface Hydrological and Hydrochemical Models.* Reviews of Geophysics. 29.

Mann, J.F. 1977. Wastewaters in the vadose zone of arid regions. *Hydrologic Interactions. Groundwater.* 14(6).

Mantoglou, A. and L.W. Gelhar. 1987a. Stochastic modeling of large-scale transient unsaturated flow systems. *Water Resour. Res.* 23(1): 37-46.

Mantoglou, A. and L.W. Gelhar. 1987b. Capillary tension head variance, mean soil moisture content, and effective specific soil moisture capacity of transient unsaturated flow in stratified soils. *Water Resour. Res.* 23(1): 47-56.

Mantoglou, A. and L.W. Gelhar. 1987c. Effective hydraulic conductivities of transient unsaturated flow in stratified soils. *Water Resour. Res.* 23(1): 57-67.

Martinez, M.J. 1988. *Capillary-Driven Flow in a Fracture Located in a Porous Medium.* Sandia National Laboratories report SAND-84-1697. Albuquerque, New Mexico. 52pp.

McCord, J.T., D.B. Stephens, and J.L. Wilson. 1988. Field-scale unsaturated flow and transport in a sloping uniform porous medium: field experiments and modeling considerations. *Validation of Flow and Transport Models for the Unsaturated Zone.* P.J. Wierenga and D. Bachelet, eds. 256-267.

McCord, J.T. and D.B. Stephens. 1989. *Analysis of Soil-Water Movement on a Sandy Hillslope.* WRRI Report No. 245. New Mexico Water Resources Research Institute. Las Cruces, New Mexico. 94pp.

McCord, J.T. and D.A. Zimmerman. 1990. Using a stochastic variably saturated flow model to simulate tracer migration in the Los Alamos Caisson experiments. *Am. Geophys. Union Spring Meeting Abstracts.* EOS. 517.

McCord, J.T., D.B. Stephens, and J.L. Wilson. 1991. Toward validating state-dependent macroscopic anisotropy in unsaturated media: Field experiments and modeling considerations. In: P.J. Wierenga (Guest-Editor), Validation of Flow and Transport Models for the Unsaturated Zone. *J. Contam. Hydrol.* 7: 147-177.

McIntosh, D. 1990. UDEX: unsaturated zone dispersion experiment. *EPRI Journal.* 42-45.

Miller, E.E., and R.D. Miller. 1955. Theory of capillar flow: I. practical implications, II. experimental information. *Soil Sci. Soc. Proc.* 267-275.

Miller, E.E. and R.D. Miller. 1956. Physical theory for capillary flow phenomena. *J. Appl. Phys.* 27:324-332.

Milly, P.C.D. 1988. Advances in Modeling of Water in the Unsaturated Zone. *Transport in Porous Media*, 3(5):491-514.

Mishra, S. and J.C. Parker. 1990. On the relation between saturated conductivity and capillary retention characteristics. *Groundwater*, Vol 28:775-777.

Moltyaner, G.L. 1990. Field studies of dispersion: radioactive tracer experiments on scales of 20, 40, and 260 metres. *Dynamics of Fluids in Hierarchial Porous Media.* J. Cushman, ed. New York, NY: Academic Press. Chapter II.

Montazer, P. and W.E. Wilson. 1984. *Conceptual Hydrologic Model of Flow in the Unsaturated Zone, Yucca Mountain, Nevada.* U.S. Geological Survey Water Resources Investigations report 84-4345. 55pp.

Montazer, P., E.P. Weeks, F. Thamir, S.N. Yard, and P.E. Hofrichter. 1985. *Monitoring the Vadose Zone in Fractured Tuff, Yucca Mountain, Nevada.* U.S. Geological Survey, Denver, Colorado. 30pp.

Moore, R. E. 1939. *Water Conduction from Shallow Water Tables.* Hilgardia. v12(6). 383-426.

Moss, M., et al. 1982. *Effects of Composition, Porosity, Bedding Plane Orientation, Water Content and a Joint on the Thermal Conductivity of Tuff.* Sandia National Laboratories report SAND84-1164. Albuquerque, New Mexico. 28pp.

Mualem, Y. 1976. *A Catalogue of the Hydraulic Properties of Unsaturated Soils.* Hydrodynamics and Hydraulic Laboratory, Research Project No. 442. Technian Institute of Technology. Haifa, Israel. 100pp.

NAGRA Bulletin. 1988. Special english edition. M. Güntensperger ed. Baden, Switzerland. 62 pp.

Narasimhan, T.N., P.A. Witherspoon, and A.L. Edwards. 1978. Numerical model for saturated-unsaturated flow in deformable porous media; 2: The Algorithm. *Water Resour. Res.* 14: 255-261.

Narasimhan, T.N. 1982. Multidimensional numerical simulation of fluid flow in fractured porous media. *Water Resour. Res.* 18(4): 1235-1247.

Neretnieks, I., Abelin, H., and Birgersson, L. Some recent observations of channeling in fractured rocks: its potential impact on radionuclide migration. *Geostatistical, Sensitivity, and Uncertainty Methods for Groundwater Flow and Radionuclide Transport Modeling.* B. E. Buxton ed., Columbus, Ohio, pp. 387-410.

Neuman, S.P. and J.S. Depner. 1988. Use of variable-scale pressure test data to estimate the log hydraulic conductivity covariance and dispersity of fractured granites near Oracle, Arizona. *J. of Hydrology.* 102: 475-501.

Neuman, S.P. 1990. Universal scaling of hydraulic conductivities and dispersivities in geologic media. *Water Resour. Res.* 26(8): 1749-1758.

Neuman, S.P., Y.-K. Zhang, and O. Levin. 1990. Quasi-linear analysis, universal scaling, and Lagrangian simulation of dispersion in complex geologic media. *Dynamics of Fluids in Hierarchial Porous Media.* Chapter XIII. J. Cushman, ed. New York: Academic Press.

Nielsen, D.R., J.W. Biggar and K.T. Ehr. 1973. Spatial variability of field-measured soil water properties. *Hilgardia.* 42: 215-260.

Nielsen, D.R., M.Th. van Genuchten, and J.W. Biggar. 1986. Water flow and solute transport processes in the unsaturated zone. *Water Resour. Res.* 22(9): 89S-108S.

Nimick, F.B. and B.M. Schwartz. 1987. *Bulk, Thermal, and Mechanical Properties of the Topopah Spring Member of the Paintbrush Tuff, Yucca Mountain, Nevada.* Sandia National Laboratories Report SAND85-0762. Albuquerque, New Mexico.

Nitao, J.J. 1989. *On the Infiltration of a Liquid Front in an Unsaturated, Fractured Porous Media (Part II).* Lawrence Livermore National Laboratory report UCID-21743. Livermore, California.

Nitao, J.J. and T.A. Buscheck. 1989. On the infiltration of a liquid front in an unsaturated, fractured porous medium. *Proceedings, American Nuclear Society Topical Meeting on Nuclear Waste Isolation in the Unsaturated Zone (FOCUS 89).* September 17-21, 1989. Las Vegas, Nevada.

Norris, A.E., K. Wolfsberg and S.K. Gifford. 1985. *Chlorine-36 Measurements of the Unsaturated Zone Flux at Yucca Mountain.* Los Alamos National Laboratory report LA-UR-85-2408. Los Alamos, New Mexico. 10pp.

Norris, A.E., K. Wolfsberg, S.K. Gifford, H.W. Bentley, and D. Elmore. 1987. *Infiltration at Yucca Mountain, Nevada, traced by ^{36}Cl.* New York, NY: Elsevier Science Publishers Co., Inc.

Nuclear Waste Policy Amendments Act. 1987. Public Law 100-203, Title 42, Section 10101, United States Code.

Ortiz, T.S., R.L. Williams, F.B. Nimick, B.C. Whittet, and D.L. South. 1985. *Three-Dimensional Model of Reference Thermal/Mechanical and Hydrological Stratigraphy at Yucca Mountain, southern Nevada.* Sandia National Laboratories report SAND84-1076. Albuquerque, NM. 80pp.

Parker, J. C. 1989. *Multiphase Flow and Transport in Porous Media.* Reviews of Geophysics. 27(3). August 1989.

Peters, R.R., E.A. Klavetter, I.J. Hall, S.C. Blair, G.W. Heller, and G.W. Gee. 1984. *Fracture and Matrix Characteristics of Tuffaceous Materials from Yucca Mountain, Nye County, Nevada.* Sandia National Laboratories report SAND84-1471. Albuquerque, New Mexico. 63pp.

Peters, R.R., J.H. Gauthier and A.L. Dudley. 1985. *Effect of Percolation Rate on Water-Travel Time in Deep, Partially Saturated Zones*. Sandia National Laboratories report SAND85-0854C. Albuquerque, New Mexico. 43pp.

Peters, R.R., E.A. Klavetter, J.T. George, and J.H. Gauthier. 1986a. *Measuring and Modeling Water Imbibition into Tuff*. Sandia National Laboratories report SAND86-1757C. Albuquerque, New Mexico. 26pp.

Peters, R.R., J.H. Gauthier, and A.L. Dudley. 1986b. *The Effect of Percolation Rate on Water-Travel Time in Deep, Partially Saturated Zones*. SAND85-0854. Sandia National Laboratories. Albuquerque, N. Mex.

Peters, R.R. and E.A. Klavetter. 1988. A continuum model for water movement in an unsaturated fractured rock mass. *Water Resour. Res.* 24(3): 416-430.

Philip, J.R. 1969. Theory of infiltration. *Advances in Hydroscience, Volume 5*. New York, NY: Academic Press.

Polmann, D.J., E.G. Vomvoris, D. McLaughlin, E.M. Hammick, and L.W. Gelhar. 1988. *Application of Stochastic Models to the Simulation of Large-Scale Unsaturated Flow and Transport*. U.S. Nuclear Regulatory Commission NUREG/CR-5094. Washington, DC.

Polmann, D.J., D. McLaughlin, L.W. Gelhar, and R. Ababou. 1991. Stochastic modeling of large-scale flow in heterogeneous unsaturated soils *Water Resour. Res.* 27(7):1447-1458.

Power, W.L. and T.E. Tullis. 1991. Euclidian and fractal models for the description of rock surface roughness. Abstract 8165 (*J. Geophys. Res.*) Geophys. Abstr. in press. January. p. 11.

Prill, R.C. 1977. *Movement of Moisture in the Unsaturated Zone in a Loess-Mantled Area, Southwestern Kansas*. USGS Prof. Paper 1021.

Pruess, K., J.S.Y. Wang, and Y.W. Tsang. 1986. Effective continuum approximation for modeling fluid flow in fractured porous tuff. Sandia National Labs. Report SANF86-7000. Albuquerque, NM.

Pruess, K. and T.N. Narasimhan. 1988. *Numerical Modeling of Multiphase and Nonisothermal Flow in Fractured Media*. Lawrence Berkeley Lab report LBL-25547. 22pp.

Pruess, K., J.S.Y. Wang, and Y.W. Tsang. 1988. *Effective Continuum Approximation for Modeling Fluid and Heat Flow in Fractured Porous Tuff: Nevada Nuclear Waste Storage Investigations Project*. Sandia National Laboratories report SAND-86-7000. Albuquerque, NM. 100pp.

Pruess, K., J.S.Y. Wang, and Y.W. Tsang. 1990a. On thermohydrologic conditions near high-level nuclear wastes emplaced in partially saturated fractured tuff, 1. simulation studies with explicit consideration of fracture effects. *Water Resour. Res.* 26(6): 1235-1248.

Pruess, K., J.S.Y. Wang, and Y.W. Tsang. 1990b. On thermodhydrologic conditions near high-level nuclear wastes emplaced in partially saturated fractured tuff, 2. effective continuum approximation. *Water Resour. Res.* 26(6): 1249-1261.

Purtymum, W.D. 1973. *Underground Movement of Tritium from Solid-Waste Storage Shafts.* Los Alamos Scientific Laboratory Informal Report LA-5286-MS, Los Alamos Scientific Lab., New Mexico.

Raats, P.A.C. 1971. Some properties of flows in unsaturated soilds with an exponential dependence of hydraulic conductivity upon the pressure head. *J. of Hydrology.* 14: 129-138.

Rasmussen, T.C. 1990. Steady fluid flow and travel times in partially saturated fractures using a discrete air-water interface. Department of Hydrology and Water Resources, University of Arizona. Tucscon, Arizona. *Abstract, EOS Transactions of the Amer. Geophys. Union.* 71(39).

Rasmussen, T.C. and D.D. Evans. 1987. *Unsaturated Flow and Transport Through Fractured Rock Related to High-Level Waste Repositories: Final Report, Phase 2.* U.S. Nuclear Regulatory Commission NUREG/CR-4655. 500pp.

Rasmussen, T.C. and D.D. Evans. 1989. *Fluid Flow and Solute Transport Modeling Through Three-Dimensional Networks of Variably Saturated Discrete Fractures.* Report NUREG/CR-5239. U.S. Nuclear Regulatory Commission. Washington, D.C. 193pp

Rasmussen, T.C., D.D. Evans, P.J. Sheets, and J.H. Blanford. 1990. *Unsaturated Fractured Rock Characterization Methods and Data Sets at the Apache Leap Tuff Site.* NUREG/CR-5596 Report, U.S. Nuclear Regulatory Commission, Washington, DC.

Reda, D.C. 1986. *Influence of Tranverse Microfractures on the Imbibition of Water into Initially Dry Tuffaceous Rock.* Sandia National Laboratories report SAND86-0420C. Albuquerque, NM.

Richards, L.A. 1931. Capillary conduction of liquids through porous medium. *Physics* 1: 318-333.

Ross, B. 1984. A conceptual model of deep unsaturated zones with negligible recharge. *Water Resour. Res.* 20(11): 1627-1629.

Roth, K., H. Flühler, and C. Gysi. 1988. Temporal change of the spatial distribution of chlorine displaced through a heterogeneous soil. *Validation of Flow and Transport Models for the Unsaturated Zone.* P.J. Wierenga and D. Bachelet, eds. 362-366.

Roth, K. 1989a. Transport of a conservative tracer under field conditions: qualitative modeling with random-walk in a double porous medium. Abstract. *International Workshop on Field Scale Water and Solute Flux in Soils.* September 24-29, 1989. Monte-Verita, Ascona, Switzerland.

Roth, K. 1989b. *Stofftransport in Wasserungesättigten Untergrund Natürlicher, Heterogener Böden Unter Feldbedingungen.* Doctoral Thesis, Diss. ETH No. 8907, Swiss Federal Institute of Technology (ETH), Zurich, Switzerland. (in German with English abstract).

Routson, R.C., W.H. Price, D.J. Brown, and K.R. Fecht. 1979. *High-Level Waste Leakage from the 241-T-106 Tank at Hanford.* Report RHO-ST-14. U.S. Department of Energy/Rockwell International, Richland, WA.

Rulon, J., G.S. Bodvarsson, and P. Montazer. 1986. *Preliminary Numerical Simulations of Groundwater Flow in the Unsaturated Zone, Yucca Mountain, Nevada.* Lawrence Berkeley Laboratory report LBL-20553. 102pp.

Rush, F.E., W. Thordarson, and D.G. Pyles. 1984. *Geohydrology of Test Well USW H-1, Yucca Mountain, Nye County, Nevada.* USGS-WRI-84-4032. Water-Resources Investigations Report. U.S. Geological Survey Survey. Denver, Colorado.

Russell, C.E., J.W. Hess, and S.W. Tyler. 1987. Hydrogeologic investigations of flow in fractured tuffs, Rainier Mesa, Nevada Test Site. *Flow and Transport Through Unsaturated Fractured Rock.* D.D. Evans and Th.J. Nicholson, eds. Washington, DC: American Geophysical Union. 43-50.

Russo, A.J. and D.C. Reda. 1988. *Drying of an Initially Saturated Fractured Volcanic Tuff.* San National Laboratories report SAND-87-0293C. Albuquerque, New Mexico.

Russo, D. and E. Bresler. 1980. Scaling soil hydraulic properties of a heterogeneous field. *Soil Soc. Am. J.* 44: 681-684.

Russo, D. and E. Bresler. 1981. Soil hydraulic properties as stochastic processes. I: an analysis of field spatial variability. *Soil Soc. Am. J.* 45: 682-687.

Russo, D. 1983. A geostatistical approach to the trickle irrigation design in heterogeneous soils, (1): theory. *Water Resour. Res.* 19: 632-642.

Russo, D. and G. Dagan. 1991. On solute transport in a heterogeneous porous formation under saturated and unsaturated water flows. *Water Resour. Res.* 27(3):285-292.

Russo, D. 1991. Stochastic analysis of simulated vadose-zone solute transport in a vertical cross-section of heterogeneous soil during nonsteady water flow. *Water Resour. Res.* 27(3):267-283.

Sagar, B. and A.K. Runchal. 1984. Permeability of fractured rock: effects of fracture size and data uncertainties. *Water Resour. Res.* 18(2): 266-274.

Sagar, B. 1991. Hydrologic research for performance assessment. *Proceedings Workshop V: Flow and Transport Through Unsaturated Fractured Rock Related to High-Level Radioactive Waste Disposal.* January 7-10, 1991. Tucson, Arizona. D.D. Evans and T.J. Nicholson (eds). NUREG/CP-0040. U.S. Nuclear Regulatory Commission. Washington, D.C..

Scisson, J.B. and P.J. Wierenga. 1981. Spatial variability of steady state infiltration rate as a stochastic process. *Soil Sci. Soc. Am. Journal.* 45: 699-704.

Scott, R.B., R.W. Spengler, S. Diehl, A.R. Lappin, and M.P. Chornak. 1983. Geologic character of tuffs in the unsaturated zone at Yucca Mountain, southern Nevada. *Role of the Unsaturated Zone in Radioactive and Hazardous Waste Disposal.* J.W. Mercer, P.S.C. Rao, and I.W. Marine, eds. Ann Arbor, MI: Ann Arbor Science Publishers: 289-335.

Shapiro, A.M. and J. Andersson. 1983. Steady state fluid response in fractured rock: a Boundary Element solution for a coupled discrete fracture continuum model. *Water Resour. Res.* 19(4): 959-969.

Shapiro, A.M. and J. Bear. 1985. Evaluating the hydraulic conductivity of fractured rock from information on fracture geometry. *Communication at 17th Internat. Congress on Hydrogeology of Rocks of Low Permeability.* Internat. Association of Hydrogeologists. Jan. 7-10. Tucson, Arizona.

Shapiro, A.M. 1987. Transport equations for fractured porous media. *Advances in Transport Phenomena in Porous Media.* J. Bear and M.Y. Corapcioglu, eds. NATO A.S.I. Series E, No. 128: 405-471.

Sharma, M.L., G.A. Gander, and C.G. Hunt. 1980. Spatial variability of infiltration in a watershed. *J. of Hydrology.* 45: 101-122.

Simmons, C.S., D.R. Nielsen, and J.W. Biggar. 1979. Scaling of field-measured soil water properties. *Hilgardia.* 47(4): 77-173.

Sinnock, S., Y.T. Lin and M.S. Tierney. 1986. *Preliminary Estimates of Groundwater Travel Time and Radionuclide Transport at the Yucca Mountain Repository Site.* Sandia National Laboratories report SAND85-2701. Albuquerque, New Mexico. 156pp.

Sinnock, S. and Y.T. Lin. 1987. Preliminary bounds on the expected postclosure performance of the Yucca Mountain repository site, southern Nevada. *Journal of Geophysical Research.* 92(B): 7820-7842.

Sisson, J.B. and P.J. Shouse. 1990. Scaled hydraulic properties of the Apache Leap tuff. *Am. Geophys. Union Spring Meeting Abstracts.* EOS. 514.

Smoot, J. L. and B. Sagar. 1990. *Three-Dimensional Contaminant Plume Dynamics in the Vadose Zone: Simulation of the 241-T-106 Single-Shell Tank Leak at Hanford.* Pacific Northwest Laboratory. PNL-7221.

Snow, D.T. 1969. Anisotropic permeability of fractured media. *Water Resour. Res.* 5(6): 1273-1289.

Stephens, D.B., A.M. Parsons, E.D. Mattson, K. Black, K. Flanigan, R. Bowman, and W.B. Cox. 1988. A field experiment of three-dimensional flow and transport in a stratified soil. *Validation of Flow and Transport Models for the Unsaturated Zone.* P.J. Wierenga and D. Bachelet, eds. 401-413.

Streltsova, T.D. 1976. Hydrodynamics of groundwater flow in a fractured formation. *Water Resour. Res.* 12(3): 405-414.

Sudicky, E.A. 1986. A natural gradient experiment on solute transport in a sand aquifer: spatial variability of hydraulic conductivity and its role in the dispersion process. *Water Resour. Res.* 22(13): 2069-2082.

Supkow, P.G. 1974. *Tank Infiltration Test Conducted by Hydrotechnics.* Arizona Nuclear Project.

Thordarson, W. 1965. *Perched Groundwater in Zeolitized-Bedded Tuff, Ranier Mesa and Vicinity, Nevada Test Site, Nevada.* U.S. Geological Survey report TEI-862. 89pp.

Thordarson, W. 1983. *Geohydrologic Data and Test Results from Well J-13, Nevada Test Site, Nye County, Nevada.* USGS-WRI-83-4171, Water Resources Investigations Report, U.S. Geological Survey, Denver, Colorado.

Thordarson, W., F.E. Rush, R.W. Spengler, and S.J. Waddell, 1984. *Geohydrologic and Drill-Hole Data for Test Well USW H-3, Yucca Mountain, Nye County, Nevada.* USGS-OFR-84-149, Open-File Report, U.S. Geological Survey, Denver, Colorado, 28 p.

Thornburg, T.M. 1990. *Electrical Resistivity of Unsaturated, Fractured Tuff: Influence of Moisture Content and Geologic Structure.* M.S. Thesis. Dept. Hydrology and Water Resources, Univ. of Arizona. Tucson, Arizona. 196pp.

Tompson, A.F., R. Ababou, and L.W. Gelhar. 1989. Implementation of the three-dimensional turning bands random field generator. *Water Resour. Res.* 25(10): 2227-2243.

Tompson, A.F.B. and L.W. Gelhar. 1990. Numerical simulation of solute transport in three-dimensional, randomly heterogeneous porous media. *Water Resour. Res.* 26(10): 2541-2562.

Trauntwein, S.J., D.E. Daniel, and H.W. Cooper. 1983. Case history study of water flow through unsaturated soils. *The Role of the Unsaturated Zone in Radioactive Hazardous Waste Disposal,* Mercer et al., eds. Ann Arbor, MI: Ann Arbor Science.

Travis, B.J. et al. 1984. *Preliminary Estimates of Water Flow and Radionuclide Transport in Yucca Mountain.* Los Alamos National Laboratory report LA-UR-84-40. Los Alamos, New Mexico.

Tyler, S.W. 1987. *Review of Soil Moisture Flux Studies at the Nevada Test Site.* U.S. Department of Energy. DOE/NV/10384-17. 56pp.

United States General Accounting Office. 1988. *Nuclear Waste: Fourth Annual Report on DOE's Nuclear Waste Program.* GAO/RCED-88-131.

Vachaud, G., C. Dancette, S. Sanko, and J.L. Thony. 1978. Méthode de caractérisation hydrodynamique in-situ d'un sol non saturé (application à deux types de sols du Sénégal). *Annales Agronomiques*. 29(1): 1-36.

van Genuchten, R. 1978. *Calculating the Unsaturated Hydraulic Conductivity with a New Closed-Form Analytical Model*. Water Res. Program. Princeton University. 65pp.

van Genuchten, M.Th. 1980. A closed form equation for predicting the hydraulic conductivity of unsatured soils. *Soil Sci. Soc. Am. J.* 44: 892-898.

Vanmarcke, E. 1983. *Random Fields Analysis and Synthesis*. Cambridge, MA: The MIT Press. 382pp.

Vauclin, M., D. Khanji, and G. Vachaud. 1979a. Experimental and numerical study of a transient two-dimensional unsaturated-saturated water table recharge problem. *Water Resour. Res.* 15(5): 1089-1101.

Vauclin, M., R. Haverkamp and G. Vachaud. 1979b. *Résolution Numérique d'une Equation de Diffusion Nonlinéaire*. P.U.G.. Grenoble. 183pp.

Vauclin, M., J. Imbernon, and G. Vachaud. 1981. Spatial variability of some soil physical properties over one-hectar field plot. *American Geophysical Union. Chapman Conference*. Fort-Collins, Colorado. July. p.5-16].

Vauclin, M. 1982. Méthode d'étude de la variabilité spatiale des propriétés d'un sol. *Variabilité Spatiale des Processus de Transfert dans les Sols*. Avignon, France. Ed. INRA publ. 15: 9-43.

Vieira, S.R., D.R. Nielsen, and J.W. Biggar. 1981. Spatial variability of field-measured infiltration rate. *Soil Sci. Soc. Am. J.* 45: 1040-1048.

Wang, J.S.Y., C.-F. Tsany, and R.A. Sterbentz. 1983. The state of the art of numerical modeling of thermohydrologic flow in fractured rock masses. *Environmental Geology*. 4(314): 133-199.

Wang, J.S.Y. and T.N. Narasimhan. 1984. *Hydrologic Mechanisms Governing Fluid Flow in Partially Saturated, Fractured, Porous Tuff at Yucca Mountain*. Lawrence Berkeley Laboratory report LBL-18473. Berkeley, California. 58pp.

Wang, J.S.Y. and T. N. Narasimhan. 1985. Hydrologic mechanisms governing fluid flow in a partially saturated, fractured, porous medium. *Water Resour. Res.* 21(12): 1861-1874.

Wang, J.S.Y. and T.N. Narasimhan. 1986. *Hydrologic Mechanisms Governing Partially Saturated Fluid Flow in Fractured Welded Units and Porous Non-Welded Units at Yucca Mountain*. Sandia National Laboratories report SAND85-7114. Albuquerque, New Mexico. 83pp.

Wang, J.S.Y. and T.N. Narasimhan. 1988. *Hydrologic Modeling of Vertical and Lateral Movement of Partially Saturated Fluid Flow Near a Fault Zone at Yucca Mountain.* Sandia National Laboratories report SAND-87-7070. Albuquerque, New Mexico. 76pp.

Warren, J.E. and P.J. Root. 1963. The behavior of naturally fractured reservoirs. *Soc. Pet. Eng. Jour.* pp. 245-255.

Warrick, A.W. and D.O. Lomen. 1976. Time dependent linearized infiltration, III: strip and disc sources. *Soil Sci. Soc. Am. J.*, 40:4-17.

Warrick, A.W., G.J. Mullen, and D.R. Nielsen. 1977. Scaling field-measured soil hydraulic properties using a similar media concept. *Water Resour. Res.* 13: 355-362.

White, I. and M.J. Sully. 1987. Macroscopic and microscopic capillary length and time scales from field infiltration. *Water Resour. Res.* 23(8): 1516-1522.

White, I. and M.J. Sully. 1988. Field characteristics of the macroscopic capillary length or alpha parameter. Conference Proceedings. *Validation of Flow and Transport Models for the Unsaturated Zone.* P.J. Wierenga and D. Bachelet, eds.

Whitfield, M.S., Jr., E.P.Eshom, W. Thordarson, and D.H. Schaefer. 1985. *Geohydrology of Rocks Penetrated by Test Well USW H-4, Yucca Mountain, Nye County, Nevada.* USGS-WRI-85-4030, Water-Resources Investigations Report, U.S. Geological Survey, Denver, Colorado.

Wierenga, P.J., L.W. Gelhar, C.S. Simmons, G.W. Gee, and T.J. Nicholson. 1986a. *Validation of Stochastic Flow and Transport Models for Unsaturated Soils: A Comprehensive Field Study.* Report NUREG/CR-4622 (U.S. Nuclear Regulatory Commission), Pacific Northwest Laboratory, Richland, Washington.

Wierenga, P.J., I. Porro, W. Strong, J. Vinson, D. Hudson, M. Nash, and A. Schneeberger. 1986b. *Validation of Stochastic Flow and Transport for Unsaturated Soils.* Research Report 86-SS-01, Dept. Agronomy Agric., New Mexico State University, Las Cruces, New Mexico.

Wierenga, P.J. 1988. Validation of flow and transport models at the Jornada test facility. *Validation of Flow and Transport for the Unsaturated Zone.* P.J. Wierenga and D. Bachelet, eds. Conference Proceedings. 525-530.

Wierenga, P.J. and D. Bachelet (eds.). 1988. *Validation of Flow and Tranport Models for the Unsaturated Zone.* Conference Proceedings. May 23-26, 1988. Research Report 88-SS-04. Dept. Agronomy and Horticulture, New Mexico State University. Las Cruces, New Mexico. 545pp.

Wierenga, P.J., A.F. Toorman, D.B. Hudson, J. Vinson, M. Nash, and R.G. Hills. 1989. *Soil Physical Properties at the Las Cruces Trench Site.* U.S. Nuclear Regulatory Commission NUREG/CR-5441. Washington, DC.

Winograd, I.J., and W. Thordarson. 1975. *Hydrogeologic and Hydrochemical Framework, South-Central Great Basin, Nevada-California, with Special Reference to the Nevada Test Site.* U.S. Geological Survey Professional Paper 712-C, Washington, D.C., pp. C1-C126.

Winograd, I.J. 1981. Radioactive waste disposal in thick unsaturated zones. *Science.* 212(4502): 1457-1464.

Winter, C.L., C.M. Newman, and S.P. Neuman. 1984. A perturbation expansion for diffusion in a random velocity field, *SIAM J. Appl. Math.* 24: 411-424.

Woodbury, A.D. and E.A. Sudicky. 1991. The geostatistical characteristics of the Borden aquifer. *Water Resour. Res.* 27(4):533-546.

Yeh, T.-C., L.W. Gelhar, and A.L. Gutjhar. 1985a. Stochastic analysis of unsaturated flow in heterogeneous soils: (1) statistically anisotropic media. *Water Resour. Res.* 21(4): 447-456.

Yeh, T.-C., L.W. Gelhar, and A.L. Gutjhar. 1985b. Stochastic analysis of unsaturated flow in heterogeneous soils: (2) statistically anisotropic media with variable α. *Water Resour. Res.* 21(4): 457-464.

Yeh, T.-C., L.W. Gelhar, and A.L. Gutjhar. 1985c. Stochastic analysis of unsaturated flow in heterogeneous soils: (3) observations and applications. *Water Resour. Res.* 21(4): 465-471.

Yeh, T.C., T.C. Rasmussen, and D.D. Evans. 1988. *Simulation of Liquid and Vapor Movement in Unsaturated Fractured Rock at the Apache Leap Tuff Site (Models and Strategies).* Report NUREG/CR-5097. U.S. Nuclear Regulatory Commission. Washington, D.C. 73 pp.

Yeh, T.C. 1989. One-dimensional steady state infiltration in heterogeneous soils. Water Resour. Res. 25 (10):2149-2121.

Yucca Mountain Project Bibliography. 1989. Office of Scientific and Technical Information, U.S. Department of Energy. A.T. Tamura and J.L. Lorenz, comp. DOE/OSTI 3406 (Suppl. 1) (Add. 2).

Zimmerman, R.W., S. Kumar, and G.S. Bodvarsson. 1990. Lubrication theory analysis of the permeability of rough-walled fractures. *Fall Meeting Amer. Geophys. Union.* October 23, 1990. EOS Transactions. 71(43).

Zimmerman, R.W., and G.S. Bodvarsson. 1990. Absorption of water into porous blocks of various shapes and sizes. *Water Resour. Res.* 26(11): 2797-2806.

Appendix:
Annotated Bibliography

Note: All references given in this Annotated Bibliography can be found in the overall list of references as well.

Barton, C.C. 1986. Fractal geometry of two-dimensional fracture networks at Yucca Mountain, southwestern Nevada. *Proceedings of International Symposium on Fundamentals of Rock Joints*. Bjorkliden, Lapland, Sweden.

Fracture traces exposed on three 214 and 260 m^2 pavements in the same Miocene ash-flows tuff at Yucca Mountain, southwestern Nevada, have been mapped at a scale of 1:50. The maps are two-dimensional sections through the three-dimensional network of strata-bound fractures. All fractures with trace lengths greater than 0.20 m were mapped. The distributions of fracture-trace lengths is log-normal. The fractures do not exhibit well-defined sets based on orientation. A fractal analysis was conducted for each network. Each network appears to be fractal, and the fractal dimensions are tightly clustered.

Borg, I.Y., R. Stone, H.B. Levy, and L.D. Ramspott. 1976a. *Information Pertinent to the Migration of Radionuclides in Ground Water at the Nevada Test Site. Part 1. Review and Analysis of Existing Information*. Lawrence Livermore Laboratory Report No. UCRL-52078 (Pt. 1). 221pp.

Borg, I.Y., R. Stone, H.B. Levy, and L.D. Ramspott. 1976b. *Information Pertinent to the Migration of Radionuclides in Ground Water at the Nevada Test Site. Part 2. Annotated Bibliography*. Lawrence Livermore Laboratory Report No. UCRL-52078 (Pt. 2). 114pp.

A history of NTS is given, the geologic and hydrologic setting is described, and the amount of radioactivity deposited within and near the main aquifers is estimated. Tritium is the most mobile radionuclide and may be the only isotope of concern. Highest priority is assigned to measurement of tritium and other radionuclides in large water samples taken from nuclear chimneys that water has re-entered after an explosion. Study of the many unplugged holes that penetrate the Tuff Aquitard; testing of the assumption that radionuclides deposited in the unsaturated zone are isolated from the saturated zone because of limited precipitation and downward movement of moisture. Part 2 of UCRL-52078 consists of the bibliography and abstracts that were compiled in the course of searching the literature for information on the migration of radionuclides in groundwater at the Nevada Test Site. The bibliography also includes numerous references to work done at foreign nuclear centers or contracted to outside agencies by these same centers.

Bowman, R.S., D.P. Grablea, J.F. Gibbens, and D.B. Stephens. 1990. Three-dimensional solute transport in a heterogeneous vadose zone. *Amer. Geophys. Union Spring Meeting Abstracts*. EOS, 514.

Instrumented irrigation plot in layered alluvial deposits, 10m x 10m, with solution samplers down to 7m in depth. Fluor-organic tracers, and bromide. Vertical tracer velocities and vertical dispersivities were both found to be log-normally distributed. Significant lateral flow.

Czarnecki, J.B. 1984. *Simulated Effects of Increased Recharge on the Groundwater Flow System of Yucca Mountain and Vicinity, Nevada-California.* U.S. Geological Survey Water Resources Investigations report 84-4344. 33pp.

A study was performed to assess the potential effects of changes in future climatic conditions on the groundwater system in the vicinity of Yucca Mountain by simulating the groundwater system using a two-dimensional, finite-element groundwater flow model. The simulated portion of the water table rose as much as 130 m near the area of the repository for a simulation involving a 100 percent increase in precipitation.

Daily, W., W. Lin, and T. Buscheck. 1987. Hydrological properties of Topopah Spring Tuff - laboratory measurements. *Journal of Geophysical Research.* 92(B8): 7854-7864.

The purpose of this work is to study the transport of liquid and vapor water from the Topopah Spring welded unit under conditions expected in the near-field environment of a high-level nuclear waste container. A naturally fractured sample of the Topopah Spring Tuff and well J-13 water were used. During the more than six month experiment duration, water permeability decreased by approximately three orders of magnitude. The most likely mechanism is the redeposition of silica in the fracture. Results also indicate that the sample dehydrates and rehydrate nonuniformly.

Daily, W. and A. Ramirez. 1987. *An Experiment to Determine Drilling Water Imbibition by In-Situ Densely Welded Tuff.* Lawrence Livermore National Laboratories. Report No. UCID-21249-Rev. 1. 8pp.

Experiments were performed to determine the extent of penetration of drill water into Grouse Canyon densely welded tuff during use of normal drilling practices. Core samples were examined from a borehole cored in a rib of the Rock Mechanics drift in G-tunnel at the Nevada Test Site, Nye County, Nevada. Methylene blue dye was added to the drill water to act as a tracer which stained the rock blue on contact. We found that in the imbibition process, the dye and water separated such that the water penetrated the matrix to a much greater depth. This result meant that any interpretation of drill water imbibition in borehole core based on this dye as a tracer is unreliable. More important, however, is the conclusion that the presence of methylene blue dye on the rock indicates the presence of tracer water flow, but the absence of the dye does not rule out the presence of water flow.

Duffy, C.J. and S. Al-Hassan. 1987. Time and frequency domain analysis of tracer migration in crushed tuff. *Workshop on Modeling of Solute Transport in the Unsaturated Zone.* Los Alamos, New Mexico. NUREG/CR-4615. 2: 82-116.

The time moment method as presented by Valocchi (1985) and Himmelbau (1970) is compared with the frequency domain method for transport parameter estimation for the LANL caisson experiments. Parameters for several tracers are estimated and compared using the time and frequency domain methods. Descriptions of the models are given. Some speculation is presented

regarding the nature of local and macrodispersive effects in the experiment, including some indication concerning the effect of uncertainty in the velocity, source strength, and random measurement errors on the overall interpretation of the experiment. Descriptions of the models are given.

Dykhuizen, R.C. 1988. *Transport of Solutes Through Unsaturated Fractured Media: Nevada Nuclear Waste Storage Investigations Project.* Sandia National Laboratories report SAND-86-0940. Albuquerque, NM. 16pp.

A numerical model is presented to represent the transport of solutes through a highly fractured unsaturated, porous medium. To accomplish this, the solute is tracked separately in two flow systems a matrix pore flow system and a fracture network, with interaction terms. Compatible hydraulic equations for such a dual system are also presented to enable solution of the solute transport. The hydraulic equations chosen use the equivalent porous media concept. These equations can also be applied to a saturated medium without modification. However, many of the transport terms will be negligible for such an application. A brief sample calculation illustrates the method.

Eaton, R.R. and N.E. Bixler. 1986. *Analysis of a Multiphase, Porous-Flow Imbibition Experiment in Fractured Volcanic Tuff.* Sandia National Laboratories report SAND86-1679C. Albuquerque, NM. 18pp.

A sub-meter-scale imbibition experiment has been analyzed using a finite element, multiphase-flow code. In the experiment, an initially dry cylindrical core of fractured tuff was saturated by contacting the ends with pressurized water. The model used discretely accounts for three primary fractures that may be present in the core. Results show that vapor transport has a small (less than five percent) effect on the speed of the wetting front. By using experimental results to estimate apparent spatial variations in permeability along the core, good agreement with measured, transient, saturation data was achieved. The sensitivity of predicted transient wetting fronts to permeability data indicates a need for more extensive measurements. It is concluded that it will be difficult to characterize an entire repository, where inhomogeneities due to variations in matrix and fracture properties are not well known, solely from the results of sub-meter-scale laboratory testing and deterministic modeling.

Eaton, R., K.S. Udell, and M. Kaviany. 1988. Drying of an initially saturated fractured volcanic tuff. *Multiphase Transport in Porous Media.* American Society of Mechanical Engineers: 55-60.

The isothermal drying of an initially saturated welded tuffaceous rock was studied experimentally. Gamma-beam densitometry was used to measure the material's effective porosity distribution prior to the drying experiment. It was then used to measure liquid saturation distributions during a 1400 hour drying period. The core selected for study was taken from the Busted Butte outcrop at the Nevada Test Site, part of the Topopah Spring Member of Paintbrush tuff. This specimen contained several microfractures transversely oriented to the direction of the water or vapor

migration. These fractures were found to be regions of rapid dryout or low saturation even though they were displaced from the surface over which dry nitrogen was flowing. An imbibition experiment was performed earlier on the same core. In the imbibition experiment the presence of most of these microfractures was detected by discontinuities in the measured saturation curves, which indicated a delay in liquid transport past the microfractures.

Elabd, H., I. Porro, and P. J. Wierenga. 1988. *Estimation of Field Transport Parameters Using the Convection Dispersion Equation.* Conference Proceedings, [in Wierenga and Bachelet, 1988]. Department of Agronomy and Horticulture. Las Cruces, New Mexico.

The results of a field experiment are reported in this paper. The experiment took place on the Jornada range, 40 km northeast of Las Cruces, New Mexico. An initially dry field plot was irrigated with a 9x4 m highly uniform drip system. The irrigated area was covered to prevent evaporation. The plot was irrigated with tritiated water for the first two weeks and non-tritiated water thereafter. The tritiated water front was found to lag behind the water front. The amount of lag increased with depth indicating that, during the process of wetting dry soil, the initial water in the soil is displaced by the added water. The tritiated water breakthrough curves at different depths were fitted to a solution of the one-dimensional deterministic convection dispersion equation. After calibrating the model at the 0.5 m depth, tritiated water breakthrough curves were predicted at underlying sampling locations. The model overestimated the downward speed of the tritiated water. The pore water velocity was calculated assuming that water first displaces the resident soil water and then fills the pores to the final water content before downward movement occurs. With the corrected pore water velocity, the model was more successful in predicting tritiated water breakthrough curves.

Erickson, J.R. and R.K. Waddell. 1985. *Identification and Characterization of Hydrologic Properties of Fractured Tuff Using Hydraulic and Tracer Tests: Test Well USW H-4, Yucca Mountain, Nye County, Nevada.* U.S. Geological Survey Water Resources report 85-4066. 30pp.

The test well penetrates volcanic tuffs through which water moves primarily along fractures. Data collected from hydrologic and tracer tests and an acoustic-televiewer log, were used to quantify intrawell-bore flow directions and rates, permeability distribution, fracture porosity, and orientations of the hydraulic conductivity ellipsoid for the test well. This report also presents results and interpretations of hydrologic and tracer tests used to identify and characterize fractures contributing to groundwater flow in the well.

French, R.H. 1986. *Daily, Seasonal, and Annual Precipitation at the Nevada Test Site, Nevada.* U.S. Department of Energy. DOE/NV/10384-01. 64pp.

A comprehensive understanding of the temporal and spatial distribution of precipitation is crucial from the viewpoint of understanding the hydrologic cycle. In this report, the daily precipitation data base which has been digitized from the raw data available for the Nevada Test Site and a program which can be used to interrogate this data base are discussed. The daily precipitation

data base includes all data for the period 1957 through 1985 inclusive. In addition, this report discusses several methods to use the precipitation data available at gauged locations to estimate the precipitation at ungauged locations on daily, seasonal, and annual time scales. Finally, a number of conclusions and recommendations regarding precipitation data for the Nevada Test Site are stated. Among these conclusions are recommendations that before any of fifteen precipitation stations with long and reliable periods of record are discontinued careful consideration be given to the impact of such an event. It is also noted that the western area of the Nevada Test Site has inadequate precipitation gauge coverage.

French, R.H. 1987. *Effects of the Length of Record on Estimates of Annual and Seasonal Precipitation at the Nevada Test Site, Nevada.* U.S. Department of Energy. DOE/NV/10384-18. 50pp.

The goal was to examine, in some detail, the effect of the period of record available for analysis on estimates of annual and seasonal precipitation, examine the effect of changing estimates of annual precipitation on estimates of regional groundwater recharge, and to discuss the possibility of a period of severe erosion occurring on the Nevada Test Site in the near future. The conclusions were: reasonably large changes in the calculated annual and seasonal precipitation must be expected as the period of record available for analysis lengthens; there appears to be a positive trend in the calculated annual precipitation at six of the eleven precipitation stations examined in this study; and in the case of annual precipitation, the variability of precipitation has increased at some stations and has decreased at others as the period of record has lengthened. In the case of seasonal precipitation, the variability of the precipitation has increased at ten of the eleven stations for the summer season and decreased at all stations for the winter season.

Gutjahr, A.L., C.T. Kincaid, J.W. Mercer, I.P. Murarka, M.D. Siegal, and P.J. Wierenga. 1987. Panel summary report. *Workshop on Modeling of Solute Transport in the Unsaturated Zone.* Los Alamos, New Mexico. NUREG/CR-4615. 2: 174-199.

The objective of this report is to summarize the various modeling approaches that were used to simulate solute transport in a variable saturated emission. In particular, the technical strengths and weaknesses of each approach are discussed, and conclusions and recommendations for future studies are made. Five models are considered: 1) one-dimensional analytical and semianalytical solutions of the classical deterministic convection-dispersion equation (van Genuchten, Parker, and Kool); 2) one-dimensional simulation using a continuous-time Markov process (Knighton and Wagenet); 3) one-dimensional simulation using the time domain method and the frequency domain method (Duffy and Al-Hassan); 4) one-dimensional numerical approach that combines a solution of the classical deterministic convection-dispersion equation with a chemical equilibrium speciation model (Cederberg); and 5) three-dimensional numerical solution of the classical deterministic convection-dispersion equation (Huyakorn, Jones, Parker, Wadsworth, and White). The models were used in a data analysis mode, as opposed to a predictive mode. Also, all the approaches were similar in that they were based on a convection-dispersion model of solute transport.

Gvirtzman, H., J. Dvorkin, and A. Nur. 1990. Revising Kozeny equation for partly saturated porous media. *Fall Meeting Amer. Geophys. Union.* October 23, 1990. EOS Transactions. 71(43).

The authors attempt to apply the Kozeny formula to the relative permeability, k, of a porous medium with a mobile non-wetting phase in the presence of an immobile wetting phase. In this two phase system, they define "porosity", P, as the partial volume occupied by the mobile phase, and S as its specific surface area. Because both P and S change as the degree of saturation of the immobile phase increases, the original Kozeny equation (relating permeability to P and S) fails to predict the relative permeability through such diverse systems as thin tapered cracks or grains in contact. Using the Kozeny equation at the initial stage of saturation of the pore space by the immobile phase, an increase of k is obtained where decrease is intuitively expected. This artifact is due to small reduction of porosity at the initial stage of saturation while the specific surface area decreases significantly. To correct this, they introduce a modified version of the Kozeny equation for media with thin tapered cracks and pores having thin tapered appendixes. Analytical expressions of k are derived for cases where the shape of cracks can be described by power laws. The revised equation for the relative permeability includes the saturation of pore space by immobile phase, Z, as well as the original porosity, P_o, and specific surface area, S_o, of porous medium at $Z = 0$. The predicted relative permeability as proposed by the authors is proportional to P_o^3 and S_o^{-2}, and decreases with increasing Z.

Hoffman, D.C., W.R. Daniels, K. Wolfsberg, J.L. Thompson, R.S. Rundberg, S.L. Fraser, and K.S. Daniels. 1983. *Review of a Field Study of Radionuclide Migration from an Underground Nuclear Explosion at the Nevada Test Site.* Los Alamos National Laboratory report LA-UR-83-493. 17pp.

Results from a long-term (nine year) field study of the distribution of radionuclides around an underground nuclear explosion cavity at the Nevada Test Site are reviewed. The goals of this Radionuclide Migration project are to examine the rates of migration underground in various media and to determine the potential for movement, both on and off the Nevada Test Site, of radioactivity from such explosions, with particular interest in possible contamination of water supplies. Initial studies were undertaken near the site of the low-yield test Cambric, which was detonated 73 m beneath the water table in tuffaceous alluvium. Solid samples were obtained from just below ground surface to 50 m below the detonation point, and water was sampled from five different regions in the vicinity of the explosion. Ten years after the test, most of the radioactivity was found to be retained in the fused debris in the cavity region and no activity above background was found 50 m below.

Huyakorn, P.S., B.G. Jones, J.C. Parker, T.D. Wadsworth, and H.O. White Jr. 1987. Finite element simulation of moisture movement and solute transport in a large caisson. *Workshop on Modeling of Solute Transport in the Unsaturated Zone.* Los Alamos, New Mexico. NUREG/CR-4615. 2: 117-173.

The results of the solute transport experiments performed on compacted, crushed Bandelier Tuff in caisson B of the experimental cluster described by DePoorter (1982) are simulated. Both one- and three-dimensional simulations of solute transport have been performed using two selected finite element codes. Results of bromide and iodide tracer experiments conducted during near-steady flow conditions have been analyzed for pulse additions made on December 6, 1984, and followed over a period of up to 60 days. In addition, a pulse addition of nonconservative strontium tracer on September 28, 1984, during questionably steady flow conditions has been analyzed over a period of 240 days. One-dimensional finite element flow and transport simulations were carried out assuming the porous medium to be homogeneous and the injection source uniformly distributed. To evaluate effects of the nonuniform source distribution and also to investigate effects of inhomogeneity porous medium properties, three dimensional finite element analyses of transport were carried out. Implications of the three-dimensional effects for the design and analysis of future tracer studies are discussed.

Jacobson, R.L., M.S. Hence, and J.W. Hess. 1986. *A Reconnaissance Investigation of Hydrogeochemistry and Hydrology of Rainier Mesa.* U.S. Department of Energy. DOE/NV/10384-05. 62pp.

Rainier Mesa, in the northern part of the Nevada Test Site, provides an opportunity to study unsaturated flow in volcanic tuffs. This was accomplished by sampling soil waters on the mesa top and comparing them with waters in tunnels 200 to 350 meters below the surface. Discharge measurements were also made in the tunnels. The sampling was undertaken as a function of time over approximately a six month period in 1980. Analyses demonstrate the effects of evaporation and soil mineral dissolution on the concentration ratio of cations to silica. The residence time of Rainier Mesa waters was estimated in two ways. The first used a long-term trend in the cation to silica ratio observed in the tunnels which showed a maximum in June which might correspond to recharge of waters six weeks to three months prior. Groundwater seepage rates into the tunnels was the second method. Increased tunnel discharge was observed between three and six months after the estimated recharge event. Both methods indicate relatively short water residence times.

Khaleel, R. 1990. Porous medium models for advective transport through colonnade networks. *Fall Meeting Amer. Geophys. Union.* October 23, 1990. EOS Transactions. 71(43).

The use of continuum models in modeling advective transport through fractured basalt dense interiors is examined. Numerical simulations are performed to evaluate the length scale requirements for an equivalent porous medium approximation for advective transport and to determine differences, if any, in the scale requirements for fluid flow and advective transport. Simple network models of hexagonal colonnades and entablatures are used. A particle tracking procedure is used to compute the equivalent porosities for various orientations of flow regions (or hydraulic gradients). For a continuous network of hexagonal colonnades with uniform apertures, the computed equivalent porosities compare favorably with those based on "theoretical considerations." For a colonnade network with uniform apertures, however, the porosity values drop sharply for orientations of hydraulic gradient such that a fracture set becomes perpendicular to the applied gradient and thereby becomes nonconductive. With lognormally distributed

apertures, the effect of a particular fracture perpendicular to the gradient is overshadowed by the effect of distributed velocities. For both colonnade and entablature network models, the computed length scale requirements for an accurate Equivalent Porous Medium approximation are smaller for transport than for fluid flow. According to the authors, the goal of this study was to provide guidance in selecting an acceptable block size for use in a continuum model of groundwater flow and transport through colonnade networks with varying apertures.

Klavetter, E.A. and R.R. Peters. 1986. *Estimation of Hydrologic Properties of an Unsaturated, Fractured Rock Mass*. Sandia National Laboratories report SAND84-2642. Albuquerque, NM. 49pp.

This document presents a general discussion of 1) the hydrology of Yucca Mountain and the conceptual hydrologic model currently being used for the Yucca Mountain site, 2) the development of models that may be used to simulate flow in a fractured porous media, and 3) comparison of these models.

Lin, W. and W. Daily. 1984. *Transport Properties of Topopah Spring Tuff*. Lawrence Livermore National Laboratory report UCRL-53602. Livermore, CA. 20pp.

Electrical resistivity, ultrasonic P-wave velocity and water permeability were measured simultaneously on both intact and fractured Topopah Spring Tuff samples at a confining pressure of 5.0 MPa, pore pressure to 2.5 Mpa, and temperatures to 140°C. Results indicate that the fractured sample dehydrates and rehydrate nonuniformly, whereas the intact sample does so uniformly. The wetting front moved 100 times faster within the dry fractured sample relative to that of the dry intact sample. The wetting and drying cycle decreased the fracture permeability as a result of fracture healing caused by silica dissolution and redeposition.

Martinez, M. 1988. *Capillary-Driven Flow in a Fracture Located in a Porous Medium*. Sandia National Laboratories report SAND-84-1697. Albuquerque, NM. 52pp.

Capillary-driven immiscible displacement of air by water along an isolated fracture located in a permeable medium is induced by an abrupt change in water saturation at the fracture inlet. In one case, the fracture is idealized as a "smooth slot with permeable walls." The model is applied to materials representative of the Yucca Mountain region of the Nevada Test Site. Fracture moisture-penetration histories are predicted for several units in Yucca Mountain and for representative fracture apertures.

McCord, J.T., D.B. Stephens, and J.L. Wilson. 1988. Field-scale unsaturated flow and transport in a sloping uniform porous medium: field experiments and modeling considerations. *Variation of Flow and Transport Models for the Unsaturated Zone*. P.J. Wierenga and D. Bachelet, eds.

McCord, J.T., D.B. Stephens, and J.L. Wilson. 1991. Toward Validating state-dependent macroscopic anisotropy in unsaturated media: Field experiments and modeling considerations. In: P.J. Wierenga (Guest-Editor), Validation of Flow and Transport Models for the Unsaturated Zone. J. Contam. Hydrol. 7: 147-177.

This field-scale experiment was designed to observe the migration of unsaturated tracer plume on a sandy hillslope under relatively dry conditions. The site is a small sand dune, about 900 m^2, located next to the Rio Salado, an ephemeral tributary to the Rio Grande, near Sorocco, New Mexico (annual rainfall 200 mm). The dune is a relatively uniform sand with fine eolian cross-stratification, roughly parallel to the sloping ground surface (variable slope, 8-15 degrees). Soil water content was monitored by neutron probes down to 3 meters and suctions were measured by tensiometers down to 2.4 m, along an east-west-trending transect (25 m long). Dry bromide salt ($CaBr_2$) was buried at shallow depth, and the concentration plume movement subsequent to rainfall was then monitored by core sampling using a small diameter thin-walled tubing. The monitored concentration plume was used to estimate the direction and magnitude of water flux using a simple inference based on the shape and size of the concentration plume. The inferred flux had a large downslope component, in some cases five times larger than the orthogonal (near-vertical) flux component. In contrast, the total hydraulic head contours obtained from tensiometer data appeared to be nearly horizontal. The non-colinearity of flux and hydraulic gradient leads the authors to the conclusion that the (relatively dry) dune sand behaves anisotropically at the scale of the plume. Simplified models of unsaturated conductivity anisotropy lead to estimates of unsaturated anisotropy ratio on the order of 10/1, while independent experimental procedures indicate a small-scale anisotropy ratio of 3/2 at saturation. This appears to confirm, albeit roughly, theoretical predictions based on Mualem (1984) and Yeh et al. (1985a,b,c). In addition, McCord et al. (1991) develop a scenario to show how hysteresis-enhanced moisture content variations can cause a texturally homogeneous porous medium profile to behave anisotropically under transient unsaturated conditions. They conclude that both factors (layered heterogeneity and hysteresis-enhanced moisture content variations) contribute to the anisotropic behavior observed in the tracer experiments, but they do not quantify the relative magnitude of their contributions.

McIntosh, D. 1990. UDEX: unsaturated zone dispersion experiment. *EPRI Journal*. 42-45.

UDEX consists of two controlled tracer experiments for characterizing the hydraulic and dispersive properties of deep unsaturated soils near Riverside, California as part of EPRI solid-waste environmental studies (EPRI: Electric Power Research Institute). The Etiwanda site consists of layered alluvial deposits (loamy sand on top) and is unsaturated over a depth of 150 m. A narrow pulse of sodium bromide (NaBr) was applied over an area equivalent to a square of 80 m x 80 m by injection in irrigation water. Irrigation was continued for eight months. Concentrations were measured by ceramic suction lysimeters at 20 m intervals on a 4 x 4 grid horizontally, and down to 3 m (4.5 m in some cases) vertically. One year after the end of irrigation, the plume was sampled by six soil cores (vertically) to a depth of 25 meters (time t = 20 months). This final sampling, according to the author, indicated a bimodal concentration profile with main peak around 10-15 m depth, and secondary peak around 20-25 m depth (concentration plot not shown). Attempts at simulating plume migration with constant coefficients convective-dispersive model failed, as actual dispersivity appeared to vary as the

plume migrated. Dispersivity increased more or less linearly with advance of the plume, except at intermediate depth of 4.5 m where the leading edge of the plume appeared to be impeded in its downward movement, or compressed before advancing again. Finally, new three-dimensional experiments were also designed to measure transverse as well as longitudinal dispersion. Tracers (including chloride) where applied to 1.5 m x 1.5 m plots, which were destructively sampled by coring, and 2 m x 2 m plots which were sampled at three successive times rather than all at once. Other conditions were varied among a total of thirteen plots. One of the conclusions is that the anomaly previously observed at depth 4.5 m (impeded/compressed plume) was probably due to an increase in storage (i.e. higher moisture) at that depth, resulting in higher concentrations and less vertical spreading there. Transverse plume spreading was moderate (0.5 m at 5 m depth) when the areas around the plots were submitted to the same irrigations as the plots themselves (i.e. horizontally uniform moisture conditions). However, for one plot, the soil around the plot was left dry; in this case horizontal spreading was 2 m at depth 5m, probably due to lateral flow driven by horizontal suction gradients.

Montazer, P. and W.E. Wilson. 1984. *Conceptual Hydrolgic Model of Flow in the Unsaturated Zone, Yucca Mountain, Nevada.* U.S. Geological Survey Water Resources Investigations report 84-4345. 55pp.

The geology, structure, porosity, permeability, and fracture density of the various hydrogeologic units of Yucca Mountain are used to construct a hypothetical model for flow through porous layers intercalated with double-porosity layers. In this simplified model, flow through fracture can occur at almost all stages of saturation, but the flux magnitude in fractures is largely a factor of the contrast between the matrix and fracture-hydraulic properties and the magnitude of the perturbation of flux at the flow boundaries. Flow is retarded by capillary barriers that occur at the contacts between nonwelded and welded units. The effectiveness of this capillary barrier depends on the magnitude of the flux and hydraulic-head distribution. Hysteresis during wetting phases and air entrapment may result in greater flux in fractures than would otherwise be predicted. Initiation of lateral flow also results. Both vapor transport and liquid flow can occur simultaneously within the fractured layers of this model. Net infiltration is estimated at 0.5 to 4.5 mm/yr. Water infiltrates primarily into the Tiva Canyon welded unit, but also into the alluvium, Paintbrush nonwelded unit, and Topopah Spring welded unit. Eastward lateral flow occurs within and above the upper contact of the Paintbrush Tuff nonwelded unit. This lateral flow is intercepted by structural features, which transmit most of the infiltrating water to the water table. Percolation through the matrix occurs principally vertically in the welded units and both laterally and vertically in the nonwelded units. Fracture flow is dominant in the Tiva Canyon welded unit during intense pulses of infiltration and is insignificant in the Topopah Spring welded unit except near the upper contact and near the structural features. Temporary development of perched water is possible near the structural features within and above the nonwelded units. This water drains into the structural flow paths and much of it travels directly to the water table. Possible flux ranges are given for various units that occur within Yucca Mountain.

Montazer, P., E.P. Weeks, F. Thamir, S.N. Yard, and P.E. Hofrichter. 1985. *Monitoring the Vadose Zone in Fractured Tuff, Yucca Mountain, Nevada.* U.S. Geological Survey, Denver, Colorado. 30pp.

The U.S. Geological Survey has been conducting hydrologic, geologic, and geophysical studies at Yucca Mountain to provide data for the potential suitability of the site. Hydrologic investigations were started in the unsaturated zone in 1982. A 17.5 inch borehole was drilled to a depth of 1,269 feet. Thermocouple psychrometer and pressure transducers were installed at screened intervals and monitored for two years with satisfactory results.

Moss, M., et al. 1982. *Effects of Composition, Porosity, Bedding Plane Orientation, Water Content and a Joint on the Thermal Conductivity of Tuff.* Sandia National Laboratories report SAND84-1164. Albuquerque, NM. 28pp.

This study deals with the effects of composition, porosity, bedding-plane orientation, water content and the presence of a joint on the thermal conductivity of tuff from the Grouse Canyon Member of the Belted Range Tuff, as it occurs within Rainier Mesa (Nevada Test Site).

Norris, A.E., K. Wolfsberg and S.K. Gifford. 1985. *Chlorine-36 Measurements of the Unsaturated Zone Flux at Yucca Mountain.* Los Alamos National Laboratory report LA-UR-85-2408. Los Alamos, NM. 10pp.

A new technique that measures that chlorine-36 content of the tuff from the exploratory shaft at Yucca Mountain will be used to calculate flux through the unsaturated zone over longer periods than possible with carbon-14. Measurements of the chlorine-36 "bomb pulse" in soil samples from Yucca Mountain have been used to confirm that infiltration is not an important recharge mechanism.

Norris, A.E., K. Wolfsberg, S.K. Gifford, H.W. Bentley, and D. Elmore. 1987. *Infiltration at Yucca Mountain, Nevada, traced by ^{36}Cl.* New York, NY: Elsevier Science Publishers Co., Inc.

Measurements of chloride and ^{36}Cl in soils from two locations near Yucca Mountain, Nevada, have been used to trace the infiltration of precipitation in this arid region. The results show that the ^{36}Cl fallout from nuclear-weapons testing formed a well-defined peak at one location, with a maximum $^{36}Cl/Cl$ ratio 0.5 m below the surface. The structure of the ^{36}Cl bomb pulse at the other location was much more complex, and the quantity of ^{36}Cl in the bomb pulse was less than one percent of the $6x10^{12}$ atoms $^{36}Cl/m^2$ in the bomb pulse at the first location. The data indicate hydrologic activity subsequent to the ^{36}Cl bomb pulse fallout at one location, but none at the other location.

Ortiz, T.S., R.L. Williams, F.B. Nimick, B.C. Whittet, and D.L. South. 1985. *Three-Dimensional Model of Reference Thermal/Mechanical and Hydrological Stratigraphy at Yucca Mountain, southern Nevada.* Sandia National Laboratories report SAND84-1076. Albuquerque, NM. 80pp.

A three-dimensional model of the thermal/mechanical and hydrological reference stratigraphy at Yucca Mountain has been developed for use in performance assessment and repository design studies involving material properties data. The reference stratigraphy defines units with distinct thermal, physical, mechanical, and hydrologic properties. Thickness of the repository unit and depth to groundwater are also discussed.

Peters, R.R., E.A. Klavetter, I.J. Hall, S.C. Blair, G.W. Heller, and G.W. Gee. 1984. *Fracture and Matrix Characteristics of Tuffaceous Materials from Yucca Mountain, Nye County, Nevada.* Sandia National Laboratories report SAND84-1471. Albuquerque, NM. 63pp.

Hydraulic tests were performed on tuffaceous samples from forty-eight different locations on Yucca Mountain. A wide variety of water retention values existed between the different Yucca Mountain lithologies studied. Fracture hydraulic conductivities were higher than matric hydraulic conductivities in all cases.

Peters, R.R., J.H. Gauthier, and A.L. Dudley. 1985. *Effect of Percolation Rate on Water-Travel Time in Deep, Partially Saturated Zones.* Sandia National Laboratories report SAND85-0854C. Albuquerque, NM. 43pp.

A composite-porosity, continuum model was developed to model flow in a fractured, porous medium. Simulations using data from the Yucca Mountain site and this model in the one-dimensional code TOPSAC indicate that current estimates of the percolation rate result in water movement confined to the matrix and that the water-travel time from the repository to the water table is on the order of hundreds of thousands of years. This result is sensitive to the percolation rate; a ten-fold increase in the rate of percolation may initiate water movement in the fractures, reducing the travel time significantly.

Peters, R.R., E.A. Klavetter, J.T. George, and J.H. Gauthier. 1986. *Measuring and Modeling Water Imbibition into Tuff.* Sandia National Laboratories report SAND86-1757C. Albuquerque, NM. 26pp.

Water imbibition experiment into a cylinder of tuff (from a Yucca Mountain drill core) was measured by immersing one end of a dry sample in water and noting its weight at various times. Computer simulation of the experiment using the model TOPSAC with data currently considered for use in site-scale modeling of a repository in Yucca Mountain. The measurements and the results of the modeling are compared. See also Peters et al. (1987) and references therein for imbibition and moisture retention data.

Power, W.L. and T.E. Tullis. 1991. Euclidean and fractal models for the description of rock surface roughness. Abstract 8165 (*J. Geophys. Res.* B). Geophys. Abstr. in press. January. p. 11.

This paper studies model of the topography of rock surfaces for possible applications to the flow of fluids in joints and fractures, the seismic behavior of faults, and the formation of gouge and breccia in fault zones. According to the authors in a Euclidean model, the surface is the sum of a simple, analytic, function that describes the overall form of the object, and a random or stochastic function that describes roughness. For such Euclidean surfaces, height distributions and statistical measures such as the root mean squareheight are used to quantify the roughness. Two concepts from fractal geometry, self-similar and self-affine scaling, provide useful alternatives to surface models based on Euclidean geometry. A self-similar surface, when magnified isotropically, will appear statistically identical to the entire surface. If a surface is self-affine, a portion of the surface will appear statistically identical to the entire surface only if different magnification factors are used for the directions parallel and perpendicular to the surface. Thus self-similar scaling may be considered a special case of self-affine scaling. At least two parameters are required to describe a fractal model of a surface; one parameter typically describes how roughness changes with scale, while the other specifies the variance or surface slope at a reference scale. The divider method and the spectral method are in common use to determine best fit fractal surface models from surface profile data. Power spectra from perfectly self-similar surfaces will have uniform slopes of exactly -3 on log-log plots of power spectra density versus spatial frequency, while spectra from perfectly self-affine surfaces will have slopes other than -3. Power spectra can be interpreted with greater facility if dimensionless amplitude to wavelength ratios are contoured on plots of power spectral density versus frequency. Although few natural rock surfaces follow exactly self-similar of self-affine scaling, the authors suggest that for natural surface fractal models have a significant advantage. Furthermore, the authors observe that the topography of many natural rock surfaces is approximately self-similar between wavelengths of 10 microns and 40 meters, and/or self-affine within smaller wavelength bands.

Pruess, K. and T.N. Narasimhan. 1988. *Numerical Modeling of Multiphase and Nonisothermal Flow in Fractured Media.* Lawrence Berkeley Laboratory report LBL-25547. 22pp.

The authors discuss and apply several approaches for modeling coupled multiphase fluid and heat flow in fractured media: explicit modeling of fractures, which are represented as domains with small spatial scale and large permeability; effective continuum approximations, in which one attempts to model the composite behavior of a fractured porous medium in terms of a single effective continuum; and hybrid models such as double- or multiple-porosity techniques which combine features of the explicit fracture and effective continuum approaches. The explicit fracture approach has been applied to investigate thermohydrologic conditions near high-level nuclear waste packages emplaced in partially saturated fractured tuffs. Besides providing insight into multiphase flow processes in the near field, according to the authors, this approach serves to confirm the validity of an effective continuum approximation, which leads to a drastic simplification in the modeling of fractured flow systems. A consideration for diffusive processes in rock matrix and fractures provides criteria for the validity of the effective continuum approximation; these have been verified by means of numerical experiments. Flow studies using the method of multiple interacting continua have demonstrated how effects of global flow tend

to diminish sensitivity to individual matrix block response in enhanced oil recovery and in heat mining in geothermal systems. In some cases, according to the authors, simple semi-analytical techniques are found to provide an adequate approximation to the complexities of multiple-continua behavior.

Pruess, K., J.S.Y. Wang, and Y.W. Tsang. 1988. *Effective Continuum Approximation for Modeling Fluid and Heat Flow in Fractured Porous Tuff: Nevada Nuclear Waste Storage Investigations Project.* Sandia National Laboratories report SAND-86-7000. Albuquerque, NM. 100pp.

The authors present a formulation, and partial evaluation, of an effective continuum approximation for non-isothermal multi-phase flow, which had been introduced previously only in a heuristic fashion. The key concept on which the effective continuum approach must rely is approximate local thermodynamic equilibrium between fractures and rock matrix. The applicability of this approximation is discussed and studied by means of numerical simulations for emplacement of high-level waste packages in partially saturated fractured tuff. The simulations demonstrate that the validity of the effective continuum approximation cannot be ascertained in general terms. The approximation will break down for rapid transients in flow systems with low matrix permeability and/or large fracture spacing, so that its applicability needs to be carefully evaluated for the specific processes and conditions under study. The effective continuum approximation has been applied for a preliminary study of fluid and heat flow near a high-level nuclear waste repository on a regional scale, employing a highly simplified stratigraphic description. It was found that substantial gas phase convection is taking place, with convection velocities being sensitive to permeability, porosity, and tortuosity of the fracture network.

Rasmussen, T. C. *Steady Fluid Flow and Travel Times in Partially Saturated Fractures Using a Discrete Air-Water Interface.* Department of Hydrology & Water Resources, University of Arizona. Tucson, AZ. Abstract, EOS Transactions of the Amer. Geophys. Union, Vol. 71, No. 39, Sept. 25, 1990.

Fracture flow under conditions of partial fluid saturation is studied where a portion of the fracture is filled with water and the remaining portion is filled with air. A discrete air-water interface is used to separate the saturated from the drained regions within the fracture. A laboratory flow experiment is presented which demonstrates the interface concept. the steady state air-water interface position is observed by maintaining a circular water source at constant positive pressure head between two vertical glass plates. An analytic solution to the flow problem is compared to the observed interface position and to simulated results which assume that a constant capillary pressure head can be assigned along the interface. Simulations performed for a hypothetical vertical fracture indicate zones of positive and negative pressure head in the saturated zone as well as an air-filled zone. For the hypothetical fracture examined, fluid travel times are not substantially changed as fracture saturation decreases. This result may not hold generally for all fractures.

Rasmussen, T.C. and D.D. Evans. 1987. *Unsaturated Flow and Transport Through Fractured Rock Related to High-Level Waste Repositories: Final Report, Phase 2*. U.S. Nuclear Regulatory Commission NUREG/CR-4655. 500pp.

The authors investigate physical characteristics and methodologies for performance assessment of candidate sites in unsaturated fractured rock. The focus is on the ability of the geologic medium surrounding an underground repository to isolate radionuclides from the accessible environment. Media of interest are consolidated rocks with variable fracturing, rock matrix permeabilities, contained water under negative pressure, and air-filled voids. Temperature gradients are also considered. Presentation of conceptual and theoretical considerations, physical and geochemical characterization, computer modeling techniques, and parameter estimation procedures. Radionuclide transport is considered to occur as solutes in groundwater and/or as vapor through air-filled voids. The latter may be important near a heat source (near field process). Water flow and solute transport properties of a rock matrix may be quantified using rock core analyses. Natural spatial variation dictates many samples. Observed fractures can be characterized and combined to form a fracture network for hydraulic and transport assessments. Unresolved problems include the relation of network hydraulic conductivity to fluid pressure and to scale. Once characterized, the matrix and fracture network can be coupled.

Reda, D.C. 1986. *Influence of Tranverse Microfractures on the Imbibition of Water into Initially Dry Tuffaceous Rock*. Sandia National Laboratories report SAND86-0420C. Albuquerque, NM. 40pp.

The isothermal imbibition of liquid water into initially dry, welded, tuffaceous rock was studied. Results indicate that transverse microfractures were a significant impedance to liquid transport. Comparison of saturation versus time, measured up and down gradient of the microfractures, indicated the potential occurrence of vapor-driven transport of water vapor from the fracture apertures into the matrix pore volume down gradient. The author postulates that adsorption of this vapor onto pore surfaces resulted in the formation of a thin liquid film, eventually overrun by the fracture-delayed wetting front. According to the author, combined results of this and previous investigations suggest that the detailed hydrologic characterization of tuffaceous rocks on a submeter scale will be most difficult.

Ross, B. 1984. A conceptual model of deep unsaturated zones with negligible recharge. *Water Resources Research*. 20(11): 1627-1629.

According to the author, when net recharge is less than about 0.03 mm/yr, moisture movement in deep unsaturated zones at steady state is dominated by upward movement of vapor driven by the geothermal gradient. With zero-net recharge, the downward flow of liquid water would equal the upward vapor flux. This would produce a profile of suction potential versus depth quantitatively similar to that expected if recharge is not negligible. The author concludes that the existence of a region of uniform potential is not in itself evidence of recharge.

Roth, K., H. Fluhler, and C. Gysi. 1988. Temporal change of the spatial distribution of chloride displaced through a heterogeneous soil. *Validation of Flow and Transport Models for the Unsaturated Zone*. Conference Proceedings. P.J. Wierenga and D. Bachelet, eds. 362-366.

Roth, K. 1989a. Transport of a conservative tracer under field conditions: qualitative modeling with random-walk in a double porous medium. Abstract. *International Workshop on Field Scale Water and Solute Flux in Soils*. September 24-29, 1989. Monte-Verita, Ascona, Switzerland.

Roth, K. 1989b. *Stofftransport im Wasserungesattigten Untergrund Naturlicher, Heterogener Boden unter Feldbedingungen*. Doctoral Thesis. Diss. ETH No. 8907, Swiss Federal Institute of Technology (ETH), Zurich, Switzerland. (in german with english abstract).

K. Roth and co-workers at the ETH Federal Polytechnic Institute in Zurich, Switzerland, conducted an unsaturated tracer experiment from a 12 m long, 3 m deep tunnel, in the root zone of a vegetable field in a colluvial calcareous brown-earth (clay-silt-sand ≈ 25%-35%-40%). The tunnel was instrumented with 100 tensiometers for pressure measurement and 110 suction cups for tracer sampling, using the same ceramic cups for both (30 cm long, 1.4 cm diameter). In addition, 20 TDR-probes were installed (Time Domain Reflectometry). The tracer (Cl) was applied in the form of fertilizers over an 18 m x 18 m area, and subsequently migrated downward due to a combination of irrigation and natural rainfall. The time scale of the experiment was one year. The authors found that the tracer plume split in two parts: a fast moving part (first arrival observed at 2.5 m depth after only 30 mm of water infiltration), and a slow moving part which lagged behind. This leads the authors to postulate a double-porosity model. The authors evaluate that the volume fraction of macropores may be 0.01 at most, based on tracer movement. However, there is no direct observation of fast water flow; indeed the authors note that the chances for a tensiometer to be located on a fast flow path are tenuous. In Roth (1989b), the experimental results were interpreted/simulated using an advection-diffusion particle tracking model that takes into account the existence of a "double-porosity continuum structure". Accordingly, two types of particles were tracked, say red particles in the microstructure and black particles in the macrostructure (this is similar to two-color particle models used in some multi-phase simulation approaches). Apparently, the particles of each type are allowed to occasionally migrate from one structure to the other. This transfer is in addition to spatial migration within each structure, which was modeled by advection and random walk.

Rulon, J., G.S. Bodvarsson, and P. Montazer. 1986. *Preliminary Numerical Simulations of Groundwater Flow in the Unsaturated Zone, Yucca Mountain, Nevada*. Lawrence Berkeley Laboratory report LBL-20553. 102pp.

Numerical simulations of the flow in the unsaturated zone underlying Yucca Mountain, Nevada, were performed. The model simulates two-dimensional liquid-water flow in a vertical cross section extending from the ground surface to the water table at a depth of about 650 m. Various fluxes representing the net infiltration were specified at the surface and the steady-state flux, liquid saturation distribution, and matric-potential distribution were computed. The results indicate that because of the dip of the stratigraphic units and because of their hydraulic properties, a significant proportion of the flow above and/or below the proposed repository horizon is diverted laterally into a permeable fault zone. The magnitude and location of the lateral flow depend upon whether matrix-flow or fracture-flow conditions are assumed for the

highly fractured units, upon the flux specified at the ground surface, and upon the hydraulic properties assigned to the fault zone. Various cases were considered to examine the liquid-water flux through the proposed repository unit; all of the results are controlled by poorly known hydraulic parameters such as the water retention and hydraulic conductivity curves.

Russo, A.J. and D.C. Reda. 1988. *Drying of an Initially Saturated Fractured Volcanic Tuff.* Sandia National Laboratories report SAND87-0293C. Albuquerque, NM. 6pp.

The isothermal drying of a Topopah Spring sample was studied. The specimen contained several microfractures transversely orientated to the direction of water or vapor migration. These fractures were found to be regions of rapid dryout and during imbibition studies, the microfractures inhibited liquid transport.

Russo, D. 1991. Stochastic analysis of simulated vadose-zone solute transport in a vertical cross-section of heterogeneous soil during nonsteady water flow. *Water Resour. Res.* 27(3):267-283.

Transport of a conservative nonreactive solute in a vertical cross section of a hypothetical partially-saturated, scale-heterogeneous soil, under transient water flow was analyzed. The simulated water content and the solute concentration distributions in the vertical cross section of the soil at different elapsed times were quantified in terms of space averages, and two-point autocorrelation functions. The time-evolution of the solute plume was quantified in terms of its first two normalized spatial moments, from which the time dependence of the longitudinal and the transverse components of solute velocity vector, and the spatial covariance tensor, were estimated. The simulation results indicated the considerable variability in the solute concentration in space and time due to the complex spatial heterogeneity of the soil hydraulic properties (this of course depends on the assumed soil variability). The authors concluded that some existing stochastic vadose-zone transport models may be applicable to shallow depths, but may fail to describe the actual spread of a solute plume when transport takes place to relatively large depths, mainly because of the neglect of the vertical heterogeneity in the soil hydraulic properties. The authors apparently refer here to stochastic models that take into account horizontal, but not vertical, variability of soil properties. Fully three-dimensional stochastic models are however available for testing.

Russo, D. and G. Dagan. 1991. On solute transport in a heterogeneous porous formation under saturated and unsaturated water flows. *Water Resour. Res.* 27(3):285-292

In this paper, the authors attempt to apply stochastic models of *saturated* flow and transport to *unsaturated* flow and transport. The results of a recent study of solute transport in a hypothetical scale-heterogeneous soil under transient unsaturated flow conditions, suggest that the time-dependent components of the spatial covariance tensor based on a single realization of the solute concentration in unsaturated flow are in good agreement with the components of the spatial covariance tensor based on the ensemble-average solute concentration derived for solute transport under steady saturated flow. These findings are explored in a Lagrangian formulation, using

small-perturbation, first-order approximations. Results of the analyses suggest that this agreement can be explained by the finding that under unsaturated flow conditions, there is an increase in the variability of the hydraulic conductivity K, accompanied by a decrease in the correlation scale of K relative to the saturated conditions. This stemmed from the variability in the moisture content θ, the strong nonlinear dependence of K on θ, and the negative correlation between the saturated conductivity and θ (for scale-heterogeneous soils). The results suggest that in spite of the complexity of unsaturated flow as compared with saturated flow, the former might be amenable to a similar analysis.

Sinnock, S., Y.T. Lin, and M.S. Tierney. 1986. *Preliminary Estimates of Groundwater Travel Time and Radionuclide Transport at the Yucca Mountain Repository Site.* Sandia National Laboratories report SAND85-2701. Albuquerque, NM. 156pp.

This report presents the assumptions, methods, and data used in a probabalistic approach to the calculation of groundwater travel times and total radionuclide releases to the water table below Yucca Mountain. Results from the analyses consist of distributions of groundwater travel time from the disturbed zone to the water table and the cumulative curie releases to the water table.

Sinnock, S. and Y.T. Lin. 1987. Preliminary bound on the expected postclosure performance of the Yucca Mountain repository site, southern Nevada. *Journal of Geophysical Research.* 92(B): 7820-7842.

Based on the current data and understanding of site characteristics at Yucca Mountain, the likely performance range of a mined repository for spent nuclear fuel can be calculated. The calculated travel times and mass transport of radionuclides are compared to EPA and NRC regulations.

Thordarson, W. 1965. *Perched Groundwater in Zeolitized-Bedded Tuff, Rainier Mesa and vicinity, Nevada Test Site, Nevada.* U.S. Geological Survey report TEI-862. 89pp.

Zeolitic-bedded tuff at the base of the tuff sequence within Rainier Mesa controls the recharge rate of groundwater to the underlying and more permeable Paleozoic aquifers. The zeolitic tuff is a fractured aquitard with high interstitial porosity and low interstitial permeability and fracture transmissivity. The tuff is generally fully-saturated interstitially hundreds of feet above the regional water table, yet no appreciable volume of water moves through the interstices because of the very low permeability. The only freely-moving water, observed in miles of underground workings at the Nevada Test Site occurred in fractures, usually fault zones.

Travis, B.J., et al. 1984. *Preliminary Estimates of Water Flow and Radionuclide Transport in Yucca Mountain.* Los Alamos National Laboratory report LA-UR-84-40. Los Alamos, NM. 75pp.

This paper develops a preliminary estimate of water flow and radionuclide transport for Yucca Mountain. The authors' conclusions are as follows. Significant fracture flow can occur above the water table, but only in high-saturation, low permeability tuff. Diffusion into the matrix and adsorption have a profound effect on transport. Migration times just to the water table for all but one of the important radionuclides are considerably longer than 10,000 years, and none of the radionuclides considered reaches the accessible environment in less than 10,000 years. Heat load in partially saturated tuff can result in a dry, steam-filled region extending several meters above and below a repository with recharge during cool-down phase.

Tyler, S.W. 1987. *Review of Soil Moisture Flux Studies at the Nevada Test Site.* U.S. Department of Energy. DOE/NV/10384-17. 56pp.

This report documents almost thirty years of research on soil moisture movement and recharge at the Department of Energy, Nevada Test Site. Although data is scarce, three distinct topographic zones are represented: alluvial valleys, inundated terrains, and upland terrain. Recharge in alluvial valleys was found to be very small or negligible. Ponded areas such as playas and subsidence craters showed significant amounts of recharge. Data in the upland terrains is very scarce but one area, Rainier Mesa, shows active recharge on the order of one percent (up to three percent) of the annual average precipitation in fractured volcanic tuff.

Wang, J.S.Y. and T.N. Narasimhan. 1984. *Hydrologic Mechanisms Governing Fluid Flow in Partially Saturated, Fractured, Porous Tuff at Yucca Mountain.* Lawrence Berkeley Laboratory report LBL-18473. Berkeley, CA. 58pp.

This report deals with the numerical simulation of the drainage of a fractured, unsaturated tuff column. In contrast to the saturated zone where fluid moves rapidly along fractures, the fractures (with relatively large apertures) will desaturate first during drainage processes and the bulk of fluid flow would be through the interconnected pores in the matrix. Within a partially drained fracture, the presence of a relatively continuous air phase will produce practically an infinite resistance to liquid flow in the direction parallel to the fracture. The residual liquid will be held by capillary force in regions around fracture contact areas where the apertures are small. Normal to the fracture surfaces, the drained portion of the fractures will reduce the effective area for liquid flow from one matrix block to another matrix block. (See also Wang and Narasimhan, 1986 and 1988).

Wang, J.S.Y. and T.N. Narasimhan. 1986. *Hydrologic Mechanisms Governing Partially Saturated Fluid Flow in Fractured Welded Units and Porous Non-Welded Units at Yucca Mountain.* Sandia National Laboratories report SAND85-7114. Albuquerque, NM. 83pp.

A discrete-fracture, porous-matrix model and a composite-medium model were used to study hydrological responses to cycles of pulse infiltration at Yucca Mountain. The pulses were applied to fractures at the top of a vertical column composed of alternating layers of welded and on-welded tuffs. The hydrologic response of the units from 0.1 to 0.5 mm/yr recharge pulses applied at 5,000-year intervals is discussed.

Wang, J.S.Y. and T.N. Narasimhan. 1988. *Hydrologic Modeling of Vertical and Lateral Movement of Partially Saturated Fluid Flow Near a Fault Zone at Yucca Mountain.* Sandia National Laboratories report SAND-87-7070. Albuquerque, NM. 76pp.

The objective of this work is to assess fluid flow in the partially saturated, fractured, porous tuff formations at Yucca Mountain. The effects of eastern tilting of the units at Yucca Mountain on fluid flow is studied using two-dimensional models. Ghost Dance Fault is modeled as a seepage face. Distribution of fluid flow is governed by the balance between gravity and capillary forces. Under the expected flux conditions, saturation increases just to the west of the fault, but the water does not enter the fault. Tuff matrix and fracture data are compared to the limited model parameters of the fault. Correlations between saturated conductivity and unsaturated parameters for tuff matrix, fracture, and fault are discussed in Appendix A. Model parameters were taken from the NNWSI Reference Database (RIB, April 1986) and from the general literature.

Winograd, I.J. 1981. Radioactive waste disposal in thick unsaturated zones. *Science*. 212(4502): 1457-1464.

In this paper, the author analyzes the geophysical and hydrogeologic characteristics of the man-made Sedan Crater, which he proposes as a possible site for high-level nuclear waste isolation. His arguments are summarized as follows. Portions of the Great Basin are undergoing crustal extension and have unsaturated zones as much as 600 meters thick. These areas contain multiple natural barriers capable of isolating solidified toxic wastes from the biosphere for tens of thousands to perhaps hundreds of thousands of years. An example of the potential utilization of such arid zone environments for toxic waste isolation is the burial of transuranic radioactive wastes at relatively shallow depths (15 to 100 meters) in Sedan Crater, Yucca Flat, Nevada. The volume of this man-made crater is several times that of the projected volume of such wastes to the year 2000. According to the author, disposal in Sedan Crater could be accomplished at a savings on the order of $0.5 billion, in comparison with current schemes for burial of such wastes in mined repositories at depths of 600 to 900 meters, and with an apparently equal likelihood of waste isolation from the biosphere. The downward percolation rate (velocity) through the unsaturated valley fill is estimated to be roughly on the order of 2 mm/year, or 2 meters per millennia.

Woodbury, A.D. and E.A. Sudicky. 1991. The geostatistical characteristics of the Borden Aquifer. *Water Resour. Res.* 27(4):533-546.

A complete reexamination of Sudicky's (1986) field experiment for the geostatistical characterization of hydraulic conductivity at the Borden Aquifer in Ontario, Canada is performed.

The sampled data reveals that a number of ouliers (low log-conductivity values) are present in the data base. These low values cause difficulties in both variogram estimation and determining population statistics. The analysis shows that assuming either a normal distribution or exponential distribution for log-conductivity is appropriate. The classical Cressie/Hawkins and SMAD estimators are used to compute experimental variograms. None of these estimates provides completely satisfactory variograms for the Borden data with the exception of the classical estimator with outliers removed from the data set. Theoretical exponential variogram parameters are determined from non-linear estimation. Differences are obtained between non-linear fits and those of Sudicky (1986). For the classical-screened estimated variogram, non-linear fits produce a log-conductivity (ℓn K) variance of 0.24, nugget of 0.07, and integral scales of 5.1 m horizontal and 0.21 m vertical along transect A-A'. For transect B-B' these values are 0.37, 0.11, 8.3, and 0.34. The fitted parameter set for B-B' data (horizontal and vertical) is statistically different than the parameter determined for A-A'. The authors also evaluate a probabilistic form of Dagan's (1982, 1987) equations relating geostatistical parameters to a tracer cloud's spreading moments. The equations are evaluated using the parameter estimates and covariances determined from transect A-A' as input, with a velocity equal to 9.0 cm/day. The results are compared with actual values determined from the field test, as estimated by Freyberg (1986) and and others. The geostatistical parameters developed from this study produce an excellent fit to both sets of calculated plume moments when combined with Dagan's time-dependent stochastic solution.

Zimmerman, R.W., S. Kumar, and G.S. Bodvarsson. 1990. Lubrication theory analysis of the permeability of rough-walled fractures. *Fall Meeting Amer. Geophys. Union.* October 23, 1990. EOS Transactions. 71(43).

The flow of a fluid through a rough-walled rock fracture can be modeled in detail by the Navier-Stokes equation. However, since this set of three nonlinear partial differential equations is difficult to solve, even by numerical methods, the equations are often replaced by the Reynolds equation of lubrication theory. One of the conditions necessary for this simplification is that the Reynolds number of the flow be low, and another is that the variations in the aperture be "slow" in some sense. The first (dynamical) condition is very often satisfied by flows of geophysical interest. The other (geometrical) condition is the object of this paper. The authors first discuss the work of Brown (1989). Brown carried out numerical solutions of the lubrication equations for fractures with fractal aperture distributions. His results suggested that the hydraulic aperture, h_H, could be correlated with the mean aperture, h_M, and the standard deviation of the surface roughness profile, σ, by an equation of the form $(h_H/h_M)^3 = 1 - A \exp(-Bh_M/\sigma)$, with $A \approx 0.7$, and $B \approx 0.5$. The parameters A and B were very weakly dependent on the fractal dimension. Guided by these results, the authors studied idealized fractures with sinusoidally-varying apertures, for which analytical solutions of the lubrication equation are possible. The results reproduce those of Brown "fairly closely," suggesting an applicability of his correlation beyond the specific statistical distribution used for his surface profiles. Within the context of the lubrication approximation, the results do not depend on the spatial wavelength of the aperture variations, λ. Some analysis was done to quantify the conditions of validity of the lubrication approximation. Brown had suggested that use of the lubrication equations required that the fracture surfaces be smooth over lengths equal to about 50σ, which is probably not the case for most fractures (authors dixit). Using perturbation solutions of the full Navier-Stokes equations,

with σ/λ as the perturbation parameter, they show that in order for the lubrication theory results to be correct to within less than 10 percent error, one need only have $\sigma/\lambda < 1$, which is a less restrictive condition.

NRC FORM 335 (2-89) NRCM 1102, 3201, 3202

U.S. NUCLEAR REGULATORY COMMISSION

BIBLIOGRAPHIC DATA SHEET

(See instructions on the reverse)

1. REPORT NUMBER (Assigned by NRC. Add Vol., Supp., Rev., and Addendum Numbers, if any.)

NUREG/CR-5743

2. TITLE AND SUBTITLE

APPROACHES TO LARGE SCALE UNSATURATED FLOW IN HETEROGENEOUS, STRATIFIED, AND FRACTURED GEOLOGIC MEDIA

3. DATE REPORT PUBLISHED

MONTH	YEAR
August	1991

4. FIN OR GRANT NUMBER

B6664

5. AUTHOR(S)

R. Ababou

6. TYPE OF REPORT

Technical

7. PERIOD COVERED *(Inclusive Dates)*

8. PERFORMING ORGANIZATION – NAME AND ADDRESS *(If NRC, provide Division, Office or Region, U.S. Nuclear Regulatory Commission, and mailing address; if contractor, provide name and mailing address.)*

Center for Nuclear Waste Regulatory Analyses
Southwest Research Institute
6220 Culebra Road
San Antonio, Texas 78228-0510

9. SPONSORING ORGANIZATION – NAME AND ADDRESS *(If NRC, type "Same as above"; if contractor, provide NRC Division, Office or Region, U.S. Nuclear Regulatory Commission, and mailing address.)*

Division of Engineering
Office of Nuclear Regulatory Research
U. S. Nuclear Regulatory Commission
Washington, DC 20555

10. SUPPLEMENTARY NOTES

11. ABSTRACT *(200 words or less)*

This report develops a broad review and assessment of quantitative modeling approaches and data requirements for large-scale subsurface flow in radioactive waste geologic repository. The data review includes discussions of controlled field experiments, existing contamination sites, and site-specific hydrogeologic conditions at Yucca Mountain. Local-scale constitutive models for the unsaturated hydrodynamic properties of geologic media are analyzed, with particular emphasis on the effect of structural characteristics of the medium. The report further reviews and analyzes large-scale hydrogeologic spatial variability from aquifer data, unsaturated soil data, and fracture network data gathered from the literature. Finally, various modeling strategies toward large-scale flow simulations are assessed, including direct high-resolution simulation, and coarse-scale simulation based on auxiliary hydrodynamic models such as single equivalent continuum and dual-porosity continuum. The roles of anisotropy, fracturing, and broad-band spatial variability are emphasized.

12. KEY WORDS/DESCRIPTORS *(List words or phrases that will assist researchers in locating the report.)*

Constitutive Relations, Darcy's Law, Dual-Porosity Models, Effective Conductivity, Equivalent Media, Fractured Media, Fractured Rock, Geologic Repository, Porous Media, Radionuclide Contamination, Random Fracture Networks, Random Media, Self-Similarity, Stochastic Flow, Three-Dimensional Numerical Simulation, Unsaturated Conductivity, Unsaturated Flow, Water Retention Curve, Yucca Mountain.

13. AVAILABILITY STATEMENT

Unlimited

14. SECURITY CLASSIFICATION

(This Page)

Unclassified

(This Report)

Unclassified

15. NUMBER OF PAGES

16. PRICE